

UNIVERSITÉ DU QUÉBEC À MONTRÉAL

DEVELOPMENT OF A MINIATURIZED PASSIVE AIR SAMPLER TO  
CHARACTERIZE THE EXPOSURE OF EMERGING CONTAMINANTS IN  
BIRDS

MASTER THESIS  
PRESENTED  
AS A PARTIAL REQUIREMENT  
OF THE MASTER'S DEGREE IN ELECTRICAL ENGINEERING

BY  
ALI REZAEI

NOVEMBER 2016

UNIVERSITÉ DU QUÉBEC À MONTRÉAL  
Service des bibliothèques

Avertissement

La diffusion de ce mémoire se fait dans le respect des droits de son auteur, qui a signé le formulaire *Autorisation de reproduire et de diffuser un travail de recherche de cycles supérieurs* (SDU-522 – Rév.07-2011). Cette autorisation stipule que «conformément à l'article 11 du Règlement no 8 des études de cycles supérieurs, [l'auteur] concède à l'Université du Québec à Montréal une licence non exclusive d'utilisation et de publication de la totalité ou d'une partie importante de [son] travail de recherche pour des fins pédagogiques et non commerciales. Plus précisément, [l'auteur] autorise l'Université du Québec à Montréal à reproduire, diffuser, prêter, distribuer ou vendre des copies de [son] travail de recherche à des fins non commerciales sur quelque support que ce soit, y compris l'Internet. Cette licence et cette autorisation n'entraînent pas une renonciation de [la] part [de l'auteur] à [ses] droits moraux ni à [ses] droits de propriété intellectuelle. Sauf entente contraire, [l'auteur] conserve la liberté de diffuser et de commercialiser ou non ce travail dont [il] possède un exemplaire.»

UNIVERSITÉ DU QUÉBEC À MONTRÉAL

DÉVELOPPEMENT D'ÉCHANTILLONEURS D'AIR MINIATURISÉS ET  
EMBARQUÉS SUR DES OISEAUX POUR LA CARACTÉRISATION DE LEUR  
EXPOSITION À DES NOUVEAUX CONTAMINANTS

MÉMOIRE  
PRÉSENTÉ  
COMME EXIGENCE PARTIELLE  
DE LA MAÎTRISE EN GÉNIE ÉLECTRIQUE

PAR  
ALI REZAEI

NOVEMBRE 2016

## REMERCIEMENTS

Je tiens à remercier mon directeur de recherche, Pr Ricardo Izquierdo, ainsi que mon codirecteur, Pr Jonathan Verreault pour leurs conseils et leurs suggestions qui m'ont été utiles durant tout mon mémoire.

Je remercie aussi madame Manon sorais, Dr Sujitra Poorahong et monsieur Mojtaba Mirzaei, Alexandre Robichaud, Dr Sujitra Poorahong, ainsi que les organisations suivantes pour leurs soutiens : UQAM, CoFaMic, TOXEN, AVITOX, RESMIQ, la Chaire de recherche du Canada, et le Fond de recherche nature et technologies.

Finalement, je tiens à remercier ma femme et ma mère, qui m'ont soutenu tout au long de ce périple, du début à la fin, des meilleurs moments aux plus difficiles.



## TABLE OF CONTENTS

LIST OF FIGURES .....	ix
LIST OF TABLES .....	xiii
RÉSUMÉ .....	xv
ABSTRACT .....	xvii
CHAPTER I	
INTRODUCTION .....	1
1.1 Project description.....	1
1.2 Passive and active air samplers .....	3
1.2.1 Passive air samplers.....	4
1.2.2 Active air samplers .....	9
1.3 Problematic and objectives .....	11
1.6 Methodology .....	13
1.5 Thesis presentation.....	14
CHAPTER II	
PASSIVE AIR SAMPLER CONCEPT DESIGNS AND SIMULATIONS .....	17
2.1 Design 1 .....	20
2.1.1 Pattern 1 .....	20
2.1.2 Design 1 simulation .....	21
2.2 Design 2 .....	24
2.2.1 Pattern 2 .....	24
2.2.2 Design 2 simulation .....	26
2.3 Design 3 .....	29
2.3.1 Pattern 3 .....	29
2.3.2 Design 3 simulation .....	31
2.4 Design 4 .....	33

2.4.1	Pattern 4 .....	33
2.4.2	Design 4 simulation .....	36
2.5	Design 5.....	39
2.5.1	Pattern 5 .....	39
2.5.1.1	Pattern 5-1.....	39
2.5.1.2	Pattern 5-2.....	43
2.5.2	Design 5 Simulation.....	45
2.6	Design 6.....	49
2.6.1	Pattern 6 .....	49
2.6.2	Design 6 simulation .....	54
2.7	PAS comparison and selection .....	58
2.7.1	PASs's drag values.....	58
2.7.2	PASs comparison and selection procedure .....	60
2.8	Resume .....	64
CHAPTER III		
PASSIVE SAMPLER FABRICATION AND TESTING .....		65
3.1	PAS fabrication .....	65
3.2	Adsorbents .....	68
3.2.1	Polyurethane foam .....	68
3.2.2	Glass fiber filter (GFF) .....	70
3.2.3	Polydimethylsiloxane (PDMS) .....	70
3.2.4	Graphene oxide .....	72
3.3	PAS onsite testing.....	72
3.4	Resume .....	75
CHAPTER IV		
EMBEDDED ELECTRONIC CIRCUIT .....		77
4.1	Sensors and their utilization .....	77
4.2	Airspeed measurement electronic circuit .....	83
4.3	PAS concept design (modified to embed the sensors) .....	88
4.4	Simulation.....	92

4.5 Sensor validation and calibration .....	96
Summary and discussion .....	102
Conclusion .....	105
References .....	107





## LIST OF FIGURES

Figure 1.1 : Flame and non-flame retardant papers testing against fire.....	2
Figure 1.2 : Birds flying around landfill and searching for food .....	3
Figure 1.3 : A usual passive air sampler schematic with one sample medium inside ..	5
Figure 1.4 : A usual passive air sampler schematic with two sample mediums inside.	6
Figure 1.5 : A real passive air sampler during sampling process .....	6
Figure 1.6 : A helmet used as a passive air sampler with an inside sampling medium	7
Figure 1.7 : Flow-through sampler .....	8
Figure 1.8 : An active air sampler.....	10
Figure 2.1 : PAS first concept design .....	20
Figure 2.2 : 3D view of design 1 .....	21
Figure 2.3 : Volume Tetra angle non-structural mesh on design 1 – side view.....	22
Figure 2.4 : Design 1 vectorial airflow result on PAS, side view, middle plane .....	23
Figure 2.5 : Design 1 vectorial airflow result on PAS, top view .....	23
Figure 2.6 : Design 1 vectorial airflow result, top view, PAS body included .....	24
Figure 2.7 : PAS second concept design.....	25
Figure 2.8 : PAS second concept design 3D view .....	25
Figure 2.9 : Volume Tetra angle non-structural mesh on design 2, Top view.....	27
Figure 2.10 : Design 2 vectorial airflow result, top view.....	27
Figure 2.11 : Design 2 vectorial airflow result, 3D side view, PAS body included ...	28
Figure 2.12 : Design 2 vectorial airflow result, 3D top view, PAS body included ....	28
Figure 2.13 : PAS third concept design .....	30
Figure 2.14 : PAS third concept design 3D view. (a) Bottom view. (b) Top view.....	30
Figure 2.15 : Volume Tetra angle non-structural mesh on design 3 – side view.....	31
Figure 2.16 : Design 3 vectorial airflow result, side view .....	32

Figure 2.17 : Design 3 vectorial airflow result, top view .....	32
Figure 2.18 : Design 3 vectorial airflow result, 3D view .....	33
Figure 2.19 : PAS fourth concept design bottom part .....	34
Figure 2.20 : PAS fourth concept design 3D view .....	34
Figure 2.21 : PAS fourth concept design top part .....	35
Figure 2.22 : PAS fourth concept design top part 3D view.....	35
Figure 2.23 : PAS fourth concept design parts positioning in 3D view .....	36
Figure 2.24 : Volume Tetra angle non-structural mesh on design 4, side view .....	37
Figure 2.25 : Design 4 vectorial airflow result, side view.....	38
Figure 2.26 : Design 4 vectorial airflow result, 3D view, PAS body included .....	38
Figure 2.27 : Design 4 vectorial airflow result, 3D view, PAS body included .....	39
Figure 2.28 : PAS fifth (5-1) concept design bottom part .....	40
Figure 2.29 : PAS fifth (5-1) concept design bottom part 3D view .....	41
Figure 2.30 : PAS fifth (5-1) concept design top part .....	42
Figure 2.31 : PAS fifth concept design bottom part 3D view .....	42
Figure 2.32 : PAS fifth concept design parts positioning in 3D view .....	43
Figure 2.33 : PAS fifth (5-2) concept design bottom part.....	44
Figure 2.34 : PAS fifth (5-1) concept design bottom part 3D view .....	44
Figure 2.35 : PAS fifth concept design parts positioning in 3D view .....	45
Figure 2.36 : Volume Tetra angle non-structural mesh on design 5, side view .....	46
Figure 2.37 : Design 5 vectorial airflow result, side view, supports included .....	47
Figure 2.38 : Design 5 vectorial airflow result, side view, gap included .....	47
Figure 2.39 : Design 5 vectorial airflow result, top view, results on Z plane .....	48
Figure 2.40 : Design 5 vectorial airflow result, 3D view, PAS body included .....	48
Figure 2.41 : PAS sixth concept design bottom part .....	50
Figure 2.42 : PAS sixth concept design bottom part 3D view .....	51
Figure 2.43 : PAS sixth concept design top part .....	52
Figure 2.44 : PAS sixth concept design top part 3D view.....	52
Figure 2.45 : PAS sixth concept design parts positioning in 3D view .....	53

Figure 2.46 : Volume Tetra angle non-structural mesh on design 6, side view.....	54
Figure 2.47 : Design 6 vectorial airflow result, side view, supports included.....	55
Figure 2.48 : Design 6 vectorial airflow result, side view, gap included.....	55
Figure 2.49 : Design 6 vectorial airflow result, 3D side view .....	56
Figure 2.50 : Design 6 vectorial airflow result, top view, results on Z plane.....	56
Figure 2.51 : Design 6 vectorial airflow result, top view, results on Z plane.....	57
Figure 2.52 : Design 6 vectorial airflow result, 3D view, PAS body included.....	57
Figure 2.53 : Experimentally measured Drag coefficients for certain shapes .....	59
Figure 3.1 : Accepted PAS fabricated with 3D printing technology .....	67
Figure 3.2 : Natural Tubular Teflon ribbon used to mount the PAS on the birds.....	68
Figure 3.3 : Polyurthane foam.....	69
Figure 3.4 : PDMS mould for forming the uncured PDMS.....	71
Figure 3.5 : Mounted PAS on a bird, using the Teflon ribbon in bird's colony .....	74
Figure 3.6 : Mean total mass (ng) of $\Sigma 15$ PBDE, HBB, and $\Sigma 3$ Dec.....	74
Figure 4.1 : Pitot, Static and Pitot-Static tube example .....	80
Figure 4.2 : Differential pressure sensor. (a) Different packages and tube direction .	82
Figure 4.3 : Temperature-humid sensor .....	83
Figure 4.4 : Schematic diagram of sensors and controllers .....	84
Figure 4.5 : Designed and adapted PCB to be installed inside the PAS .....	87
Figure 4.6 : A complete electronic board including all components .....	87
Figure 4.7 : Modified PAS concept design top part 4 side view .....	88
Figure 4.8 : Modified PAS concept design third part 4 side view .....	89
Figure 4.9 : Electronic components 3D diagram .....	89
Figure 4.10 : Modified PAS concept design middle part 4 side view.....	90
Figure 4.11 : Modified PAS parts installation sequence.....	90
Figure 4.12 : Modified PAS complete pack 4 side view, electronic parts included ...	91
Figure 4.13 : Complete and final modified PAS cross sectional cut .....	92
Figure 4.14 : CFD simulation on complete PAS, results on Y plan .....	93
Figure 4.15 : CFD simulation on modified PAS, results on Z plan .....	94

Figure 4.16 : CFD simulation on modified PAS, results on Z plan .....95

Figure 4.17 : CFD simulation on modified PAS, results on Z plan top view .....95

Figure 4.20 : Modified accepted PAS for embedding the active sensors .....96

Figure 4.21 : PASCO 850 Universal anemometer .....97

Figure 4.22 : Considered setup for validation and calibration the PAS sensors .....98

Figure 4.23 : PAS preliminary and calibrated output results compared .....99

Figure 4.24 : PAS preliminary and calibrated output results compared .....100

Figure 4.25 : Temperature comparison graph .....101

Figure 4.26 : Relative humidity comparison graph .....101

## LIST OF TABLES

Table 2.1 : Pattern's drag force calculation .....	60
Table 4.1 : List of main electronic components .....	96
Table 4.2 : Design 7 drag force calculation .....	96



## RÉSUMÉ

La protection de la santé humaine et de l'environnement est une préoccupation majeure depuis plusieurs années. Cependant, l'augmentation spectaculaire du nombre de produits chimiques nocifs rejetés par les industries ainsi que le nombre croissant de produits de consommation qui contiennent des composés chimiques entraîne des défis importants. Parmi ces produits chimiques, on retrouve une grande quantité de contaminants organiques halogénés qui sont constamment rejetés dans les écosystèmes. Ces contaminants peuvent ensuite s'accumuler dans les espèces sauvages, comme les oiseaux. Toutefois, il existe d'importantes lacunes dans les connaissances sur les sources alimentaires et non alimentaires de ces contaminants et c'est le cas en particulier pour certaines substances chimiques pour lesquelles aucune réglementation internationale n'existe. Par conséquent, une étude sur les sources atmosphériques de retardateurs de flamme halogénés (y compris les éthers diphényles polybromés (PBDE)) est nécessaire. Afin de réaliser cette étude, deux échantillonneurs miniaturisés pouvant être portés par des oiseaux ont été développés pour la première fois. Il s'agit d'un échantillonneur d'air passif (PAS) où uniquement un filtre est utilisé comme capteur et d'un deuxième où des capteurs électroniques sont intégrés. Différentes architectures ont été conçues en utilisant des simulations de mécanique des fluides numériques (CFD) afin d'évaluer le flux d'air à l'intérieur et à l'extérieur du PAS et la façon dont la surface des absorbants est exposée à l'air qui y circule. Le dispositif a été fabriqué en utilisant une imprimante 3D et peut être équipé de différents absorbants. Il a par la suite été monté sur des goélands afin de retracer les sources de retardateurs de flamme dans la région de Montréal. Finalement, le dispositif retenu a été muni d'un capteur commercial afin d'obtenir des données complémentaires pour de meilleures analyses d'absorbant. Ce projet fait partie d'un projet global en collaboration entre des groupes de recherche du département de biologie et informatique de l'UQAM.



**MOTS-CLÉS :** Échantillonneur d'air passif, Échantillonneur d'air actif, PAS, Adsorber, Simulation CFD, Retardateur de flamme, PBDE, Impression 3D.

## ABSTRACT

Protection of human health and the environment has been one major concern in recent years, however, the dramatic increase in the number of noxious chemicals produced by industries causes an important challenge. Among these chemicals, there is a group of organic contaminants, flame retardants, which are discharged into the wildlife environment and could become concentrated inside the bodies of different species in different ways. However, there is a lack of knowledge related to the dietary and non-dietary sources of these contaminants, especially for the type of chemicals for which is no international restriction. Therefore, an investigation on the atmospheric sources of flame retardants, both gas and particle phase (including Polybrominated diphenyl ethers (PBDEs)), can help us to have a better understanding about their effects on ecosystems. In order to address this investigation, for the first time, a miniaturized bird-borne passive air sampler was developed. This project was a part of a global project undertaken in a collaboration between research groups from computer science and biology departments of UQAM. In order to optimize the sampler, several patterns were designed and studied as a point of airflow, inside and outside the geometries, using computational fluid dynamic (CFD) simulation. Then, our colleagues from biology were responsible to select the most appropriate design based on their requirements. The design was fabricated using 3D printing technology, equipped with different kinds of sampling media and mount on a ring-billed gulls in order to track the sources of flame retardants in Montreal area. Finally, the approved passive air sampler was modified to be equipped with some commercial sensors in order to have complementary data for better adsorbents analysis.

**KEYWORDS** : Passive air sampler, Active air sampler. PAS, Adsorber, CFD simulation, Flame retardant, PBDE, 3D printing.



## CHAPTER I

### INTRODUCTION

#### 1.1 Project description

This thesis project is part of a more global project which is realized through a collaboration between research groups in microelectronics engineering and biology. The global project has the title: “Combining High-Resolution Biotelemetry and Passive Air Sampling Techniques: A Novel Approach to Understand the Intra-Specific Variations in Emerging Contaminant Exposure in Birds” and concerns about the source of the pollution in environment and their effect on ecosystems. Several endangered species live close to the water sources where different sources of contaminants can be founded. Among those sources of contamination, a group of organic contaminants that can bioaccumulate in some species such as birds, are continuously releasing into ecosystems. Among all those pollution, the flame retardant compounds, including the polybrominated diphenyl ethers (PBDEs), are a group of chemicals that massively used in industries. These chemicals are added to different kinds of products such as furniture, electronic components and boards, isolators to reduce the fire hazards (Figure 1.1).

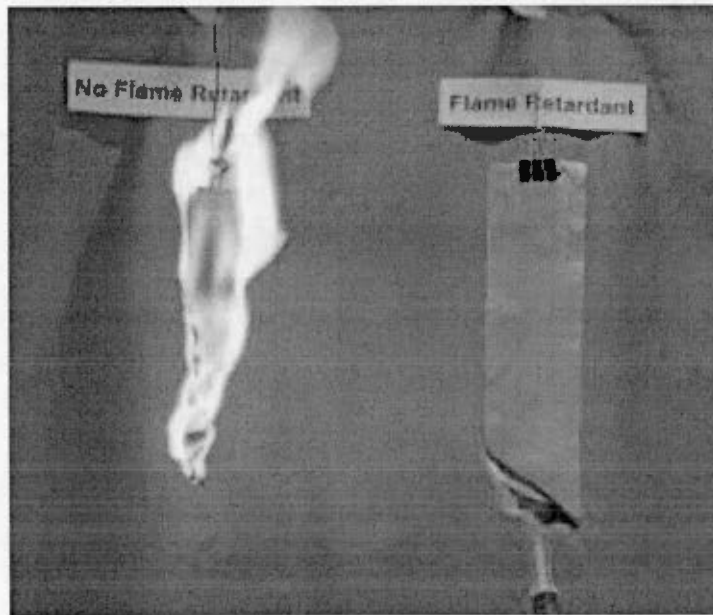


**Figure 1.1 : Flame and non-flame retardant papers testing against fire**

Retrieved from: [http://www.rutlandplastics.co.uk/advice/plastics\\_additives\\_fr.html](http://www.rutlandplastics.co.uk/advice/plastics_additives_fr.html)

A research study administered by a group (Canada Research Chair in Comparative Avian Toxicology) from the biology department of UQAM University, reported high accumulation of PBDEs and a series of other types of flame retardant compounds in tissues of birds living around Montreal. They proposed that the dietary of a kind of bird (ring-billed gulls) could be a reason that they expose to these types of chemicals besides the atmospheric pollution. As an omnivore species (Figure 1.2), these birds can be studied for environmental contamination related to dietary, in Montreal area. This can be accomplished by using these birds to find the source of these Contaminants using an air sampling device mounted on them. Air sampling consists in capturing the contaminant from a volume of air, measuring the amount of captured contaminants and reporting the results as a concentration. In order to do so, the air is passed through a sampling medium (could be a variety type of absorbers) which captures the pollutants. Then, the amount of pollutants captured in the sampling media is measured by various

analytical techniques. Finally, the volume of sampled air is reported against the amount of pollution captured and this gives the concentration, which is expressed as milligrams per cubic meter ( $\text{mg}/\text{m}^3$ ) or part per million (ppm). This process can be done by passive or active air sampling. Detailed information about this technique and related instruments will be provided in the following.



**Figure 1.2 : Birds flying around landfill and searching for food**

Retrieved from: <http://www.gettyimages.ca>

## 1.2 Passive and active air samplers

There are two principal means of monitoring the pollution of the air, passive sampling and active sampling. In the following section we will present various techniques and systems that have been reported for active and passive air sampling.

### 1.2.1 Passive air samplers

A passive air sampler (PAS) is a very simple device that does not need any pump and electrical parts. Generally, a passive air sampler consists of a housing and internal structure to hold different types of absorbers. The housing can be designed in different shapes and it will protect the internal parts of rain or direct sun light exposure. It also helps the intake air to have better circulation inside the housing in order to have maximum exposure to the absorbers. Depending on PAS applications, different types of internal structures can be designed to use different types of absorbers. This type of sampler can be installed wherever that air sampling is needed such as: offices, rooms, parking or outdoor places. In order to have enough sampling air Influence on the absorbers, the PAS can be maintained in a place from several days to several weeks. The time of sampling, depends on absorbers saturation time and application requirements. There are different types of design for PASs. One of the most reported one is made from two different sizes half spherical stainless steel housing (Figure 1.3) and installed in a way that they could cover the inside sampling media (Abdallah et Harrad, 2010). The two housing parts are fixed on top of each other using a central long screw. The sampling media or any further mechanical parts can be installed inside the PAS by using this central long screw. Based on this design, the sampling air can enter the PAS through the existing gap between top and bottom housing parts. After Influencing through the sampling media or absorbers, the sampled air can come out from the embedded holes at the bottom of the smaller housing part. Other roles of these two housings parts are: to protect the inside media from direct deposition of particulates, to reduce the effect of the fluid flow velocity (Hazrati et Harrad, 2007) and to protect the inside samplers from direct exposure to sun light for some applications where light protection is important.

Depending on the type of pollution that need to be studied, different kinds of absorbers can be used inside the PAS. As an example, the polyurethane foam (PUF) filters are

known to capture compounds in the vapor phase (Abdallah et Harrad, 2010) and glass fiber filters (GFF) are known to sample the particulate phases (Abdallah et Harrad, 2010) (Figure 1.4). Other types of materials such as Polydimethylsiloxane (PDMS) (Park *et al.*, 2014) or Graphene oxide (GO) can also be used as an absorber to check their functionality. In this PAS configuration, different kinds of absorbers can be used alone or coupled together (Abdallah et Harrad, 2010). This can be done by using the long central screw to mount various absorbers. The usage of the long central screw also brings the advantage of being able to do distance modification among the various PAS consisting of parts and installing the complete PAS for inside or outside usages (Figure 1.5).

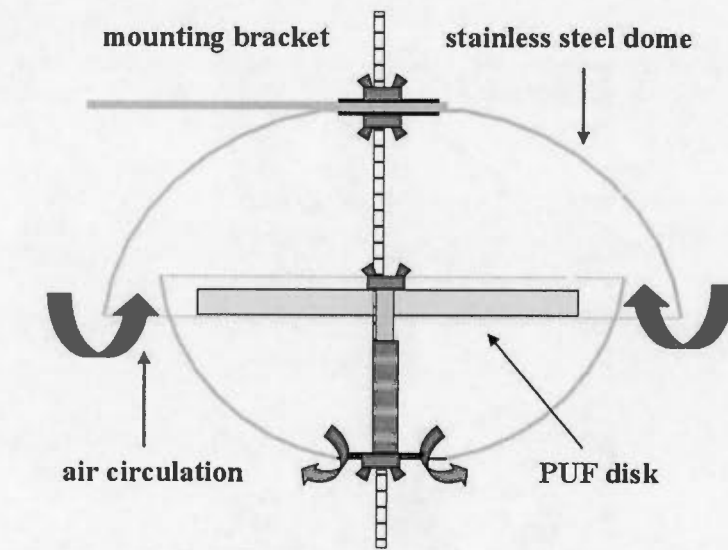
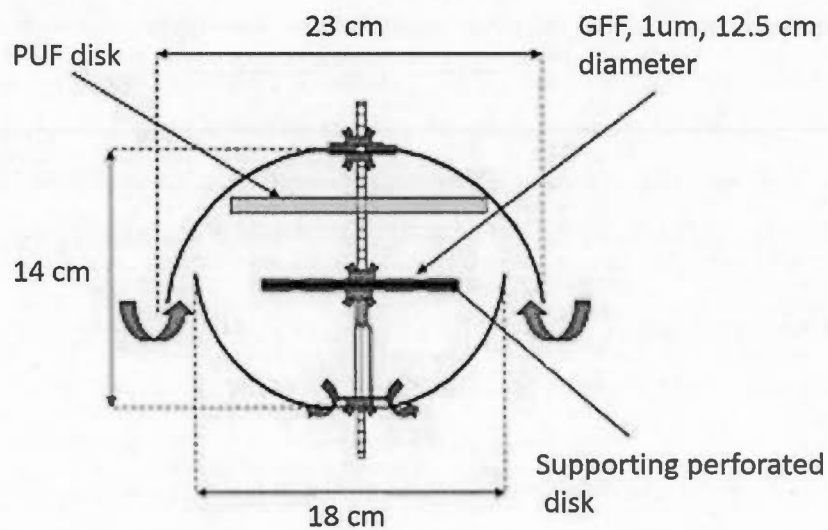


Figure 1.3 : A usual passive air sampler schematic with one sample medium inside

Retrieved from: <http://www.monairnet.eu/index-en.php?pg=methods--passive-air-sampling>





**Figure 1.4 : A usual passive air sampler schematic with two sample mediums inside (Abdallah et Harrad, 2010)**



**Figure 1.5 : A real passive air sampler during sampling process**

Retrieved from: <http://www.monairnet.eu/index-en.php?pg=methods--passive-air-sampling>

In another study which was focused on two industrial sites (alloy industry and coke plant) the PAS was embedded in the worker's helmet (Bohlin *et al.*, 2010) (Figure 1.6). In fact workers' helmets was modified in a way that it acts as a PAS. A small piece of PUF was deployed into their helmet and the workers carried them during working hours. The PUFs were exposed to the air and when they became saturated they were analyzed for extracting results.

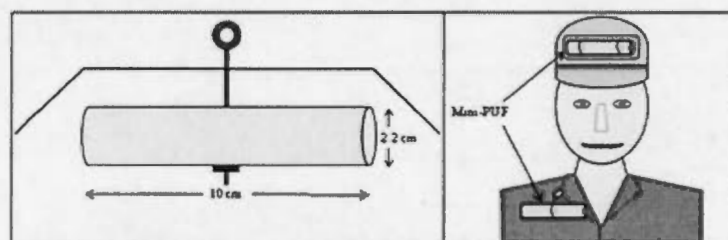


**Figure 1.6 : A helmet used as a passive air sampler with an inside sampling medium (Bohlin *et al.*, 2010)**

In another study a different type of PAS called “flow through sampler” was presented (Xiao *et al.*, 2007) (Figure 1.7). This different PAS was modified and adapted to highly increase the sampling rate of air without using a pump (Xiao *et al.*, 2007) or any electrical device. This PAS consists of a horizontal tube that can force the air to blow through the absorbers and a vertical fin part (acts like aircraft rudder) that allow the PAS to turn into the wind direction. In this way more air can blow through the sampling media and this will decrease the time of saturation of the media. This type of PAS is more suitable for applications with limited study time.

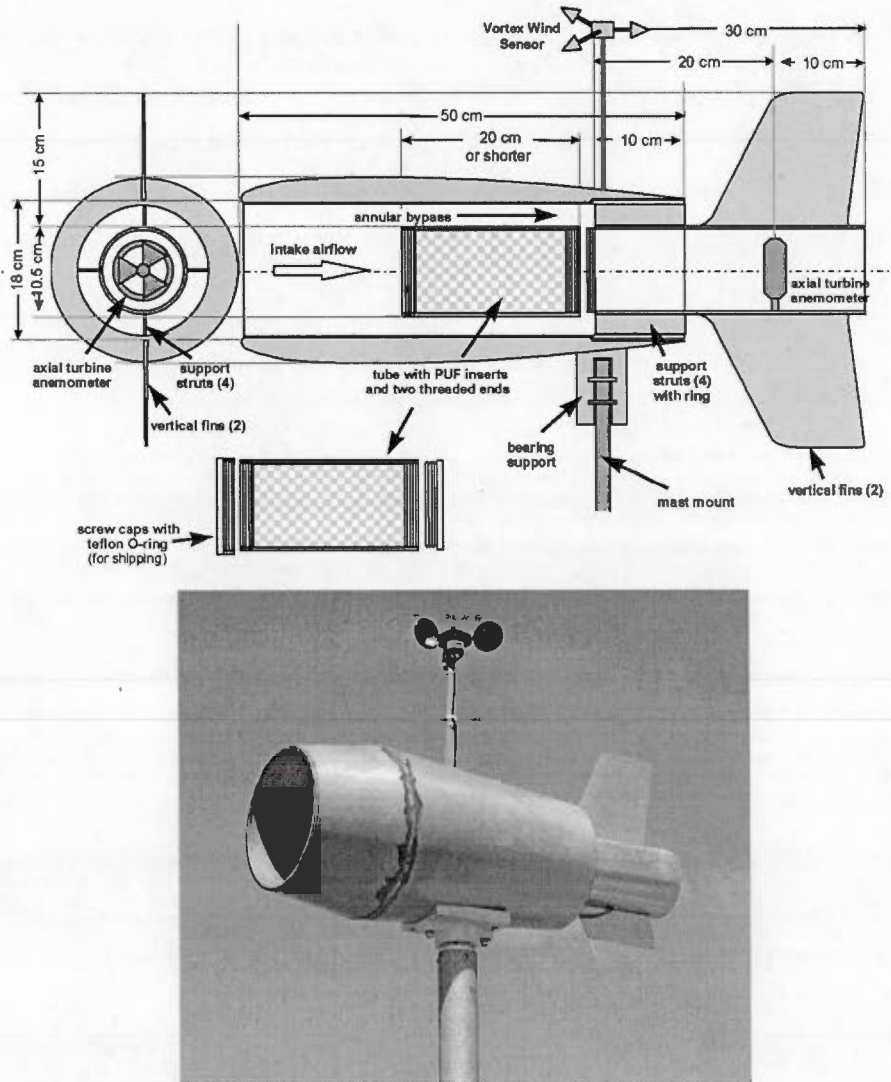


Figure 1.7 : Flow-through sampler (Xiao et al., 2007)

The conventional type of PAS can be installed everywhere (in places such as offices, schools, cars, roofs, land fields, etc.), however, the PUFs can be exposed with different air velocity and this can affect PUFs sampling rate (Tuduri *et al.*, 2006). A study with the title of “wind effect on sampling rate” (Tuduri *et al.*, 2006) reports that by exposing PUFs to PCB contaminated environment (PCB: polychlorinated biphenyl) in a wind

tunnel with a variety wind velocity, absorber sampling rate was increased inchmeal and after reaching a certain speed it increased sharply while the design of the housings could damp the wind effect (Tuduri *et al.*, 2006). In this case calculating the wind speed around the PAS can helps to validate the PUFs analysis results.

In addition, understanding of air circulation, air velocity inside and outside a PAS and the way that sampling air expose to the PUF disks, could help better comprehension of the PAS's entire system functionality for better PAS design and better positioning of different types of absorbers (Tuduri *et al.*, 2006). Also, two other studies present the computational fluid dynamic (CFD) simulation on PUF disk and typical PAS to model the air circulation and velocity around and inside the PAS. Based on those CFD simulations, they proved that the uptake rate of absorbers are dependent on external wind speed. Also, varying the boundary conditions around the PUF disk will result in varying relations between absorbed pollution and wind speed (Thomas *et al.*, 2006). Moreover, CFD simulation confirms the Integrity of previous reports about increasing in sample rate due to the increase of the wind velocity. They also show that the increase in the sample rate also depends on ambient wind angle (May *et al.*, 2011). Finally, the reported results, showing the advantage of proceeding to CFD simulation before building a new design.

### 1.2.2 Active air samplers

One of the most common active air samplers is shown on figure 1.8. This system uses a suction pump or fan to draw air to be sampled into a container. This container is equipped with different kinds of filters and absorbers, which depend on the active air sampler functionality. As it is clear from this description, this device consists of electrical and mechanical parts and they need enough power to work.

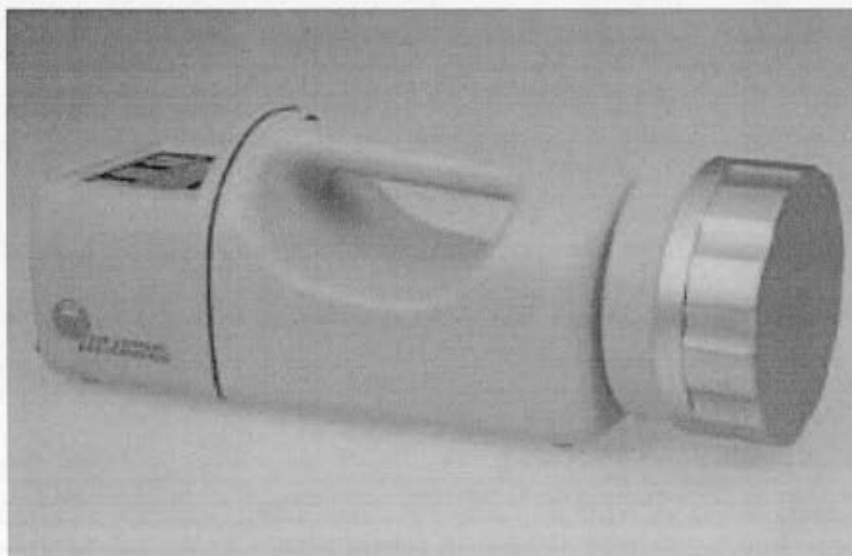


**Figure 1.8 : An active air sampler**

Retrieved from: [http://www.biosci-intl.com/products/sas\\_100\\_180.htm](http://www.biosci-intl.com/products/sas_100_180.htm)

Some studies were focused on a specific gas using active air sensors. Based on the targeted gas characteristics, a type of material or combination of several layers of different materials can be used to detect the specific kind of gas molecules. These materials change their electrical characteristics (resistivity, capacity, conductivity, etc.) when they enter in contact with those kinds of gas molecules and by measuring the variation of these characteristics the target gas can be detected.

Active gas samplers could also be built using microfluidic techniques. By using microfluidic devices, it is possible to have several inlets and each inlet can be designed for a special material such as water, air, gases, etc. From this point many new techniques can be used for gas detection. For example, it can be used to fabricate “bubble-based gas sensor” (Bulbul *et al.*, 2014) which mixes the liquid entering one channel with the gas entering from another channel in order to create small bubbles, containing the target gas to be measured. By measuring the size of the created bubbles

and using customized software the type of the entered gas can be detected. In another study, a “microfluidic gas centrifuge” was presented. It uses the gas molecular weight to separate a mixture of gases (Li *et al.*, 2007).

Generally, in microfluidic devices, a pump is required to inject the liquids or gases inside the fluidic channels. In those cases, a small micro pump can be integrated into the device in order to move the gas inside the channels (Martini *et al.*, 2012). In this study, thermal variation was used to serve as the pumping system along the micro channels in order to guide the gas into the channels (Martini *et al.*, 2012).

Additionally, the fluidic channels can be used to guide the intended gas into the main chamber which is fabricated on top of a CMOS readout chip (Mu *et al.*, 2012; Ward *et al.*, 2012). The chip could include an accrete chemiresistor (CR) array which is designed to amplify and condition the detected signal. The combination of CR arrays, CMOS chip and microfluidic techniques could be used to build a micro gas chromatograph (Mu *et al.*, 2012; Ward *et al.*, 2012).

### 1.3 Problematic and objectives

All the presented samplers are too big compared with the medium size of a bird and it is not possible that they be mounted and carried by birds. We then need to modify the samplers design in order to adapt them to the birds.

As it is clear from previous sections, the active air sampler requires several electrical-mechanical parts and it is not suitable for our application. On the other hand, passive air sampling has several advantages compared with active air sampler. It is a low-cost technique which does not need any electrical parts. In this case, for this study a passive air sampler (PAS) can be a promising device to capture the halogenated flame retardants compounds.

This device will be used to passively capture PBDEs compounds and other types of flame retardants existing in air in both the vapor and particulate phases during the period of time (one, two and three weeks). The designs will be based on existing passive air sampler which is well described by Abdallah and Harrad (May *et al.*, 2011).

After fabricating and testing PAS device, it will be interesting to evaluate the possibility of implementing some electronics sensors in it, in order to collect more complementary data when it is under testing.

Since this project has been done in collaboration with the biology department, the first step to launch this project is to design the appropriate PAS. In this case the following objectives have been set in order to fulfill all explanations above:

- 1- Miniaturize and validate a passive air sampler (PAS) that can be transported by a medium-size bird and trap both particle- and gas-phase halogenated flame retardant contaminants.
- 2- Design and fabricate a low power consumption electronic circuit that can operate during the passive air sampling period while it is embedded inside a modified PAS in order to provide some complementary data for better adsorbents analyses.

## 1.6 Methodology

In order to build a device with the small size and weight needed for this application, available practical microfabrication techniques will be evaluated and the most suitable one will be chosen by the final user (collaborators in the biology department) based on the bird's limitations.

The sampling housing can be fabricated by using the soft lithography technique. In this technique, first a mould could be made using the photo resist materials; then, by casting the polydimethylsiloxane (PDMS) on the mould, the main chamber and related channels will be formed and after curing process it can be peeled off from the mould for more manipulation (Qin *et al.*, 2010). PDMS physical characteristics make it appropriate for this type of application (harsh weather environment) due to its resistant against thermal and physical shocks. Alternatively, the PAS chamber can be fabricated using 3D printing technology. Recently the 3D printing technology has seen massive development and the new printers can print walls as narrow as 0.5 mm and layers as thin as 50 micrometers. The size and design of the chamber can easily be modified and scaled by using both techniques. Before fabrication, different concept patterns will be designed and simulated to study the fluid flow circulation inside and outside the PAS and achieve the best fluid flow control. The concept designs will be done in a way that it could be equipped with different kinds of absorbers. This new device can be used for different toxicology and pollution monitoring application. It will be designed in a way that it could be carried by the medium size bird for passive air sampling monitoring. In future it can be equipped with some sensors, specially designed for specific compounds. This will change the role of this device from passive air sampler to active air sampler which can also send online reports or data to the laboratory.



In this case, 3D design software (design Spark mechanical and Catia) were used in order to design concept patterns. Then the computational fluid dynamic (CFD) test can be done on designed patterns by using ANSYS FLUENT 15 to study the effects of the fluid flow (in our case it is air) on it. The pattern and its related results will be provided to the biology department in order to know if there are any weaknesses or critical problems on the design. In the event of any problem, the pattern will be modified or a new pattern will be provided. This procedure will be repeated until a pattern that covers all project requirements be achieved and it be approved by the biology department. The approved PAS will be fabricated by 3D printer in order to be mounted on the bird for the first year of the study.

Following the first design, in order to equip the PAS with some sensors, the PAS would be redesigned and modified in a way that it respects the previous design while it could carry electronic circuits including sensors. The new design will be fabricated and equipped with electronic circuits and adsorbents in order to be tested in field.

For the active part of the PAS, sensors and processors should be as small as possible and also they should be selected from the ultra-low power category. The printed circuit board (PCB) and its related schematic will be designed by circuit maker software (from Altium design Co.), then it will be fabricated using PCB fabrication machine (LPKF machine – LPKF Laser & electronics AG).

## 1.5 Thesis presentation

Based on the table of contents, in chapter 2, all the concept designs will be presented including their CFD simulation results. Also, patterns' actual size, their 3D and line-dote design will be presented as separated and assembled views and finally the PAS comparison and selection process will be presented which is based on CFD simulation results (Drag value) and the experiences of our colleague from the biology department.

At the beginning of chapter 3, the PAS fabrication process, results and all the necessary condition that should be respected for fabrication, will be presented. Following this, different types of adsorbents that were used and can be used with miniaturized PAS will be introduced and following that the biological results of the PAS will be presented including an image from filed work which shows a real 3D printed PAS mounted on a bird and ready to release for tests.

In chapter 4, sensors that can be applied to the miniaturized PAS and the way that they can provide some complementary data will be presented. Then the accepted PAS will be modified in a way that all new components including sensors, printed circuit boards and controllers are equipped inside the PAS. New simulation will be done on the new design in order to check PAS's functionality while the new active sensors are embedded inside the PAS. In the following, the results of the active sensors will be shown and their comparison-validation with a pre-calibrated anemometer. Finally, in conclusion, a brief explanation of all chapters will be presented.



## CHAPTER II

### PASSIVE AIR SAMPLER CONCEPT DESIGNS AND SIMULATIONS

Since this was the first time that a miniaturized PAS was designed and adapted to be installed on birds, several miniaturized PAS concept designs were made using DesignSpark Mechanical software (3D design software – Free Licence) and Catia (Dassault Systemes – Academic version at école de technologie supérieure (ETS)). On those designs we tried to consider several factors that could influence the performance of the PAS and also birds flying abilities. These factors which can also be considered as project limitations are: PAS aerodynamic shape, size and thickness (must be less than 45×35×20 mm), weight (must be less than 3% of the bird's total weight), PAS air inlet position and finally, the most effective way that the entered air can expose the sampling media. In this case, the idea of each design is based on the mentioned requirements which were provided by our collaborators from the biology department. For example, some designs would have the maximum sampling media active surface area, some would be more aerodynamic and some other could have direct air exposure. The computational fluid dynamic (CFD) simulation was done on designed patterns using ANSYS Fluent simulation software in order to understand how the designed PAS will behave before fabrication. Each design and its simulation results was proposed to our colleagues in the biology department in order to know the advantages and disadvantages of the design and getting suggestions to improving the design. At the end, the most appropriate design, the one who meets all project requirements, as suggested by the group of the biology department was fabricated and prepared to be tested on birds.

For CFD simulations, the 3D design file was exported as STereoLithography (STL) file and imported to the ANSYS software. In order to have the same simulating condition for all patterns, same settings were used during all simulation as following:

#### Area definition:

In order to make a CFD simulation on an object, this object should be defined in an area which is a 3 dimensional space. The area definition tool allows us to define this space by drawing some surfaces called walls. These walls would be a part of CFD simulation which means that the simulation software will calculate the fluid flow effects on these walls which are not desired. In order to eliminate the effects of the walls on the main objects, this area should be defined as large as possible. In CFD simulations, usually, each area dimension is considered as fifteen times bigger than related dimensions on target object.

#### Objects material:

In CFD simulations, all the designed objects (walls, main objects, fluids) should be assigned to a type of material which exists in software library. These materials can be fluids (air or chemical gazes), flexible (plastics, polymers, etc.) or rigid and non-flexible materials (such as aluminum). Since the final prototype of PAS will be fabricated from a hard plastic which is not flexible, it was defined as solid-non-flexible material in the simulation software. The flow material was defined as air with 15 m/s velocity since air will be used for normal sampling. The 15 m/s air velocity was defined based on the bird's maximum speed in order to study the PAS behaviour in the worst condition.

#### Meshing:

This step is the most important part of the simulation setting procedure since all CFD equations will be calculated based on the designated mesh. In the first step of the mesh generation, a 2D mesh will be generated on all surfaces. The size of the meshes that set in this step will affect the number of iterations during simulation. It was tried to keep

the same size for all designs in order to have the same simulation conditions. Then, these 2D mesh should be converted to 3D mesh which is called volume mesh. In our case, tetra angel non-structural mesh was defined as volume mesh type because of its easiness generation with a 1.2 exponential ratio. This ratio is related to mesh growing. This means that on important surfaces where high accuracy is needed, the mesh size will be as its default value (which will be determined by the user) and as soon as the meshes starts to draw farther from the important surfaces, they grow by designated ratio. This increase of the mesh size for certain areas will reduce simulation time.

Since the fluid flowing on the PAS surfaces is the most important parameter of the simulation, the prism mesh was defined only on object surfaces. In this case the mesh was defined as structural mesh with 1.2 exponential ratio since it gives more accurate results compared with the tetra angle mesh.

Boundary condition:

The objective of these settings is to simulate the environmental conditions that will affect the PAS during real testing. Since the PAS will be tested during summer while it is mounted on a bird, the air velocity is defined as 15 m/s. This speed is estimated to be equal to the bird's maximum speed. The temperature was defined as 25 °C and pressure was defined as being same as air pressure at sea level.

In what follows, various designs will be presented based on different ideas. CFD simulation will be done on each design in order to study the fluid flow and also calculating the drag force energy. These drag values will then use for PAS comparison and selection procedures. There will be a discussion about PAS selection and the way that the final PAS were selected.

## 2.1 Design 1

### 2.1.1 Pattern 1

The first pattern is based on birds forward flying direction. In this design it was considered that having one wide air inlet can help to intake more air into the PAS and this can be increased when the bird is flying. In this case, the PAS is designed with walls as thin as 5 mm. One inlet and one outlet are considered with a size of  $23 \times 3$  mm for both of them (Figure 2.1). The device whole size is  $27 \times 27 \times 5$  mm.

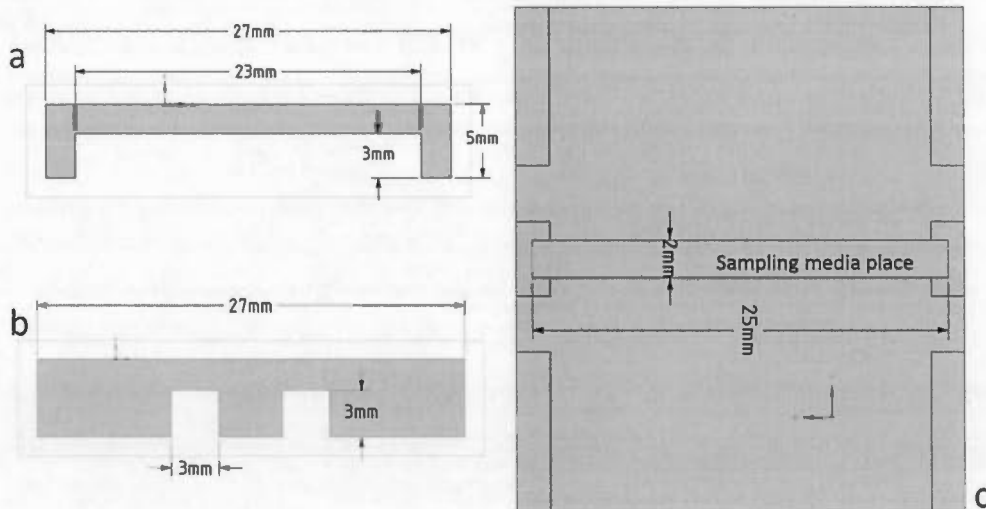


**Figure 2.1 : PAS first concept design. (a) Front view with only one wide channel as the inlet and outlet. (b) Side view with two pressure-break holes, before and after the sampling media. (c) Bottom view, the sampling media is placed in the middle of the PAS and can be exposed with air in 2 directions**

Two exit holes are considered for this design. They are situated on each side of the PAS in order to reduce the air pressure applied to the sampling media when the bird is flying or when there is a strong wind. Those holes are shown in figures 2.1 b, 2.2 a and 2.2 b.

The sampling media is positioned right in the middle of the PAS. This media has a width of 2 mm and there is a 25 mm length where the air can directly expose the sampling media (Figure 2.1 c, 2.2 a).

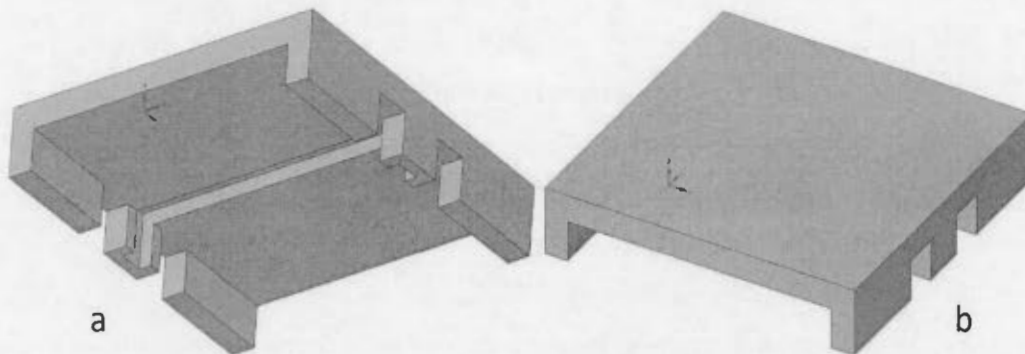


Figure 2.2 : 3D view of design 1. (a) 3D bottom view. (b) Top view

### 2.1.2 Design 1 simulation

Simulation of the first design pattern was done from its generated mesh (Figure 2.3). CFD simulation will be done on each one of the tetra angels meshed (obvious as green three angles) and this means that the fluid will flow inside these green areas. The rest empty parts are the PAS's body and there is no fluid that flows inside them as it can be seen on simulation results provided by ANSYS. When the simulation is done, a velocity vector will be provided instead of each tetra angel mesh. Each velocity vector would have direction which depends on object geometry. The results are provided as 3D views but, they should be shown on a plane for better analysis. There might be several different fluid velocity vector shown in each result output. These velocities are indicated as a legend on the right side of the output result with different colours, so it would be easy to find the fluid velocity in all parts of the design. These procedures are fixed for all designs and the only thing that might be different is results plane. Choosing



which results plane is better for studying and deep investigation depends on object geometry.

Simulation results on the first pattern shows the air circulation and its effects on the PAS. In figure 2.4, the empty spaces are related to designed geometry and only the fluid flow is visible. Each arrow (Vector) represents the fluid flow to that point. The fluid velocity is denoted by different colours according to the colour chart diagram. The lowest velocity is demonstrated by blue colour and the red colour is for the highest velocity. The lowest and highest velocity rang have been set in boundary condition. Also, the direction of vectors indicates the fluid flow direction after facing our geometry. As expected the sampling air entered into the PAS and it passed through it with the same velocity (Figure 2.4). This figure also shows that the sampling media in the middle of the PAS will directly exposed with the entered air. Due to the thin thickness of the PAS the air smoothly passed from outside of the PAS and there are no special air effects (vortex) around the PAS (Figure 2.5, 2.6).

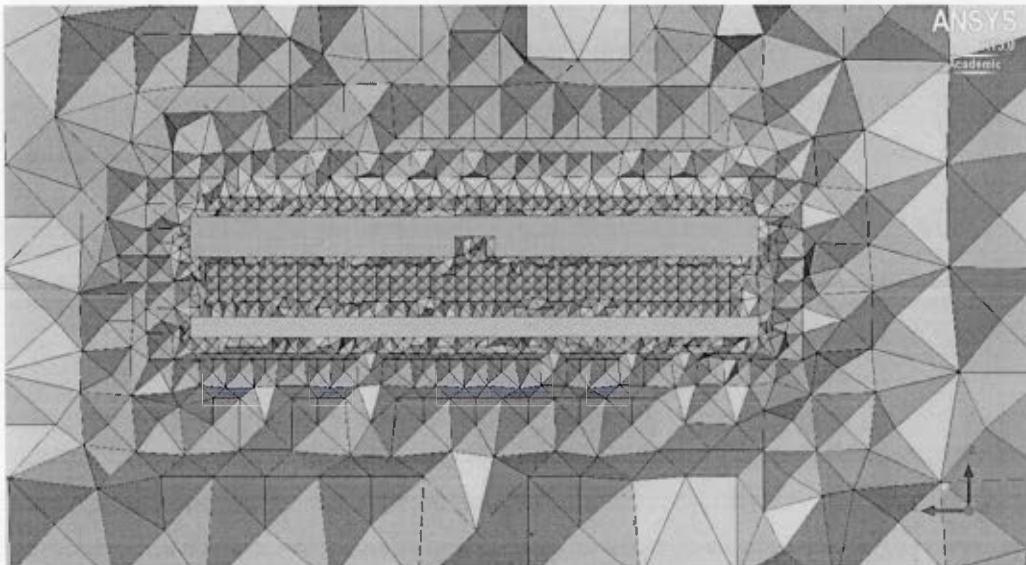
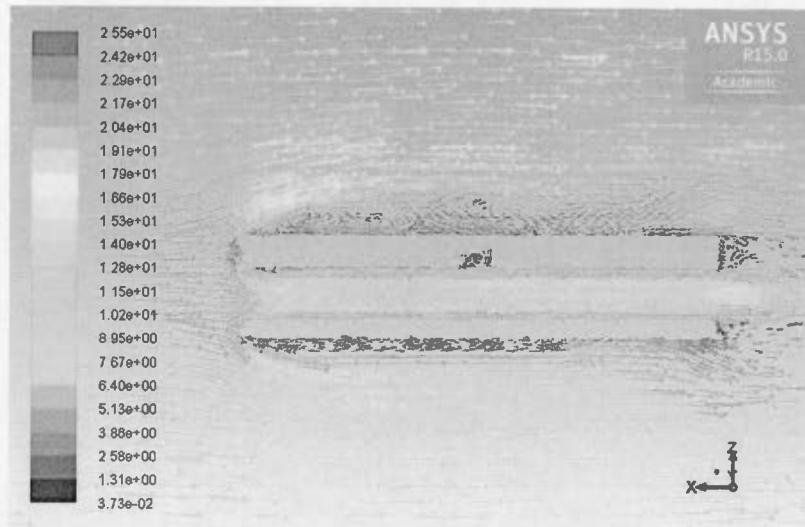


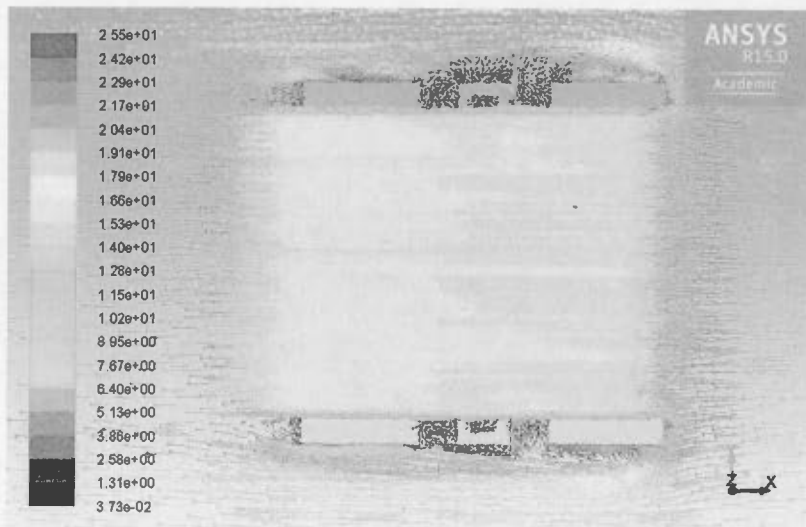
**Figure 2.3 : Volume Tetra angle non-structural mesh on design 1 – side view**



Velocity Vectors Colored By Velocity Magnitude (m/s)

Dec 29, 2015  
ANSYS Fluent 15.0 (3d, dp, pbns, lam)

**Figure 2.4 : Design 1 vectorial airflow result on PAS, side view, middle plane**



Velocity Vectors Colored By Velocity Magnitude (m/s)

Dec 29, 2015  
ANSYS Fluent 15.0 (3d, dp, pbns, lam)

**Figure 2.5 : Design 1 vectorial airflow result on PAS, top view**

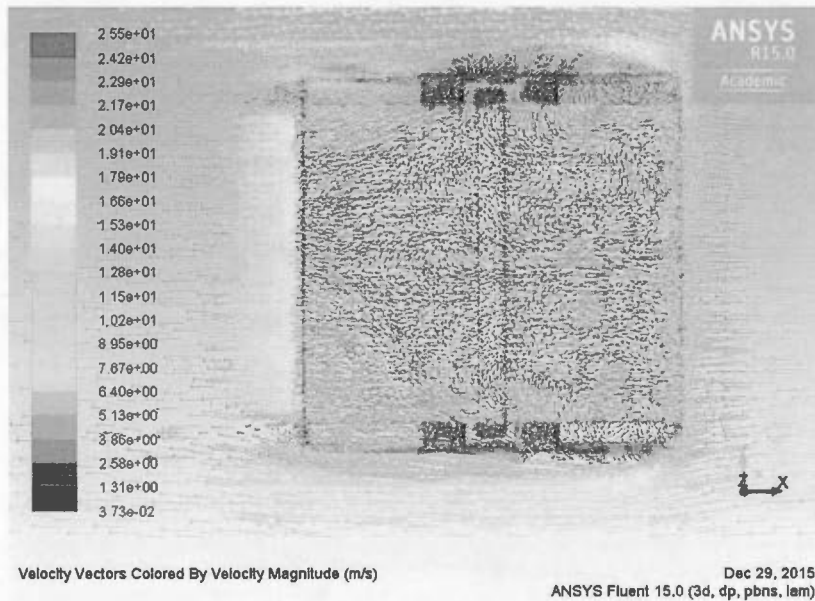


**Figure 2.6 : Design 1 vectorial airflow result, top view, PAS body included**

## 2.2 Design 2

### 2.2.1 Pattern 2

The second design (Figure 2.7) is similar to the first one except that it is narrower and also the inside design is changed in order to improve the aerodynamic shape of the design and prevent sampling media deformation from direct air exposure. The total size of the pattern is  $35 \times 16 \times 5$  mm, there is one inlet and one outlet for sampling air ( $8 \times 3$  mm) (Figure 2.7 a) and two sampling media can be placed inside the PAS with a  $15.5 \times 2$  mm dimension (Figure 2.7 c).

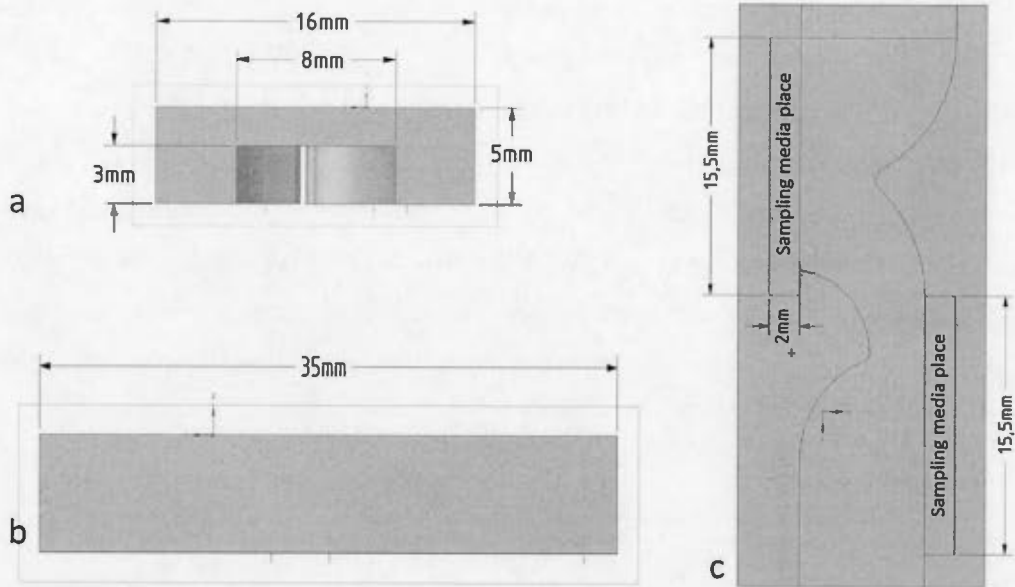


**Figure 2.7 : PAS second concept design. (a) Front view with one inlet and one outlet. (b) Side view. (c) Bottom view. The sampling mediums are places parallel to airflow direction while two curves are considered to deflect the air to the sampling media surface**

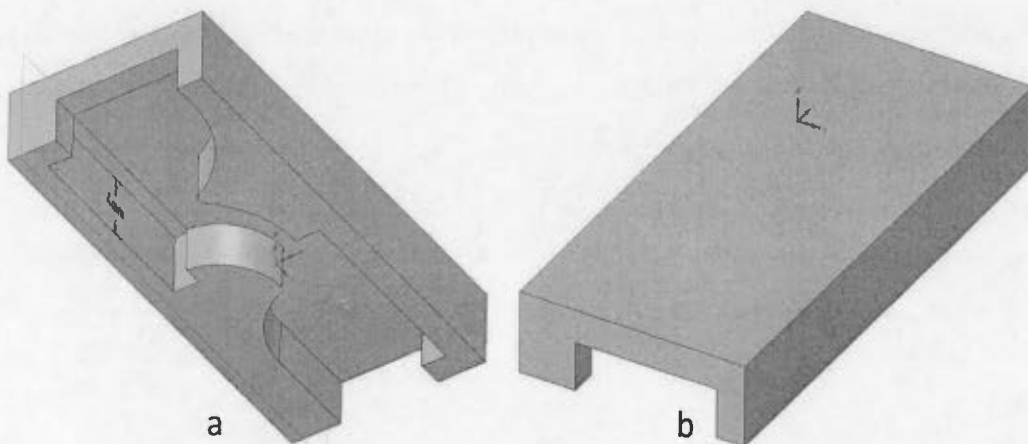


**Figure 2.8 : PAS second concept design 3D view. (a) Bottom view. (b) Top view**

The sampling mediums are positioned in the same direction as the wind flow. In this case, strong wind cannot deform them or bring them out when the bird is flying (Figure 2.7). In order to maximize air exposure to the media, the inlet channel is made narrower in the middle of the chamber using a smooth curve. These curves should have two effects. First, it tight the air exit channel and this should increase air velocity due to the larger entry (means more volume of air) and narrower exit which makes the air flow strong enough to impact to the second media. Secondly, this curve should distract the entered air to the first media in a way that it has the maximum impact to the sampling media surface (Figure 2.7, 2.8).

### 2.2.2 Design 2 simulation

CFD simulation of pattern 2, clearly shows the air circulation inside the PAS and its exposure to sampling media. It shows the reduction of the 15 m/s air velocity to approximately 4.5 m/s. The first sampling media is exposed by entering air which has the velocity of around 4.5 to 5 m/s (one third of the maximum speed). Then, the narrowed air path (due to the two implemented curve) accelerates the sampling air velocity to approximately 15 m/s (same as the outside wind speed). At this point, the sampling air velocity is high enough to expose to the second media and from there it can easily exit from the PAS (Figure 2.10).

Also, the 3D and overall views of simulation including the PAS body show that there is no special air vortex on the PAS outside body and the air smoothly passes through the PAS (Figure 2.11, 2.12).

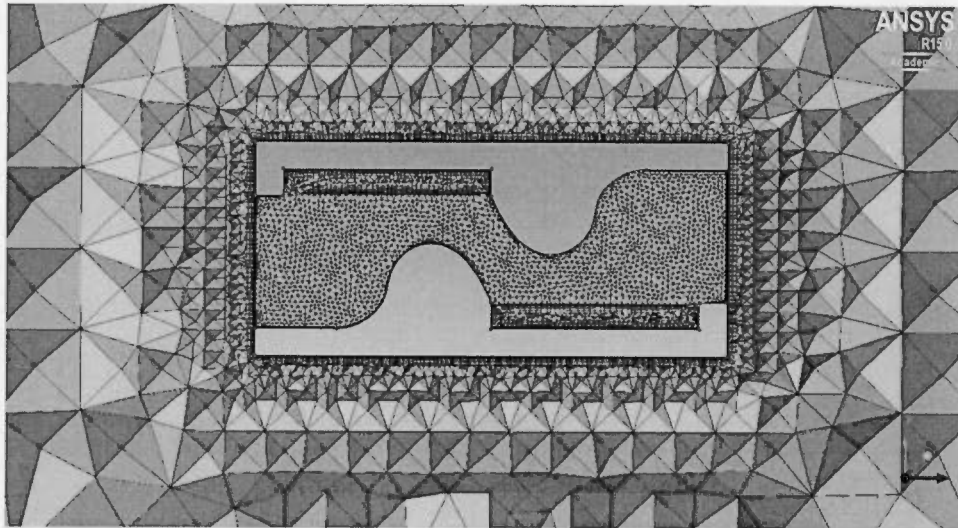
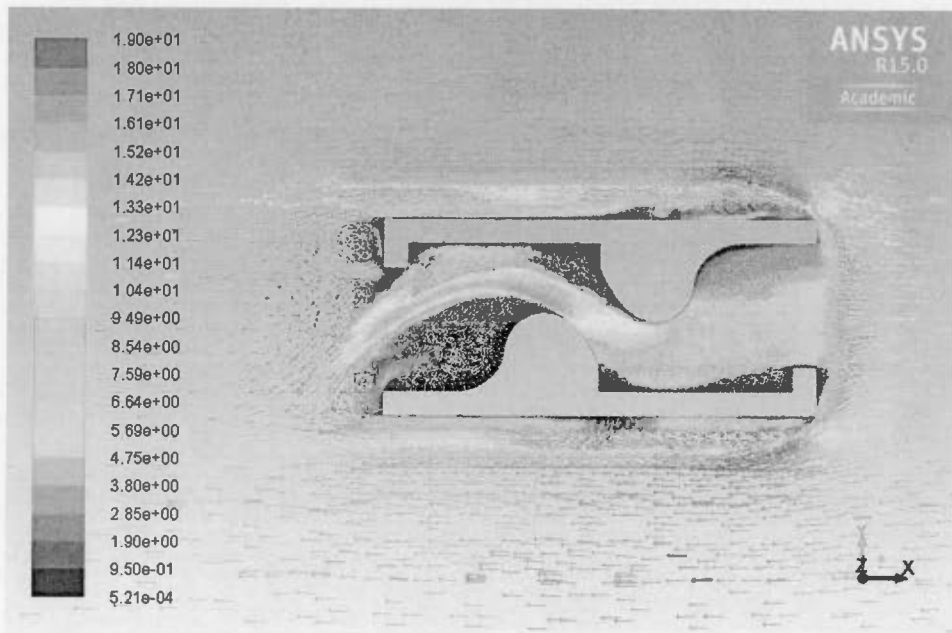


Figure 2.9 : Volume Tetra angle non-structural mesh on design 2, Top view



Velocity Vectors Colored By Velocity Magnitude (m/s)

Dec 29, 2015  
ANSYS Fluent 15.0 (3d, dp, pbns, lam)

Figure 2.10 : Design 2 vectorial airflow result, top view

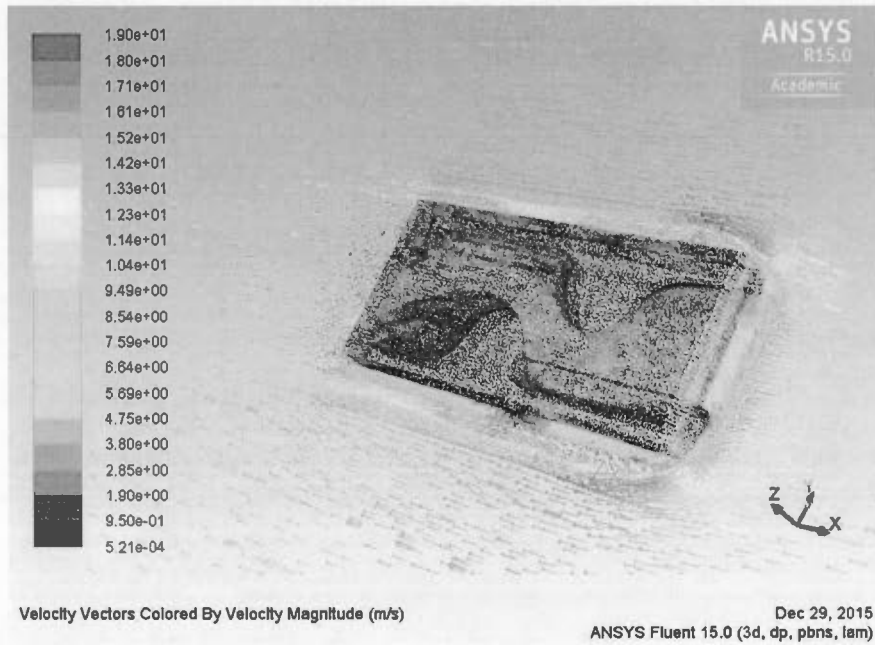


Figure 2.11 : Design 2 vectorial airflow result, 3D side view, PAS body included

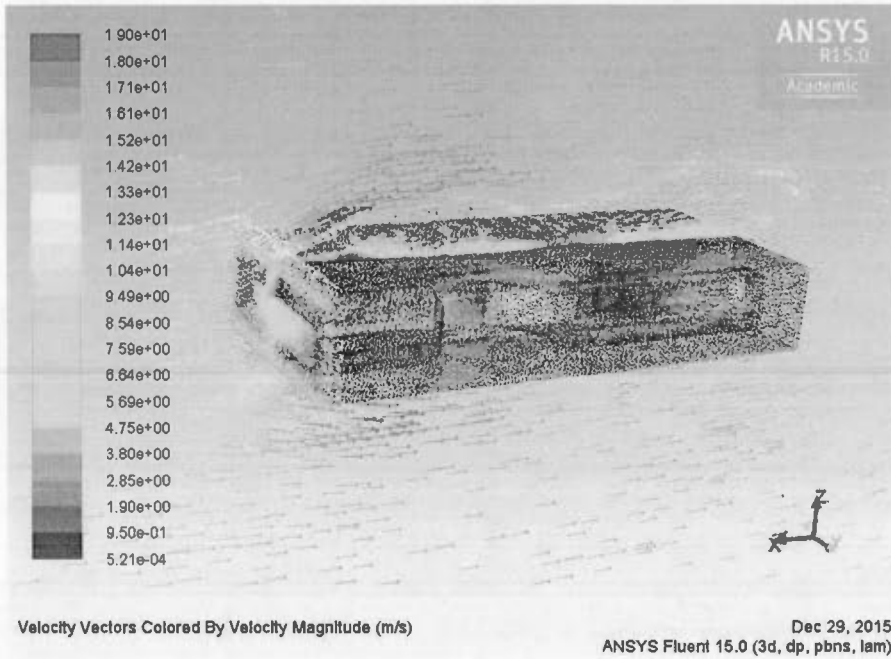


Figure 2.12 : Design 2 vectorial airflow result, 3D top view, PAS body included

## 2.3 Design 3

### 2.3.1 Pattern 3

As it was presented above, the first two patterns were designed with only one inlet and one outlet. This means that the sampling air can only enter from one direction and their maximum efficiency is during bird flying time.

In the third pattern design, it was tried to have more inlets and outlets from all sides of the PAS. In this case the sampling process would not depend on birds flying direction and sampling air could enter into the PAS from all direction (Figure 2.13). For this design, four holes were placed on top of the PAS in order to hold four sampling media with circular shape, 2 mm thickness and 4.5 mm diameter (Figure 2.13). In this case, the active surface area would be of  $3.5 \times 2$  mm.

To address these modifications, the PAS shape was changed to cube with dimensions of  $28 \times 28 \times 5$  mm. Two inlet-outlet channels were introduced on each side of the PAS. Each one can act as an inlet or outlet depending on wind direction. Each inlet is connected to another inlet which is placed on the right side of the first inlet. The combination of these two inlets makes a channel with one inlet and one outlet with 90 degree angle between them. In this way, the channel can be used in two directions (Figure 2.14).



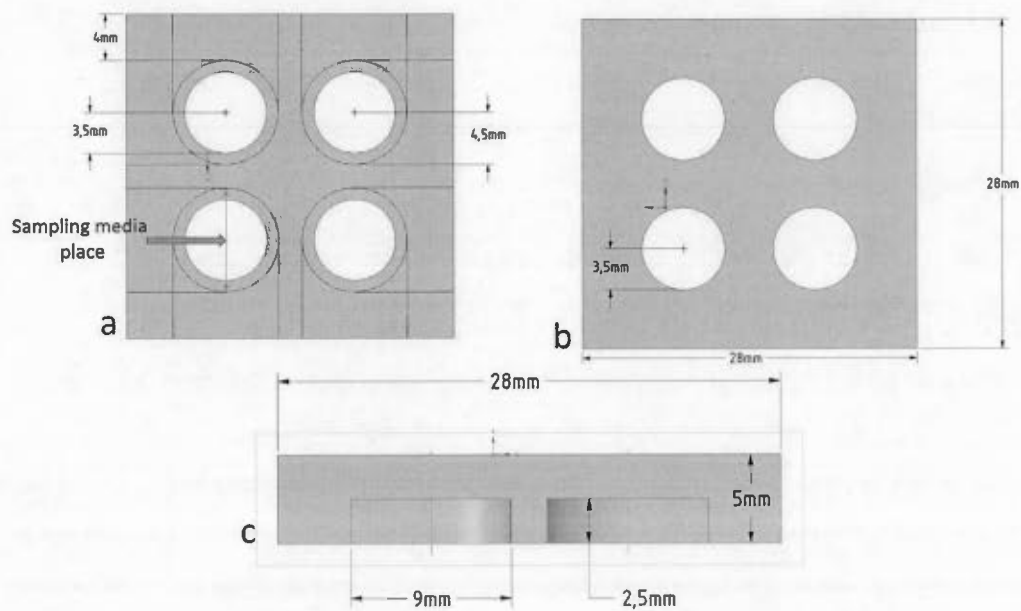


**Figure 2.13 : PAS third concept design. (a) Bottom view. (b) Top view. (c) Front view (which is same for all sides as it was designed symmetrically)**

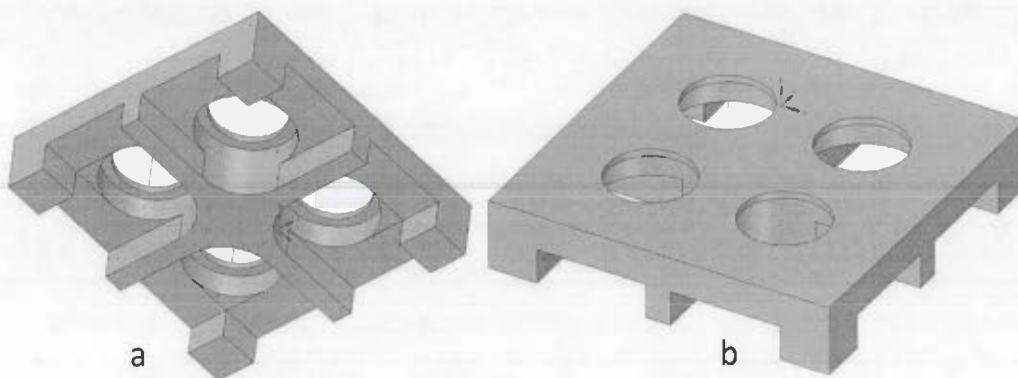


**Figure 2.14 : PAS third concept design 3D view. (a) Bottom view. (b) Top view**

### 2.3.2 Design 3 simulation

Airflow simulations on design 3 shows the effects of the entering sampling air on the two front holes. As it is shown on the figures 2.16 and 2.17, the air directly enter into the channels and due to the 90-degree turn, some of it directly exit passing through the sampling media hole due to the reflected flow and the rest come out through the channel (Figure 2.16, 2.17).

Moreover, simulation results show that a part of the sampling air that was come out through the channel and sampling media hole, enter into two back holes which was not expected during pattern design. This means that even with one direction airflow all sampling media will be exposed to the air to be sampled (Figure 2.17, 2.18).

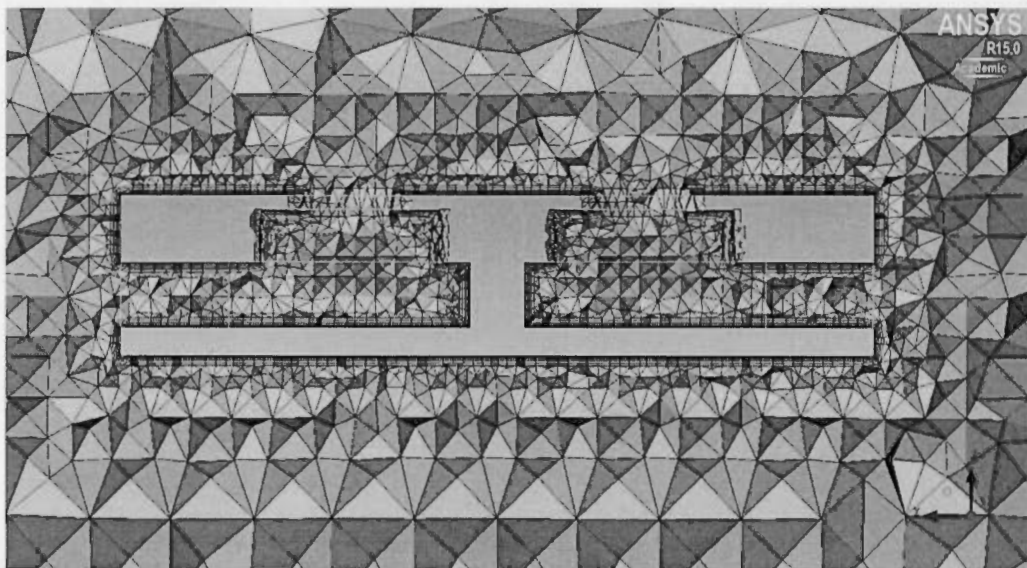


**Figure 2.15 : Volume Tetra angle non-structural mesh on design 3 – side view**

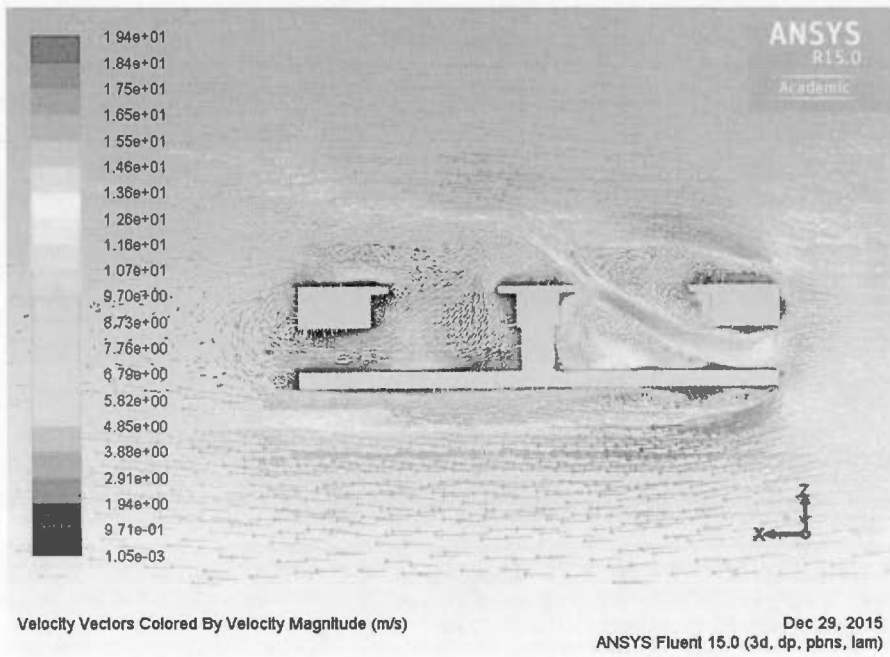


Figure 2.16 : Design 3 vectorial airflow result, side view

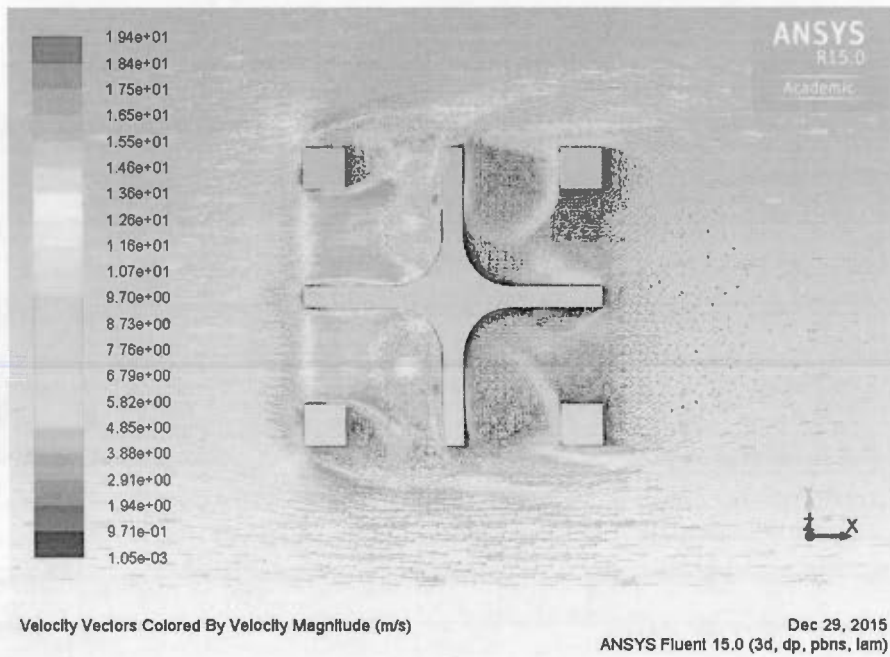
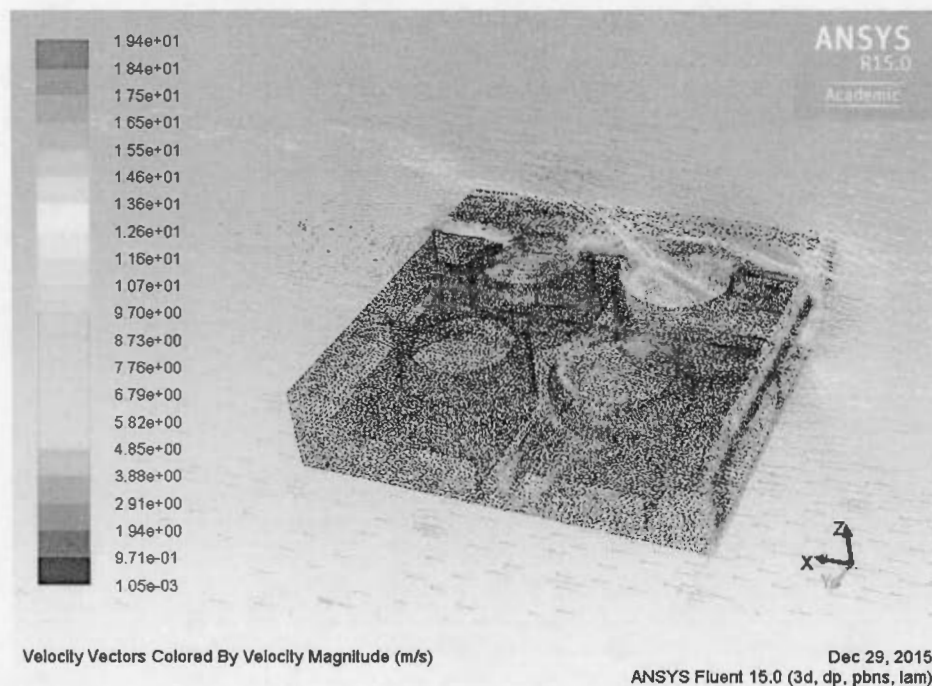


Figure 2.17 : Design 3 vectorial airflow result, top view



**Figure 2.18 : Design 3 vectorial airflow result, 3D view, PAS body included, result on Z plane**

## 2.4 Design 4

### 2.4.1 Pattern 4

From the results of the three previous designs, we evaluate that there were some points that could be improved. For example, due to the wide inlets, it is possible that water easily penetrate into the PAS. Also, in the third design it is possible that sampling media be moistened in rainy environments. Then, the fourth pattern was designed to reduce water penetration into the PAS and also to improve PAS aerodynamic shape.

The fourth pattern design consists of 2 separated parts, bottom part and top part. There is a trapezium placed in the middle of the bottom part (Figure 2.19 d) that holds the sampling media with the maximum thickness of 2 mm. At the front side of the bottom

part, there is a half-spherical curve (Figure 2.19 b) that: 1- intakes the sampling air, 2- prevents the water to come inside the PAS by increasing the thickness of the PAS entrance and 3- deflect the intake air to the sampling media surface. Also, two air exit channels were embedded in the back side of it (Figure 2.19 a, d).

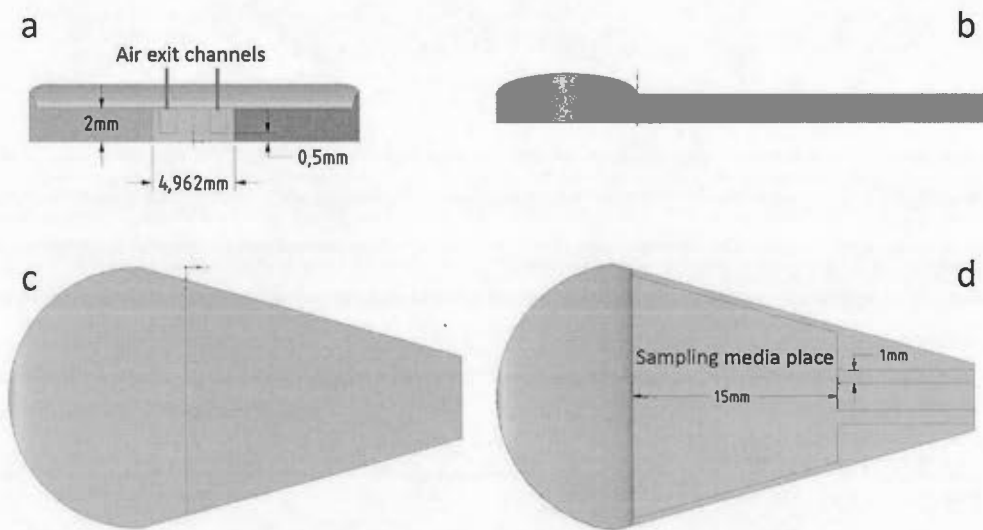


**Figure 2.19 : PAS fourth concept design bottom part. (a) Back view. (b) Side view. (c) Bottom view. (d) Top view**

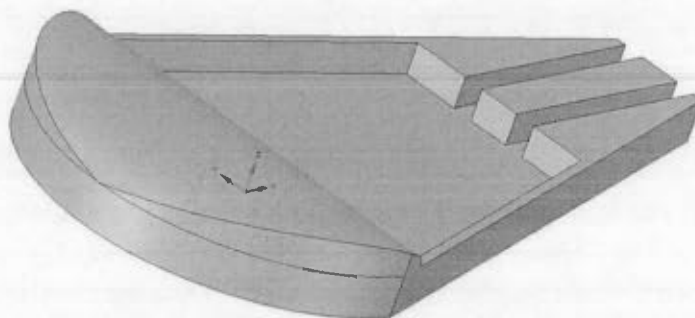


**Figure 2.20 : PAS fourth concept design 3D view**

The top part was designed as a chamber that: 1- covers the bottom part and sampling media, 2- with its rib style it could increase the aerodynamics of the PAS and 3- it increases the inside air pressure using the combination of its low slope from front to its back (Figure 2.21 b) and the narrow exit channels on the bottom part (Figure 2.19 a, d).

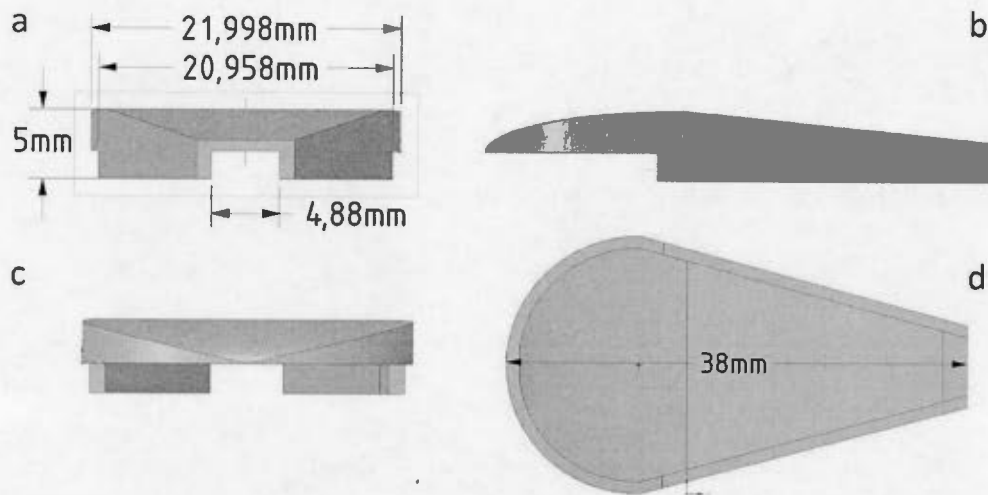


**Figure 2.21 : PAS fourth concept design top part. (a) Back view. (b) Side view. (c) Front view. (d) Bottom view**

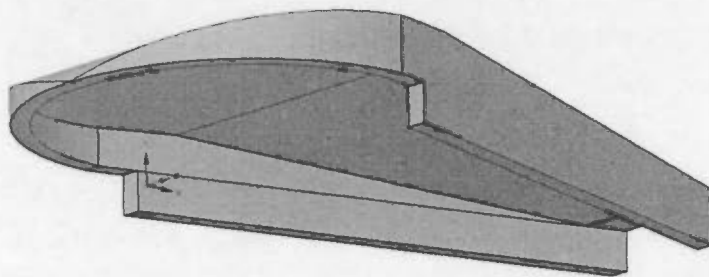


**Figure 2.22 : PAS fourth concept design top part 3D view**

After placing the sampling media inside the bottom part, the top part would be mounted on the bottom part and they will be glued together (Figure 2.23). The wide entrance, smooth slop and narrow exits holes, will increase the air pressure inside the chamber. More pressure means higher air penetration into the absorber and this can also increase the sampling rate of the PAS.

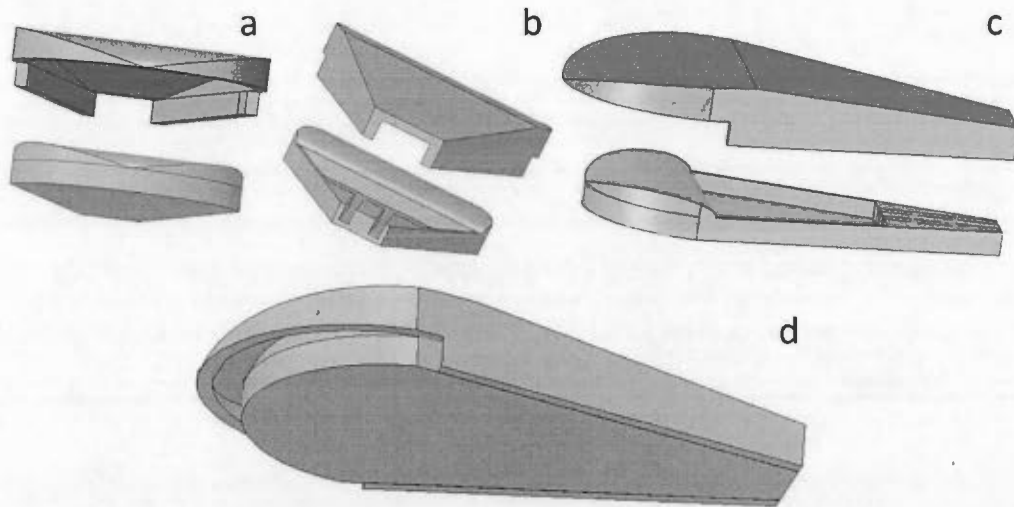


**Figure 2.23 : PAS fourth concept design parts positioning in 3D view. (a) Front view. (b) Back view. (c) Side view. (d) Complete and ready to work PAS**

#### 2.4.2 Design 4 simulation

As it was expected, the simulation results show that the designs 4 and 1 are more aerodynamic as compared with previous designs since it can smoothly rift through the front air without increasing the deflected air (part of the air that hit to the PAS body) velocity (Figure 2.25). As it is apparent in this simulation, the velocity of the deflected has approximately the same velocity as main sampling air (yellow vectors with 15 m/s speed) after hitting the PAS front side and this is due to the rib form of the PAS (Figure 2.26), there is no more velocity increment for the deflected air. The sampled air smoothly enters the PAS and after passing the small curve above the sampling media,

it moves down (Figure 2.25). This means that the entered air directly exposes the sampling media and then exits the PAS through the exit channels. Moreover, narrower exit channels cause velocity increment which means more pressure in the sampler chamber and this will increase the air exposure of the sampling media.

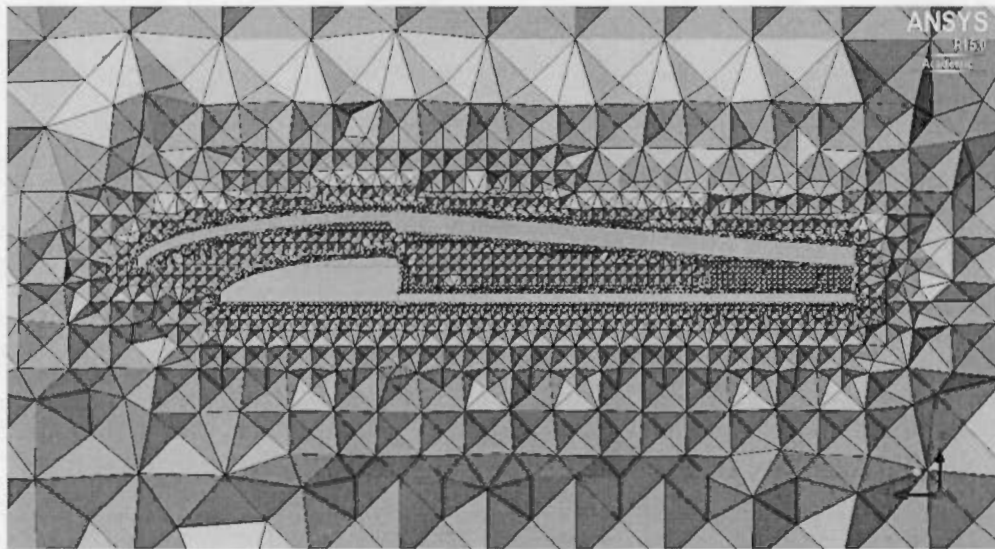


**Figure 2.24 : Volume Tetra angle non-structural mesh on design 4, side view**



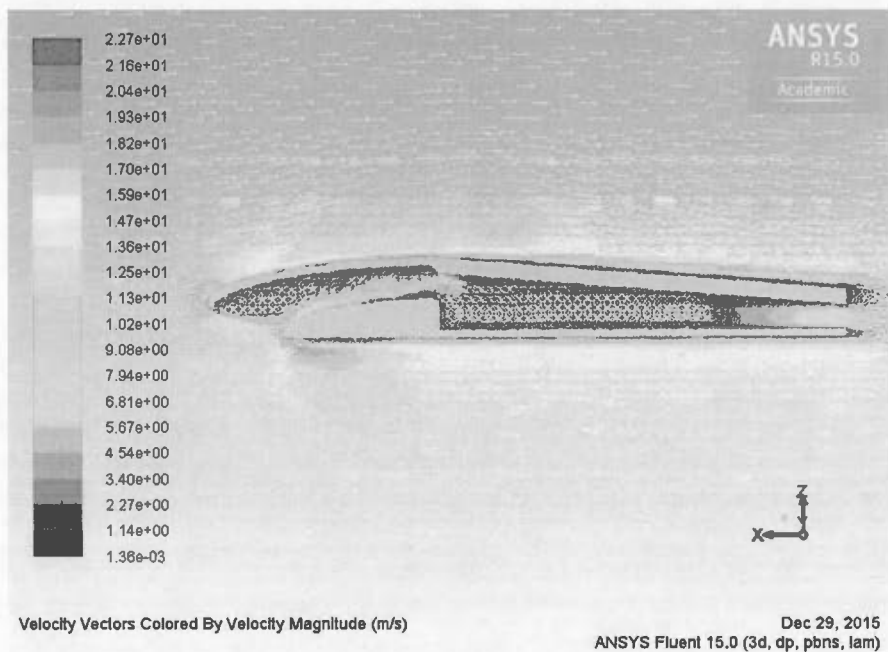


Figure 2.25 : Design 4 vectorial airflow result, side view

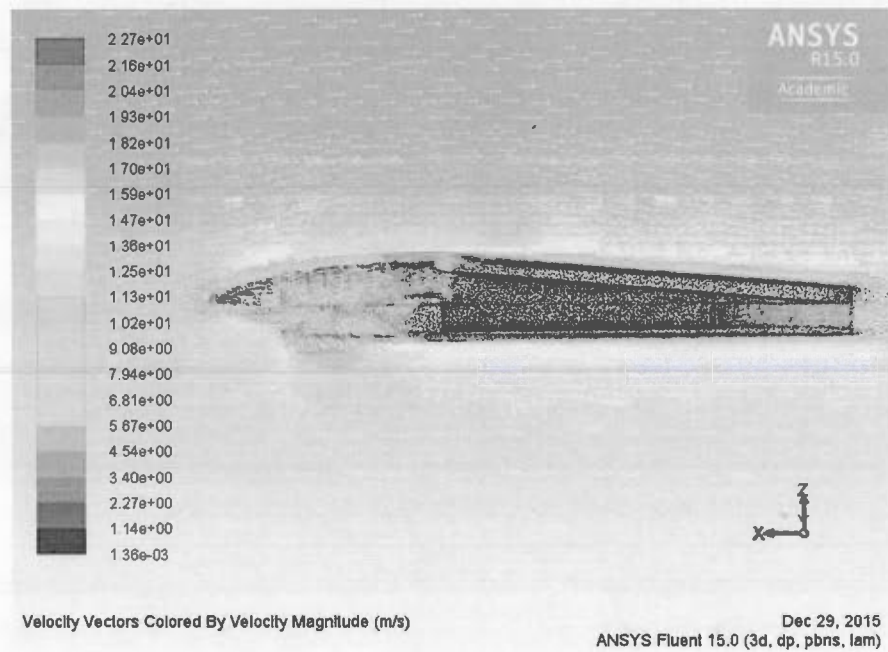
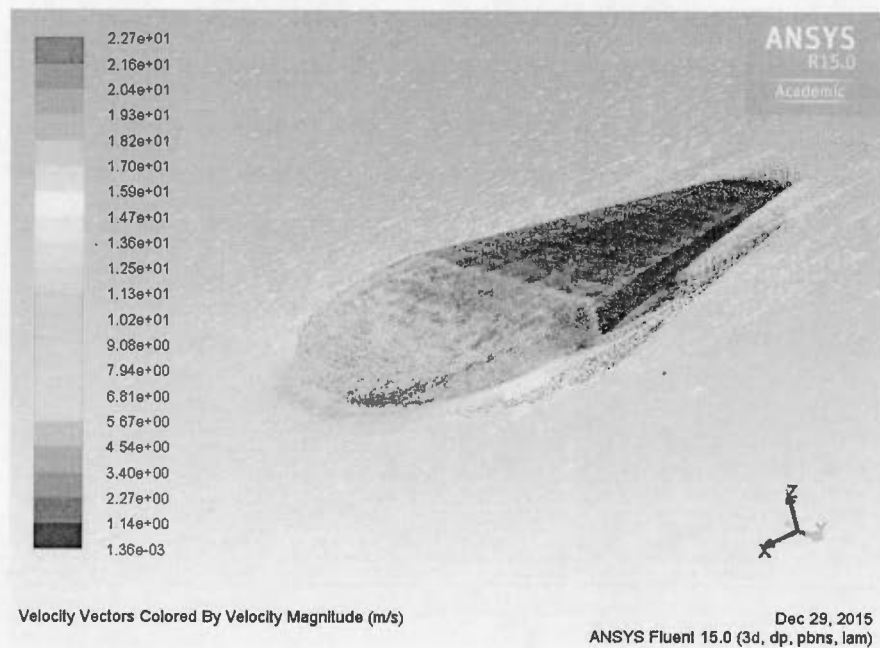


Figure 2.26 : Design 4 vectorial airflow result, 3D view, PAS body included



**Figure 2.27 : Design 4 vectorial airflow result, 3D view, PAS body included**

## 2.5 Design 5

### 2.5.1 Pattern 5

#### 2.5.1.1 Pattern 5-1

Pattern 5 was designed based on results from previous designs in order to have a PAS that will be able to: 1-intake as much air volume as possible from all directions, 2- be able to protect all the inside media from direct exposure to water and sun light, 3- have a unique sampling media with larger active surface area instead of several small surface media which helps us to have the same air exposure conditions on all sampling media for better analyzing, 4- be more aerodynamic and 5- protect sampling media from direct exposure to the high velocity air during bird flight.

In the fifth design, the PAS pattern was changed to a circular shape (Figure 2.28, 2.30). It consists of two separated parts like for design four. The sampling media would be placed at the center of the bottom part while 5 small (2 mm height) pins (Figure 2.28 a, 2.29) will support it and keep it high enough from the PAS floor for better air circulation. Four  $2.5 \times 4$  mm supports was considered to hold the top part. Under each one of them, a channel was devised as an air exit hole. 2 mm fillet was used to curve the inside wall of the PAS for better air circulation under the sampling media.

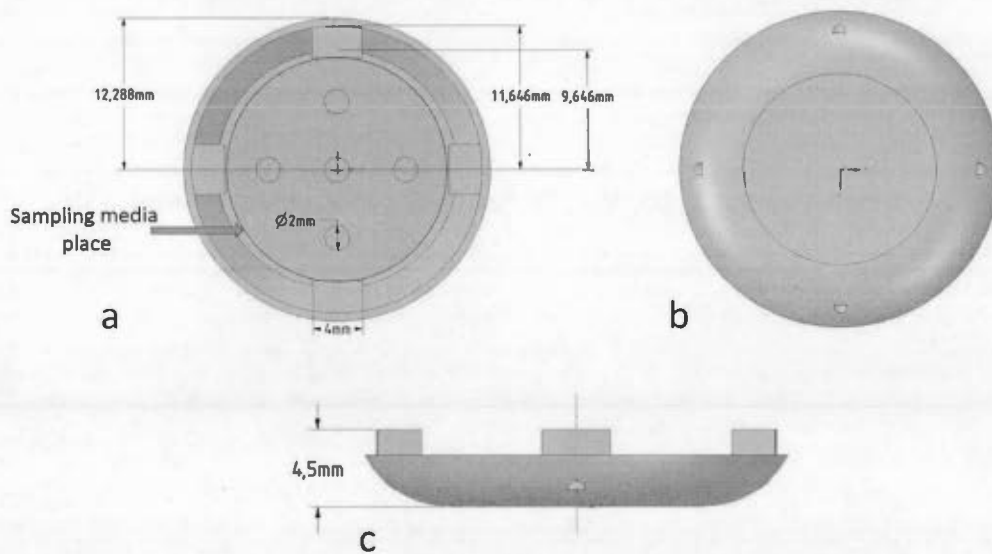
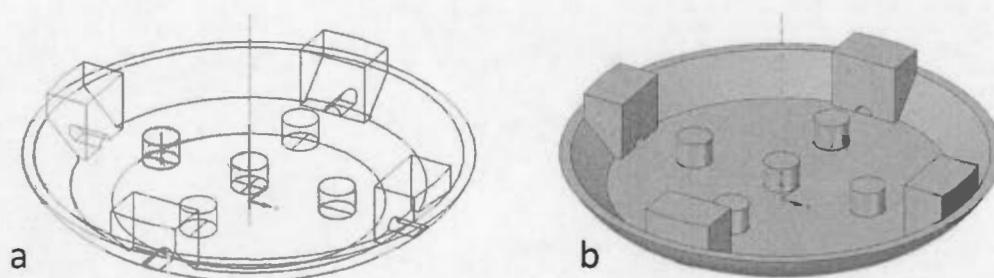


Figure 2.28 : PAS fifth (5-1) concept design bottom part. (a) Top view. (b) Bottom view. (c) Side view



**Figure 2.29 : PAS fifth (5-1) concept design bottom part 3D view. (a) Wired view. (b) Shaded view. Note that the wired view is only provided for better imagination**

The same shape was used to design the top part. The top part should be designed in such a way that it could be able to cover the bottom part and protect the inside media from high velocity air while letting some low velocity air be entered to the PAS.

In this case the diameter of the top part should be designed larger than the bottom part (Figure 2.30 a, 2.28 a). This will create some empty spaces between both parts that will act as an air entrance. In order to protect sampling media from high velocity air, the height of the four supports were kept inside the top part (Figure 2.31). This will bring the bottom part (in order to be glued together) insider to the top part and this makes some overlap between the two parts. To complete the PAS assembly, the bottom part must be glued to the four inside supports, located in the top part, using the HFR free glue (HFR: halogenated flame retardants) ensures that the sampling media is free from HFR contamination during the preparation process.

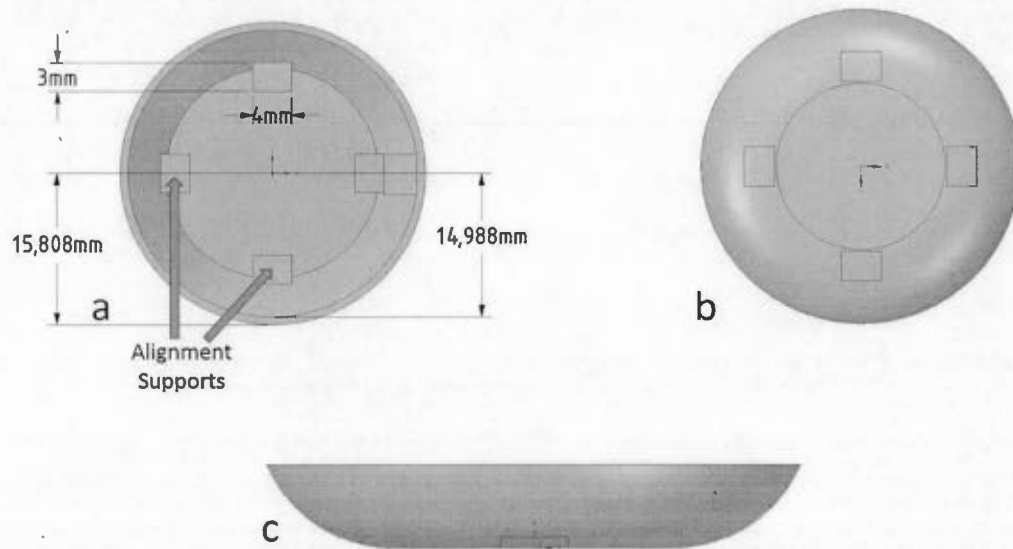


Figure 2.30 : PAS fifth (5-1) concept design top part. (a) Top view. (b) Bottom view. (c) Side view

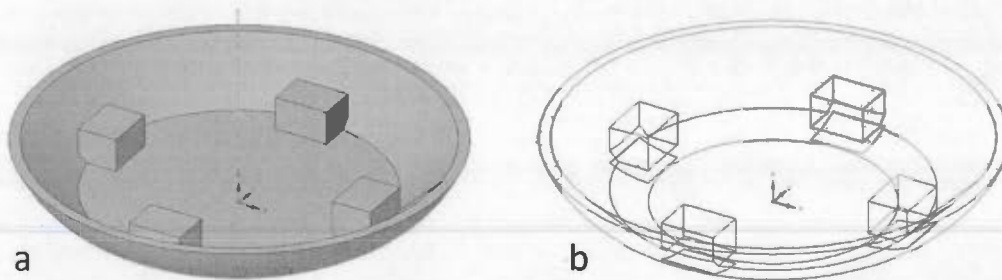
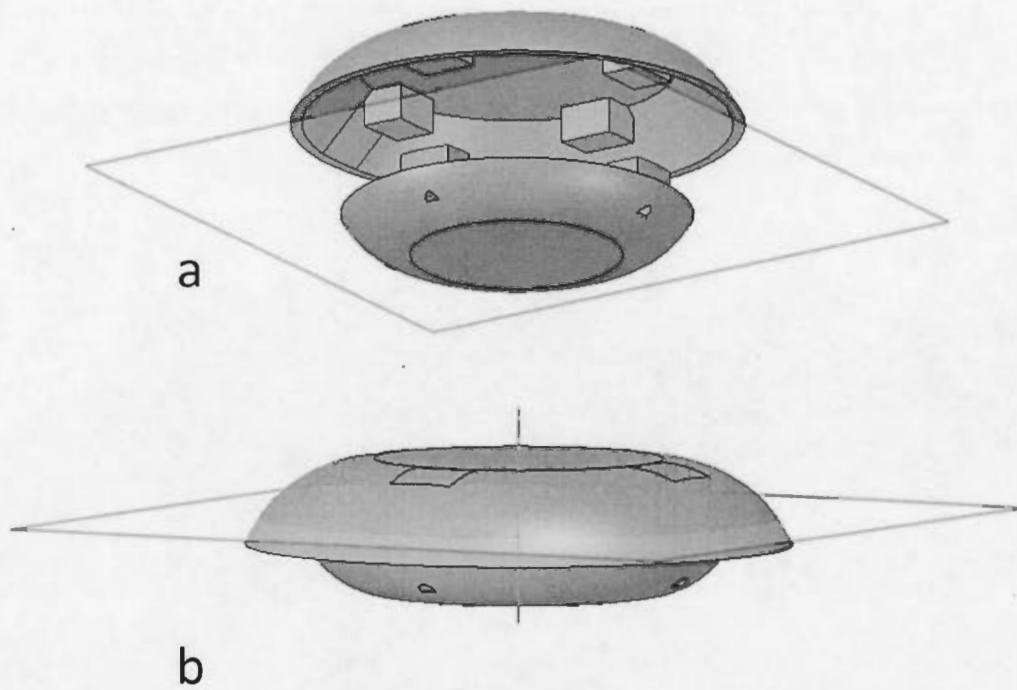


Figure 2.31 : PAS fifth concept design bottom part 3D view. (a) Shady view. (b) Wired view



**Figure 2.32 : PAS fifth concept design parts positioning in 3D view. (a) Overall view before gluing. (b) Complete and ready to work PAS**

#### 2.5.1.2 Pattern 5-2

While in design 5-1- the bottom-part fulfills most of the PAS requirements, still there could be some improvements. The ideas came from our collaborators in Biology department, and it was related to the bird's feathers.

The complete PAS should be glued on a plastic substrate in order to be mounted on the birds. However, due to its thin thickness, it is possible that bird feathers cover the PAS and prevent sampling air from entering into the PAS.

To solve the feather problem, the thickness of the bottom-part of the PAS 5-1 increased. This will make the PAS high enough to prevent feathers to cover it. Also, in order to

drive out the possible entered water into the PAS, four more water exit holes were added to the bottom part (Figure 2.33, 2.34) to reduce the possible effects of water on sampling media. After all those modifications, the final PAS becomes 8 mm thicker than the previous design (Figure 2.35).

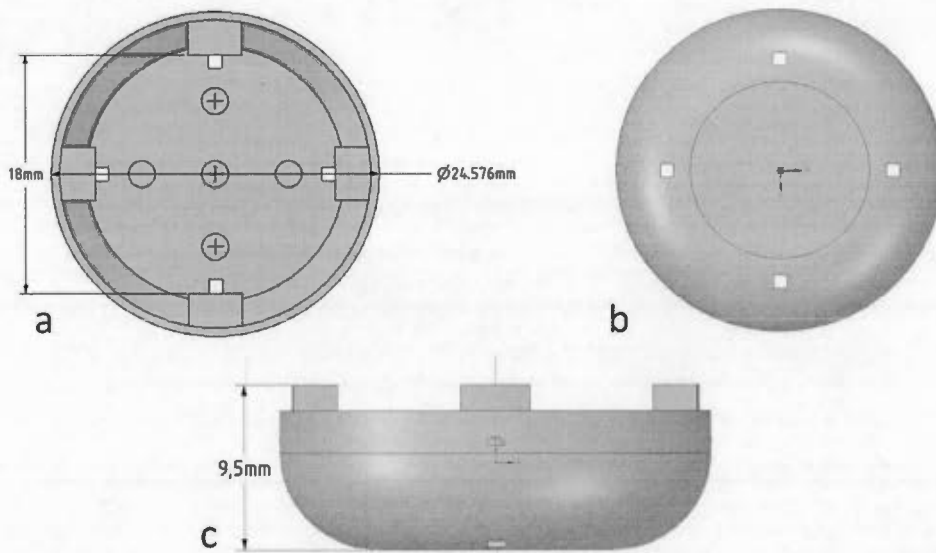


Figure 2.33 : PAS fifth (5-2) concept design bottom part. (a) Top view. (b) Bottom view. (c) Side view

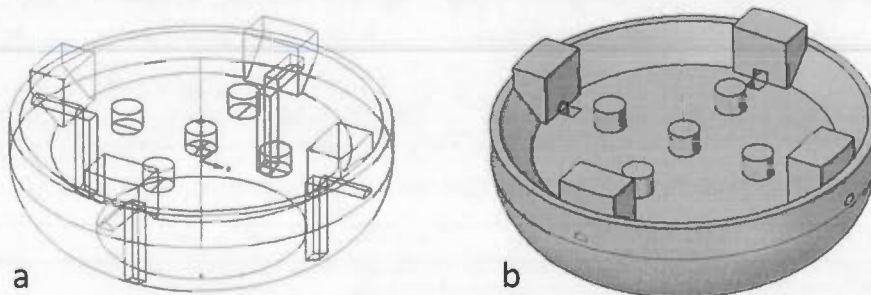
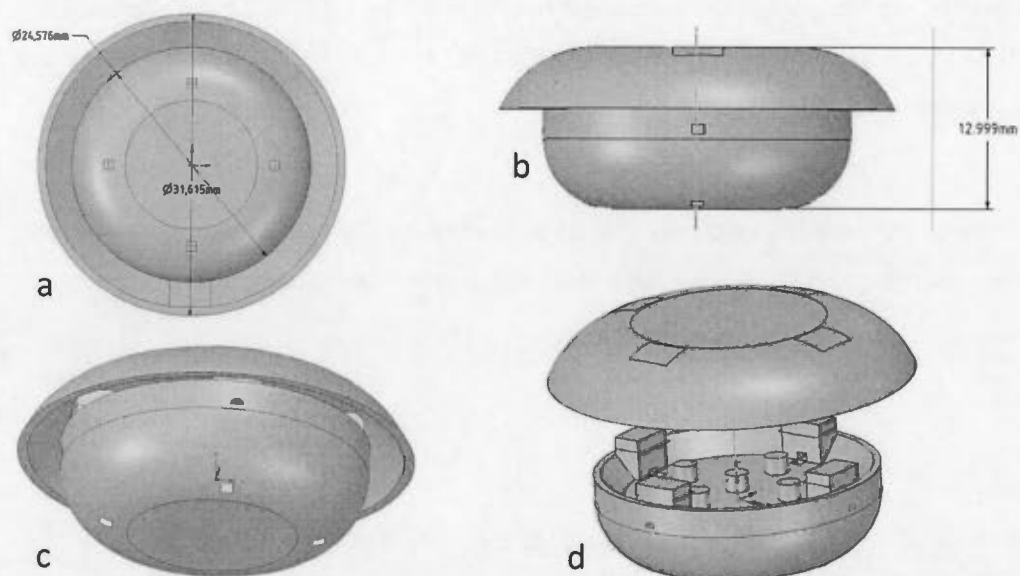


Figure 2.34 : PAS fifth (5-1) concept design bottom part 3D view. (a) Wired view. (b) Shady view



**Figure 2.35 : PAS fifth concept design parts positioning in 3D view. (a) Complete PAS bottom view, showing the air entrance gap between two parts. (b) Complete assembled PAS final thickness. (c) Complete PAS overall 3D view. (d) 3D positioning of bottom and top part for assembling**

### 2.5.2 Design 5 Simulation

Since the bottom part of the design 5-1 was not acceptable due to its thin thickness, only the design 5-2 was simulated. The results are shown in figures 2.37, 2.38. As it can be seen on the figures, the sampled air enters the PAS with a velocity around 13 m/s. After touching the top part (Figure 2.38), it reaches a smooth circulation inside the PAS with a velocity ranging between 1 and 5 m/s (Figure 2.38, 2.39). Then, it comes out from the PAS through the exit holes situated around and at the bottom of the device. Also, we can see on figure 2.37 that the front exit hole generates small turbulence under the sampling media. This effect should be avoided. As figure 2.37 shows, there is an



air turbulence where the two parts are connected due to the impact of the air into the blocked space. This might cause parts separation in high air velocity conditions. Moreover, the velocity of the air around the PAS is increased to 20 m/s after impacts to the top and bottom of the PAS while the air impacting the left and right sides of the PAS has approximately the same velocity (Figure 2.38, 2.39).

Based on simulations results some modifications should be made on this PAS design in order to decrease the velocity of air entering the PAS, to reduce the turbulent effects on the front support, to remove the air turbulence under the sampling media due to the front exit holes and to prevent air velocity acceleration.

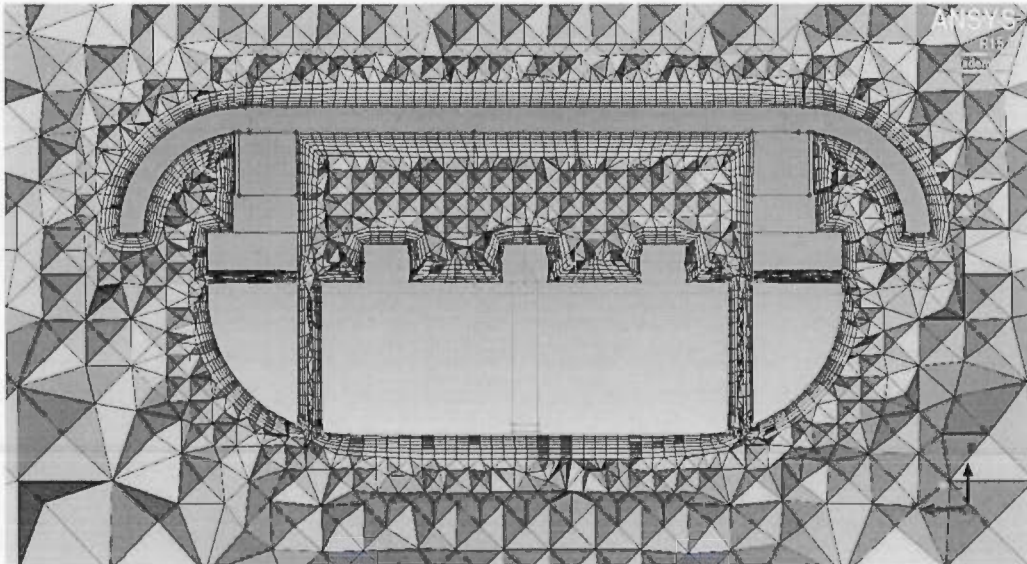
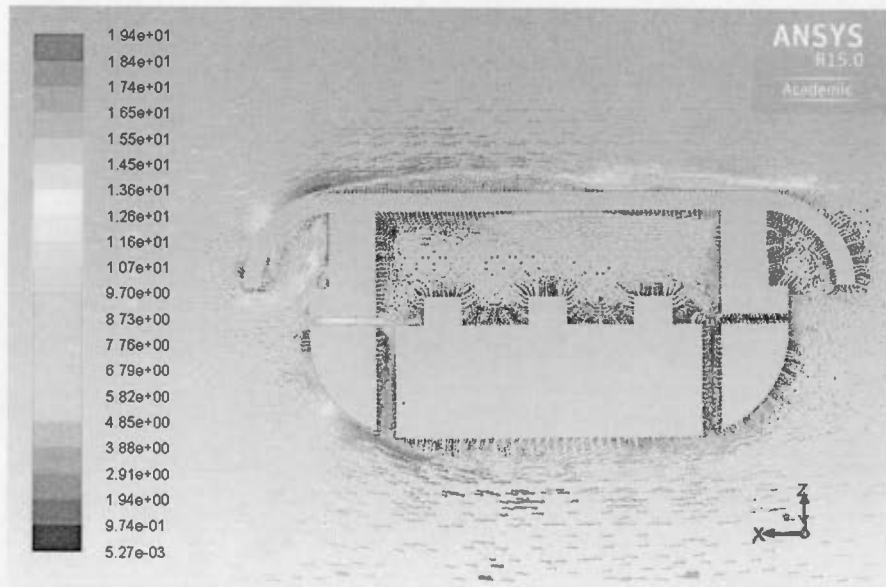


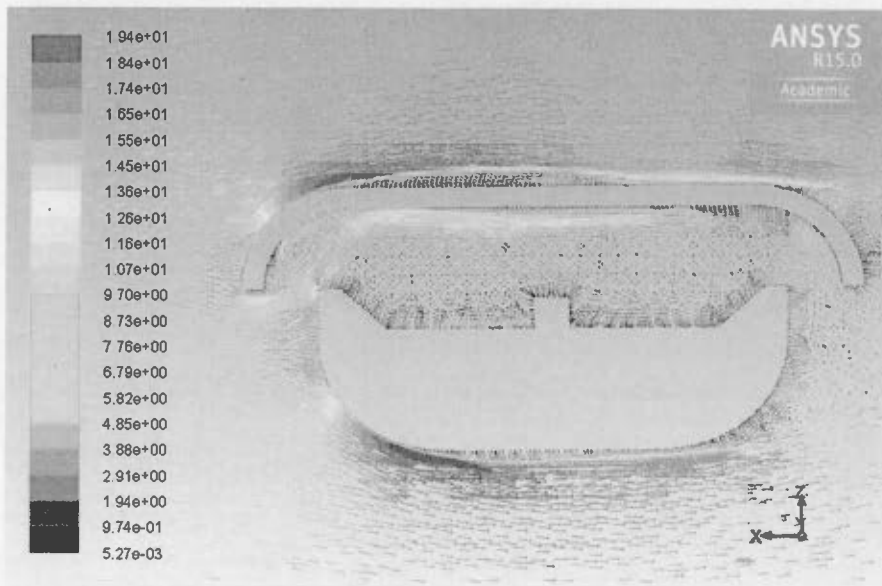
**Figure 2.36 : Volume Tetra angle non-structural mesh on design 5, side view**



Velocity Vectors Colored By Velocity Magnitude (m/s)

Dec 29, 2015  
ANSYS Fluent 15.0 (3d, dp, pbns, lam)

**Figure 2.37 : Design 5 vectorial airflow result, side view, supports included**



Velocity Vectors Colored By Velocity Magnitude (m/s)

Dec 29, 2015  
ANSYS Fluent 15.0 (3d, dp, pbns, lam)

**Figure 2.38 : Design 5 vectorial airflow result, side view, gap included**

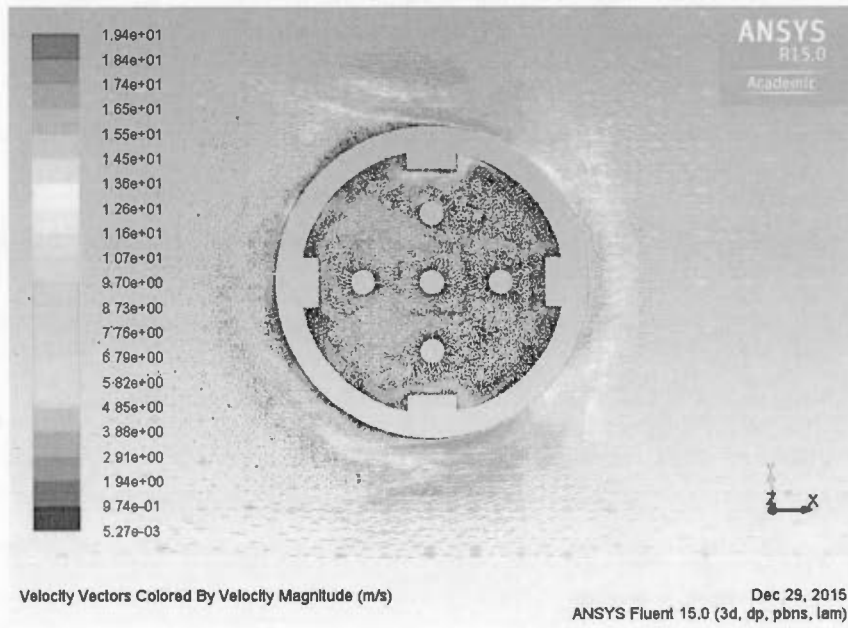


**Figure 2.39 : Design 5 vectorial airflow result, top view, results on Z plane in the middle of the PAS**

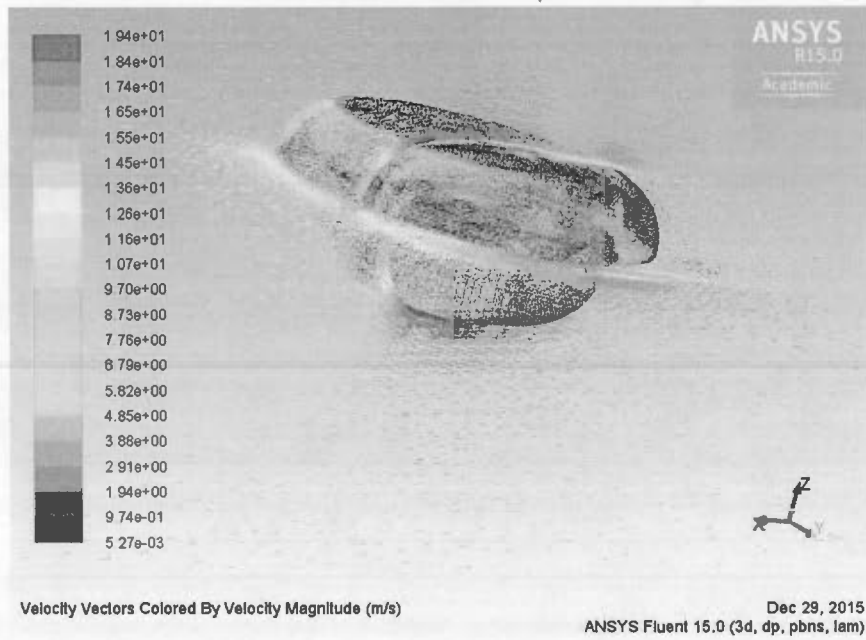


**Figure 2.40 : Design 5 vectorial airflow result, 3D view, PAS body included, results on Y and Z plane**

## 2.6 Design 6

### 2.6.1 Pattern 6

Even though design 5 covered most of the PAS requirements, still there could be some improvements that could be implemented based on simulation results. According to simulation results, the entering air hits the top part of the device with approximately the same velocity as before entering. If this velocity could be reduced, that could be used as an advantage to increase the active surface area of sampling media. This would increase the sampling rate of the PAS and could help for better analyzing. Also, a new suggestion came from our collaborators about an option for better PAS mounting that might be considered. Instead of gluing the complete PAS on a substrate for installation on birds, it could be more efficient to modify design 5 in a way that the device could be tightened around the bird by using some Teflon ribbon instead of gluing it to another substrate.

To address the new requirements, several modifications were done on design 5. The maximum size of all previous designs was based on bird's physiology constraints reported by our colleagues from the biology department. This means that the maximum width of the PAS could not be more than 30 mm. Then pattern 5 was designed to have the same size in all directions. However, after scrutinizing the pattern 5 and based on bird's physiology, it was determined by biologists that the maximum size could be increased to 45 mm but only along the bird's body. To implement the new suggestion, the circular shape of the design 5 was changed to an elliptic shape (Figure 2.41). This new shape was chosen in a way that it should reduce the velocity of the deflected air around the PAS body. This modification of shape could also lead to an increase of the active surface of the sampling media. Additionally, the thickness of the top part was increased to 2 mm which allows putting a second sampling media in the top part of the device with the same size as the sampling media in the bottom part. This additional

layer of sampling media could double the active surface area of the sampling media (Figure 2.43). Moreover, in order to reduce the velocity of the entering air, the top part was modified in such a way that it be able to cover 1 mm of the bottom part from where they have to be connected together (Figure 2.45 C, D). It was done by reducing the height of the supports (those which use to align and connect top part to bottom part) and this leads the bottom part to come more inside the top part to have contact with it for assembling process.

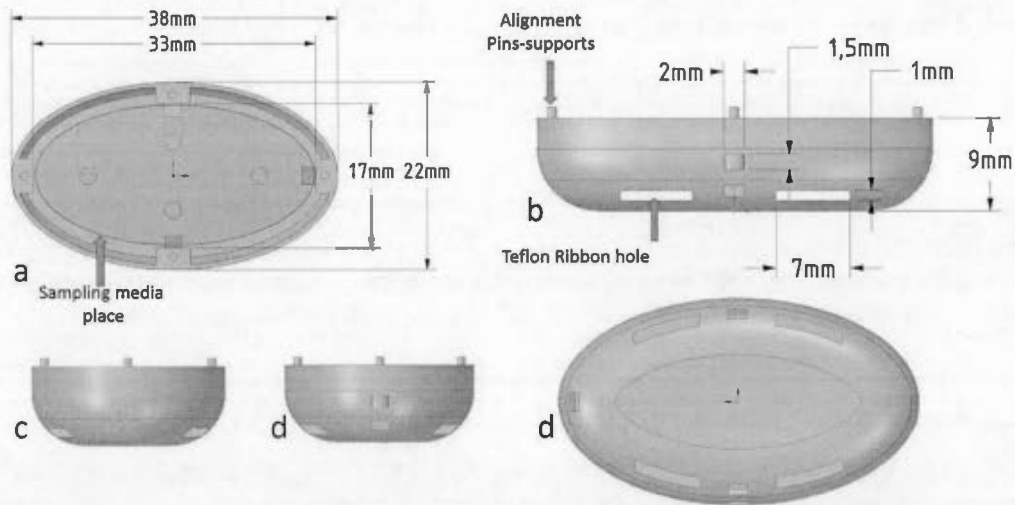


**Figure 2.41 : PAS sixth concept design bottom part. (a) Top view. (b) Side view. (c) Front view. (d) Back view. (e) Bottom view**

Four pins and holes (Figure 2.42, 2.44) (1 mm height and 0.5 mm diameter) with the same coordinates were considered on the bottom and top part's supports. In order to stick top part to bottom part the pins must be inserted into their related holes. In this case both parts would be glued exactly where they should without needing to use a high accuracy mounting alignment system.

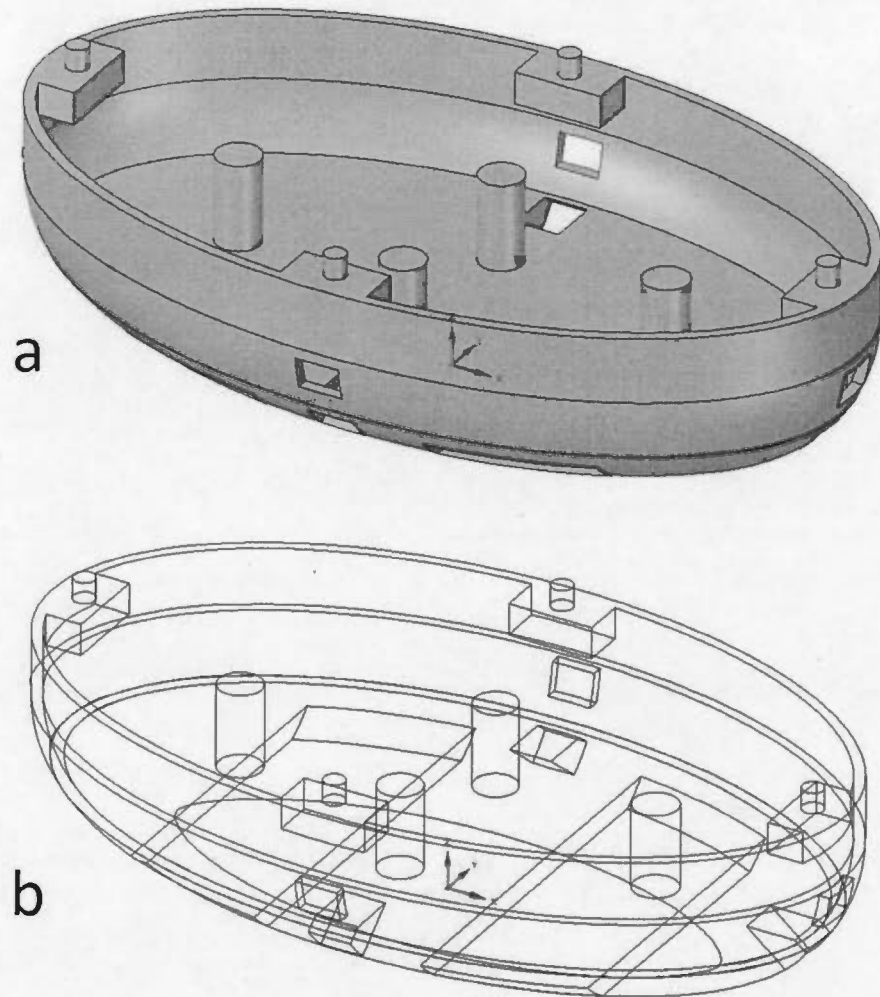


Figure 2.42 : PAS sixth concept design bottom part 3D view. (a) Shady view. (b) Wired view

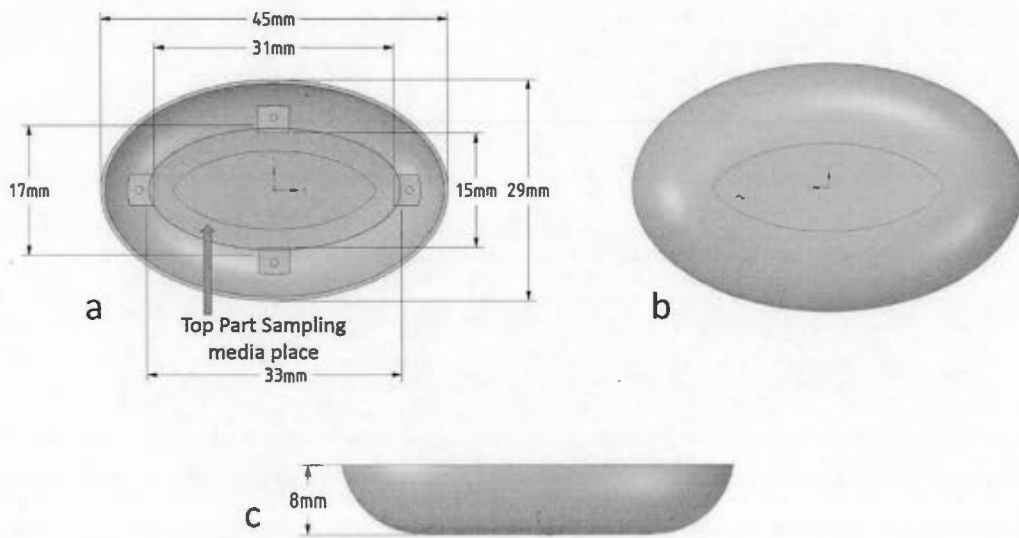


Figure 2.43 : PAS sixth concept design top part. (a) Top view. (b) Bottom view. (c) Side view

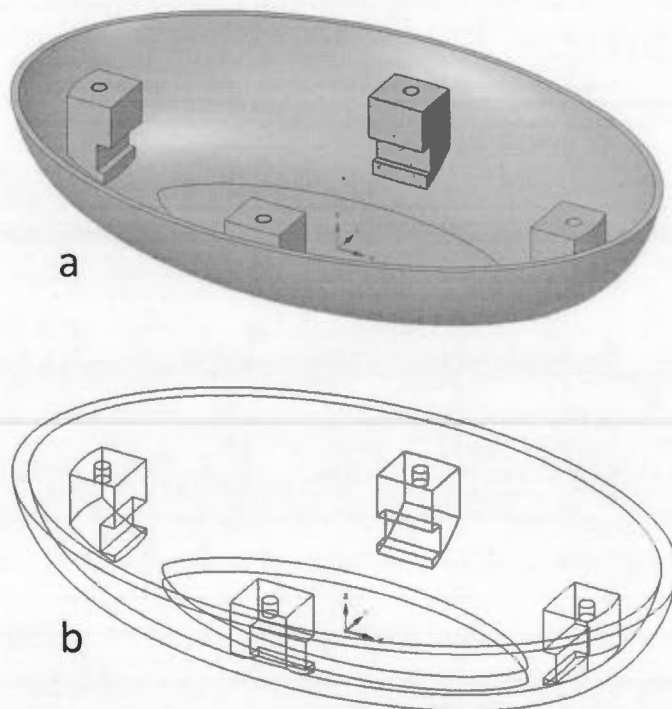
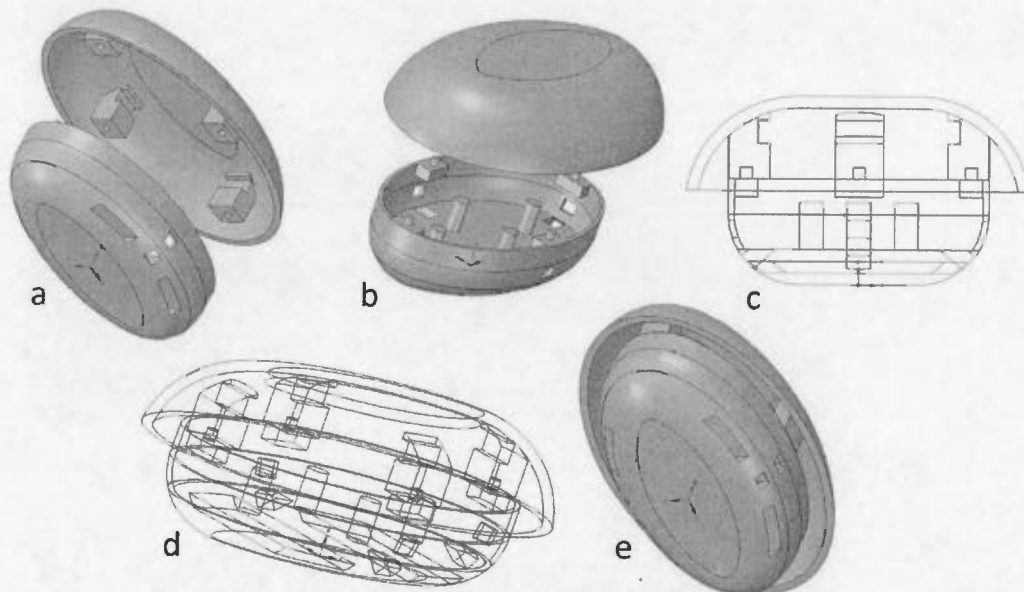


Figure 2.44 : PAS sixth concept design top part 3D view. (a) Shady view. (b) Wired view

As the thickness of the bottom part was increased to avoid feathers covering the PAS, some unused structure was created. These spaces were used to implement two separated channels on the bottom of the PAS. These channels could be used to mount the PAS on the back of birds using Teflon ribbons.

Additionally, the size of the air exit holes was increased to allow for a better air circulation. Also, the front air exit hole was removed to prevent the entering of high velocity air into the PAS (Figure 2.41 b) which will cause some turbulence under the sampling media.

Finally, three water exit holes were implanted close to the air exit holes with a 30-degree slope for better water evacuation. Their size was also increased to prevent channels being blocked with probable sand found on bird's environment (Figure 2.41 b).



**Figure 2.45 : PAS sixth concept design parts positioning in 3D view. (a) Front view (inside top - positioned). (b) Front view (inside bottom - positioned). (c) front-back wired views (parts assembled). (d) Wired 3D view (parts assembled). (e) Overall view (parts assembled)**



### 2.6.2 Design 6 simulation

The simulation of the final modified PAS (design 6) shows the advantages of all modifications that were done on design 5. The velocity of the entered sampling air is reduced to approximately 6 m/s on the top part and to around 2 m/s on bottom part (Figure 2.46, 2.47). In this case new sampling media has the great position on top part since the sampling air can directly pass through it and then make another circulation through the first sampling media on the bottom part. By removing the front exit hole, no turbulence observed under the PAS sampling media. Also, increasing the size of the exit holes leads to a better air circulation inside the PAS (Figure 2.49, 2.47). Moreover, the new PAS's shape decreases the velocity of deflected air from most parts of the PAS as compared with what was observed for design 5 (Figure 2.50, 2.51). This means that a better aerodynamic form was achieved.

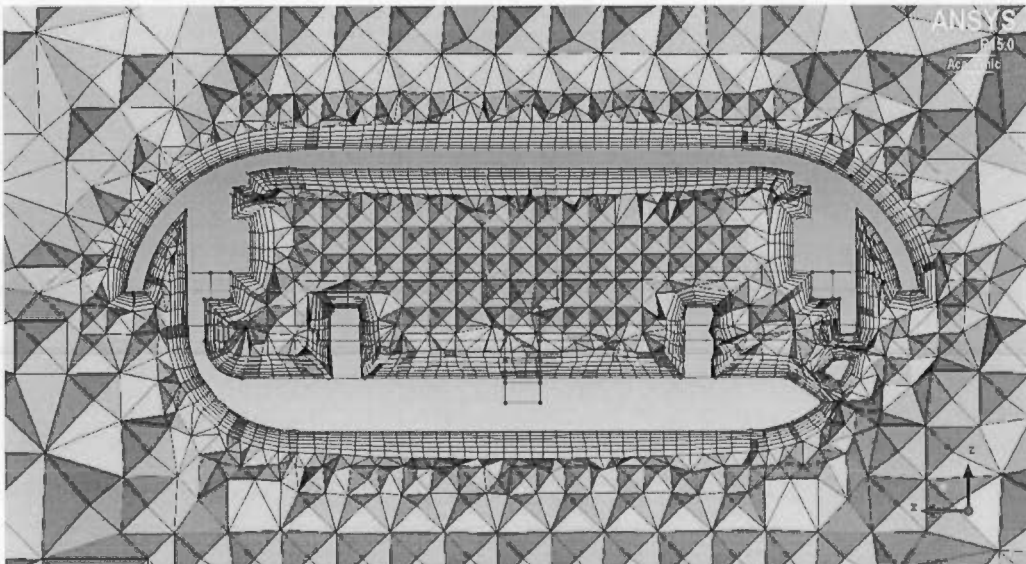
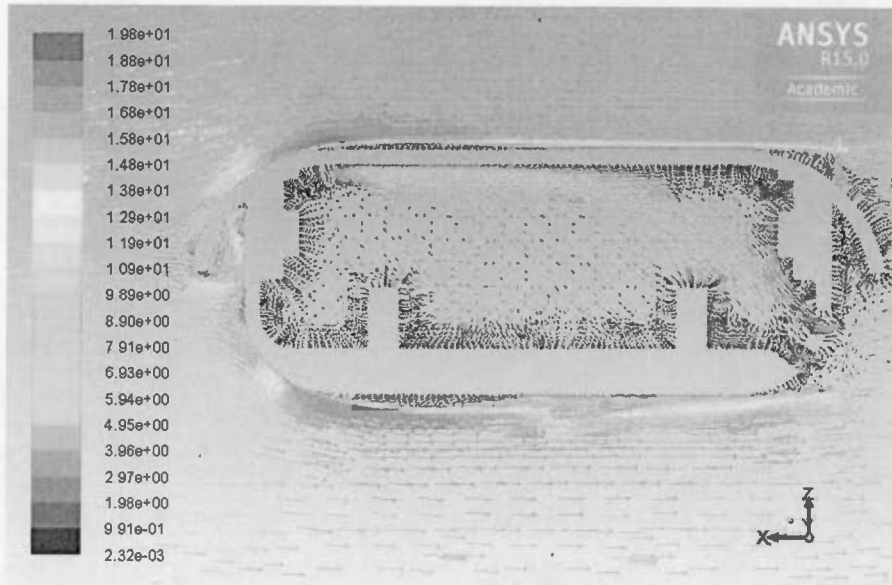


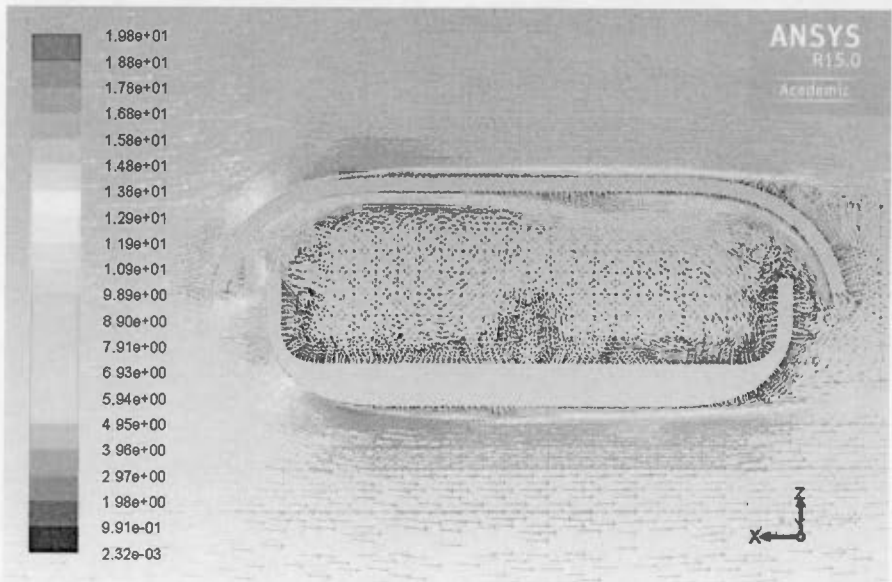
**Figure 2.46 : Volume Tetra angle non-structural mesh on design 6, side view**



Velocity Vectors Colored By Velocity Magnitude (m/s)

Dec 29, 2015  
ANSYS Fluent 15.0 (3d, dp, pbns, lam)

**Figure 2.47 : Design 6 vectorial airflow result, side view, supports included**



Velocity Vectors Colored By Velocity Magnitude (m/s)

Dec 29, 2015  
ANSYS Fluent 15.0 (3d, dp, pbns, lam)

**Figure 2.48 : Design 6 vectorial airflow result, side view, gap included**

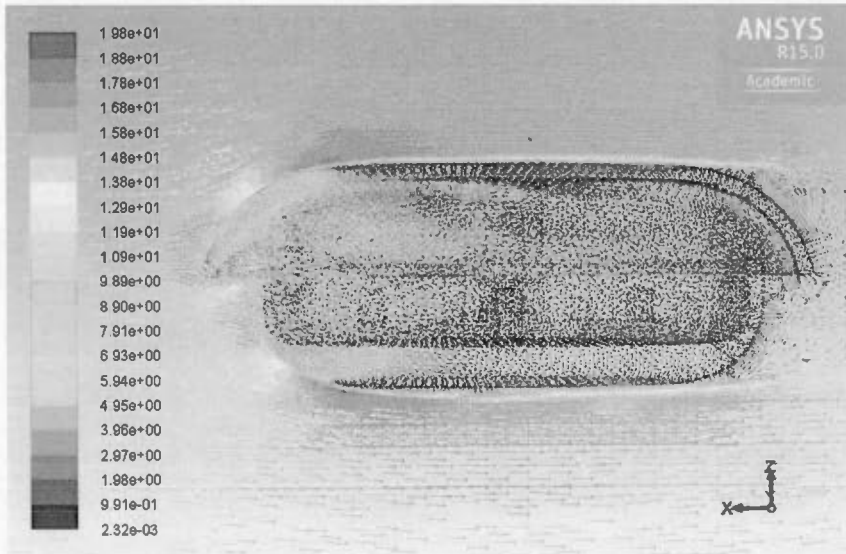


**Figure 2.49 : Design 6 vectorial airflow result, 3D side view**

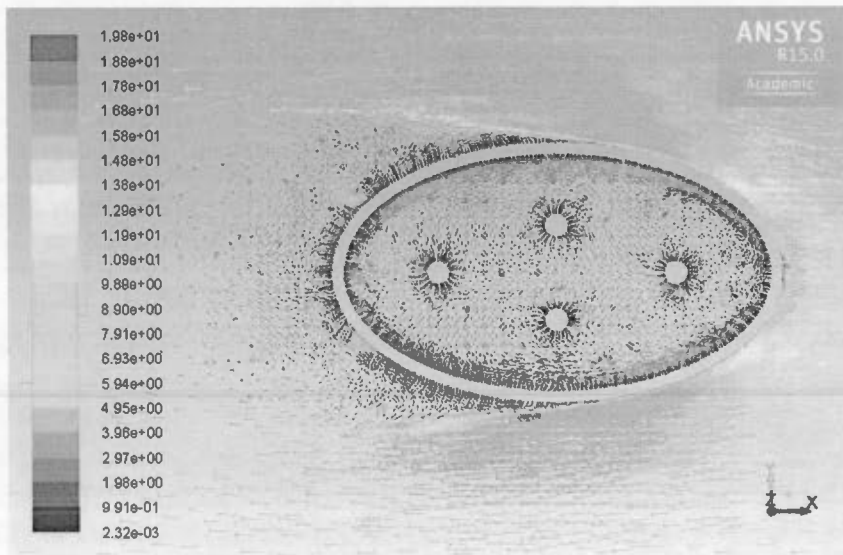


**Figure 2.50 : Design 6 vectorial airflow result, top view, results on Z plane in the middle of the PAS, bottom part**

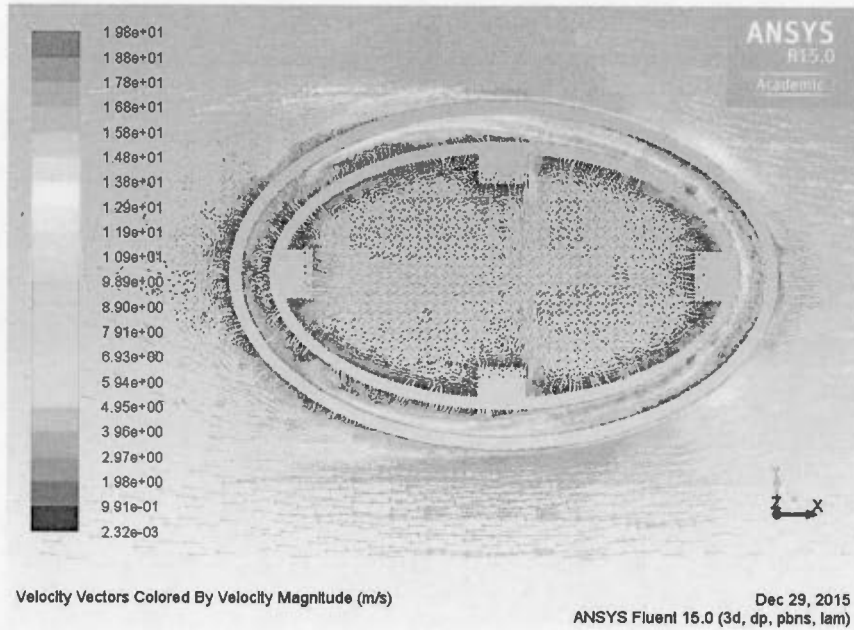


**Figure 2.51 : Design 6 vectorial airflow result, top view, results on Z plane in the middle of the PAS, overlap position**

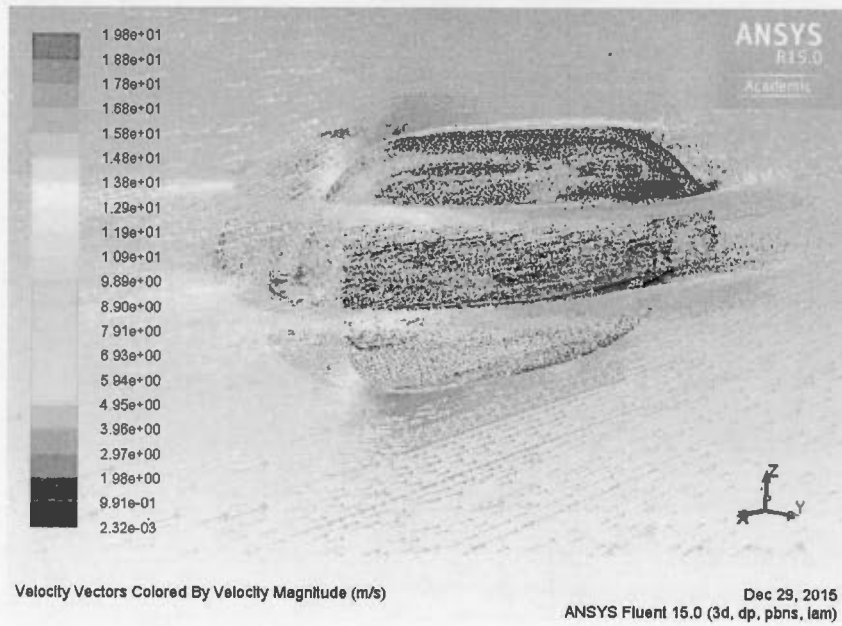


**Figure 2.52 : Design 6 vectorial airflow result, 3D view, PAS body included, results on Y and Z planes**

## 2.7 PAS comparison and selection

In this section a brief explanation of drag value energy will be presented. First, the drag value results which are calculated based on CFD simulation will be presented. Then, based on all results, a comparison will be made among all designs in order to select the most appropriate passive air sampler for our application as related to aerodynamic and airflow.

### 2.7.1 PASs's drag values

CFD simulation provides the visualized fluid flow results for better analyzing and understanding of PASs operation in outdoor environment. In addition, it provides the drag coefficient value which denoted as  $C_d$ , for calculation of magnitude of drag, designated as  $D$ , caused by air or fluid flow based on following Drag equation (Hoerner, 1965):

$$D = C_d \times \frac{\rho \times V^2}{2} \times A$$

Where:

- $D$  is magnitude drag caused by fluid flow (sometimes called air resistance) (N);
- $C_d$  is drag coefficient;
- $\rho$  is fluid density ( $\text{kg/m}^3$ );
- $V$  is fluid velocity (m/s);
- $A$  is frontal projected surface ( $\text{m}^2$ );

In fluid dynamics, drag is a kind of energy which acts against the motion of any object that moves in fluid (Hoerner, 1965). It depends on fluid density, the square of the fluid velocity, size and also shape of the object (object inclination to the fluid). Generally, the relations among object geometry, inclination and flow condition is complex. A solution to reduce this complexity is to characterize the dependence by a single variable. For drag, this variable is drag coefficient and it determined experimentally using wind tunnels and different models geometries. The drag coefficient value has been measured before by placing different shapes and geometries with the same frontal surface area in wind tunnel under the same fluid flow condition including the same velocity, density and pressure (Figure 2.53) (Hoerner, 1965) .



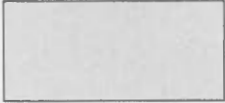

shape		Drag Coefficient
Sphere		0.47
Cube		1.05
Long Cylinder		0.82
Streamlined half-body		0.09

Figure 2.53 : Experimentally measured Drag coefficients for certain shapes (Hoerner, 1965)

This value is provided by ANSYS CFD simulation software after each simulation. It is important to have the same fluid flow condition for all geometries. In all simulations that have been done, air velocity was determined as 15 m/s, temperature equal to 25 °C and air density 1.1839 kg/m<sup>3</sup>. The drag value is then calculated based on presented equation, fluid condition and projected frontal surface area. The results of those calculations are presented on (Table 2.1).

**Table 2.1 : Pattern's drag force calculation**

Design Number	Frontal surface area (mm <sup>2</sup> )	Drag coefficient	Drag force value (Newton)
Design 1	66	0.00010697462	9.404E-07
Design 2	80	0.000082103365	8.748E-07
Design 3	140	0.00019402422	0.000003618
Design 4	110	0.00904174840	0.0001325
Design 5-2	309.42	0.033784795	0.001392
Design 6	352.09	0.0266051720	0.001248

### 2.7.2 PASs comparison and selection procedure

The PAS comparison and design process was based on CFD 3D simulation results and the suggestions from the biology department. Drag force value was used to have a better understanding of pattern's aerodynamic factor when there was a modification for better functionality. Since in most of the cases the drag coefficient value can be obtained experimentally and this is the first time that a miniaturized passive air sample was designed, there is no drag coefficient reference value, neither drag force value for

comparison but, they have used to compare the designed patterns together and keeping them for future applications as reference if be required.

After the first design, the CFD simulation showed a good fluid flow across the fluid channel and it also showed a very low drag force value. The first design should be modified in a way that it could reduce the fluid direct impact to the sampling medium since in high velocities (which is not controllable) it might be possible that sampling media come out of its position and since the fluid channel is open to the free space the sampling media could be lost. Also the size of the sampling media was too small and that was not enough to capture desired compounds.

To address this issue, the patterns two and four were proposed. In pattern two, two sampling mediums were positioned parallel to the fluid flow direction. In order to keep the maximum fluid exposure to the sampling media, the inside curves were considered to distract the fluid to the sampling media. In this case the PAS body could be narrower to increase PAS aerodynamic function. As it is obvious from table 1, this modification decreases the drag force value.

In pattern 4, a new design is proposed to protect the sampling media from direct impact while highly increasing the sampling media active surface area. It was tried to use the same design as the aircraft airfoil for better aerodynamic, since the thickness of the PAS should be increased in order to have more internal spaces for bigger sampling media. Apparently the drag force value changed but, still close to the zero.

While these two designs covered most of the project requirements, still there was a problem with fluid flow direction. For this project (inspired by an idea coming from our collaborators in the biology department) it was assumed that the most important time that a bird is getting contaminated is the time that it is sitting and waiting for foods around the land field. In this case, there is no movement to bring the sampling air inside the PAS. So the patterns should be designed in the way that fluid could flow into the



PAS from all direction and even if the bird is not moving, sampling media be exposed with fluid.

Pattern 3 was proposed in order to solve the fluid flow direction problem. During flying, the fluid could flow through the considered channels not only from forward direction but also from other directions around the PAS and expose to the sampling media. Moreover, when there is no movement, the sampling air still can expose to the sampling media surface and this is due to its locating place. As they are located inside 4 holes on the top surface of the device, in case of no movement the sampling air still can be exposed to the surface of the absorbers. The new proposed pattern had some problems based on discussions with our collaborators in the biology department. First, using the channel to guide the fluid into the sampling media, could also guide water into it. This would mean that when the bird is floating on water or when there is rain, water can easily penetrate into the sampling media. In this case the design must be modified in such a way that it could protect the sampling media. The second problem is the direct radiation of sun light to the sampling media. Since they had no study about the effect of the sun light on sampling media, the PAS must protect sampling media from direct radiation of sun light.

In this case pattern 5-1 was proposed. This pattern covers all the considerations due to its new form. In fact, its circular shape brings several advantages at the same time. It can protect the inside media while there is an entrance gap all around the PAS. In this case the fluid could flow into the PAS from all direction and even if there be no movement, the fluid still can easily flow into the PAS. Moreover, since the top part covers the bottom part, the water cannot easily enter into the PAS. The only problem with the new design was about its thickness. As it was designed as thin as possible, it was possible that bird's feathers cover the PAS. In this case the maximum thickness of the PAS was defined by our collaborators from the biology department based on their previous studies and bird's physiology.

To solve the bird's feather problem, the thickness of the bottom part was increased in pattern 5-2. Then the designed and approved PAS was fabricated using 3 D printing and tested by our collaborators in the biology department. The results showed that the sampling media active surface area (sampling media size) is too small and it should be increased for better analyze.

In order to address the new problem, pattern 6 was proposed based on bird's physiology and pattern 5-2 simulation results. The width of PAS could not be changed due to the bird's wing position but, it was possible to increase the PAS length along the bird's body. This first modification was increased the active surface area of the sampling media from  $254.34 \text{ mm}^2$  to  $440.385 \text{ mm}^2$  which means 73 % increase. Also based on pattern 5-2 simulation, another position was considered inside the top part with the same size as the one in the bottom part. In this way, new design increased the sampling surface area twice more than the previous one ( $880.77 \text{ mm}^2$ ). Also the Drag value comparison between design 5-2 and design 6 shows that the drag value was decreased from 0.001392 to 0.001248 which is another advantage of the design 6.

Since this design was covered all the requirements, it was approved by our collaborators in the biology department and it was sent for fabrication in order to be tested on birds.

## 2.8 Resume

As this was the first time that a miniaturized passive air sampler device was designed for mounting on a medium size bird, several concept designs with different characteristics were proposed and simulated. For each of the proposed architectures, it was tried to implement specific characteristics and then make a CFD simulation on them in order to understand how the designed PAS will behave and what are the advantages and disadvantages of the implemented characteristics. Some designs were made more aerodynamic in order to reduce the drag energy against the birds. Each design and its related CFD results was proposed to our collaborators from the biology department for analysis. Based on their feedback some modifications were done on the designs and in some cases the design was completely changed. Finally, a PAS concept design (design 5) was approved and some additional modifications were done on it in order to adapt it for mounting on the birds and also to increase the sampling media active surface inside the PAS (design 6). In the next chapter (chapter 3) the results from the fabrication and testing of this device will be presented. Then, this design will be modified in such a way that it be equipped with some active sensors for real time measurements (chapter 4). These sensors will help our collaborators from the biology department to consider better sampling air condition in their analyses.

## CHAPTER III

### PASSIVE SAMPLER FABRICATION AND TESTING

#### 3.1 PAS fabrication

Choosing the right technology with enough resolution and appropriate material, compatible with our requirements is the critical point when 3D printing technology is chosen as fabrication method. The more available and popular technologies are: FDM (Fused deposition modeling) (Chua et Leong, 2003), SLA (Stereolithography) (Hull, 1986), SLS (Selective laser sintering) (Kumar, 2003), DMLS (Direct metal laser sintering) (Khaing *et al.*, 2001) and Polyjet 3D printing (Barclift et Williams, 2012). Polyjet 3D printing has the capability to print 0.3 mm channel width, while it can print channels with height as thin as 50  $\mu\text{m}$  and the minimum thickness for other techniques could be 0.5 mm. The Vero (for solid-state) and Durus (for flexible-state) materials can be used as printing materials (<https://www.fablabinc.com/fr/impression-3d/materiaux#material9883>). A great advantage of 3D printing technology is that it can use different kinds of materials for printing. In addition to presented materials, other types of materials such as plastic, alumina and metals can also be used for printing.

The PAS, in order to be used and mounted on birds, should be fabricated under specific conditions. It should be fabricated from the material as light as possible. The material must be waterproof and stands during cleaning procedures with organic chemical solvents (chloroform and methanol (50:50 volume ratio), 15 min 3 times, then dried

under a fume hood for two hours). It should not be transparent in order to protect the inside sampling media from sunlight.

The first sample prototype was fabricated with Polyjet technology and from Vero material which was the most precise 3D technology available in Montreal area. This was made in order to check if the printed prototype will be acceptable from different points of view such as real printed dimensions, cleanness, assembling processes and etc. The prototype was well fabricated with accurate dimensions but it dissolved in organic solvents during cleaning process. This is not acceptable as each PAS should pass the standard cleaning process before the operation.

The second sample prototype was fabricated by Sculpteo Company (Sculpteo Inc. 169 11<sup>th</sup> Street, San Francisco, CA, USA) using a different plastic material (Polyamide model PA2200). The total weight of the complete printed PAS (Top and bottom Part) is 2.875gr which is light enough to be mounted on the birds (Figures 3.1, 3.2). Moreover, the polyamide is not affected by the cleaning process and this prototype address all the other above presented requirements. As this prototype was judged as acceptable, 100 units of PAS were ordered (6.81 US\$/Unit).

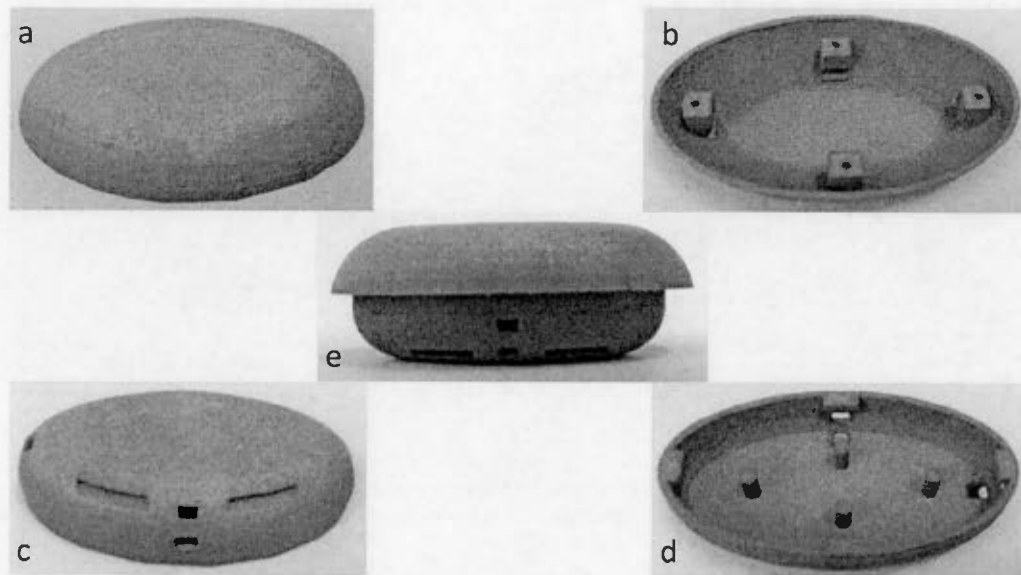


**Figure 3.1 : Accepted PAS fabricated with 3D printing technology. (a) Top part outside. (b) Top part inside. (c) Bottom part outside. (d) Bottom part inside. (e) Complete assembled PAS**

For mounting the assembled PASs, the natural Tubular Teflon ribbon (width: 3/16'') was used to attach the PAS on the birds (Figure 3.2). The ribbon passed through the considered channels on PAS's bottom part and after putting the device on back of the bird, the ribbon was tightened and hidden under the feathers.

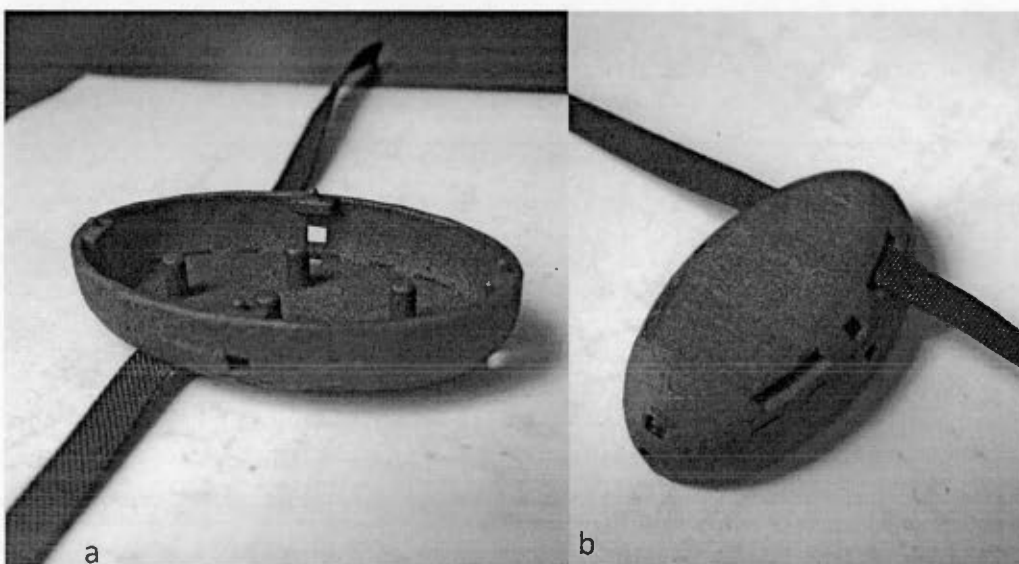


**Figure 3.2 : Natural Tubular Teflon ribbon used to mount the PAS on the birds. (a) Bottom part top view. (b) Bottom part bottom view**

## 3.2 Adsorbents

In following section, four different types of adsorbents will be presented which have been tested inside the passive air sampler. The polyurethane foam (PUF) and glass fiber filter (GFF) which are two well-known adsorbents for passive air sampling and two new types of adsorbents which are Polydimethylsiloxane (PDMS) (Park *et al.*, 2014) and graphene oxide.

### 3.2.1 Polyurethane foam

Polyurethane is a member of polymers or plastics (Bayer, 1947; Seymour et Kauffman, 1992). Polyurethane can be a solid or can have an open cellular structure (Figure 3.3),

in which case it is called foam and foam can be flexible or rigid. It is a versatile material and it can be used in different applications such as bedding, furniture, automotive or building isolator (Prisacariu, 2011).

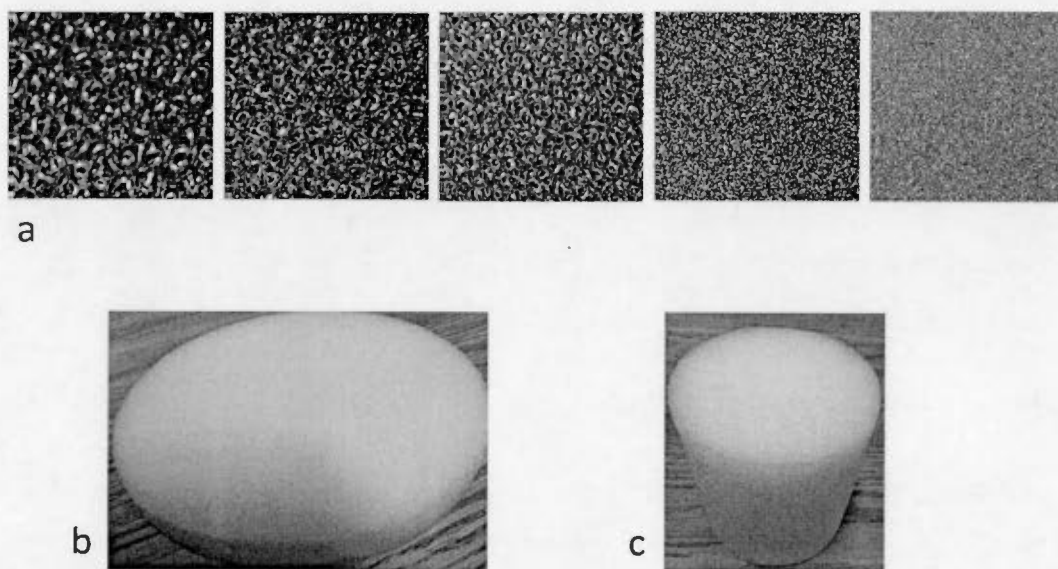


**Figure 3.3 : Polyurthane foam. (a) From left to right, open cellular structure to close cellular structure. (b) Disk shape PUF. (c) Cylinder shape PUF which has been used in this project**

In this study PUF (0.023 g.cm<sup>-3</sup> density; Shawnee Instruments, Cleves, Ohio, USA) was cut as a 2 mm-thickness disk, elliptic-shaped piece (active surface area: 400 mm<sup>2</sup>). To cut the cylinder PUF to 2 mm disk, the PUF was put in a water and froze. Then the frozen cylinder was cut by using an electrical saw into 2 mm disks. Then the disks were dried and cut into their elliptic-shaped using a FR4 mould, fabricated by LPKF CNC machine. Finally, they were pre-cleaned using chloroform and methanol solution (50:50 volume ratio) and evaporated under a fume hood for two hours and kept in a Ziploc bag for usage.



### 3.2.2 Glass fiber filter (GFF)

It was made of pure borosilicate glass fiber. It can be found in a wide range of flow rates. This type of adsorbent can be provided in different shapes, normally as a disk, and it is a well-known adsorbent in biology and environment fields.

This adsorbent was selected, bought, tested and cut into the desired shape and size by biology department (Manon Sorais) to be installed and tested inside the PAS in parallel to the other type of adsorbents. (<http://www.sterlitech.com/filters/membrane-disc-filters/glass-fiber-filter.html>).

### 3.2.3 Polydimethylsiloxane (PDMS)

PDMS is a kind of polymer that is commonly referred to silicon (European Centre for et Toxicology of, 1983). It is well-known for its flexible and hydrophobic characteristics. It widely uses in microfluidic technology. It is transparent, non-toxic and non-flammable. Its characteristics make it as a versatile material for different applications. As it was presented in some studies (Park *et al.*, 2014) that PDMS can capture some compounds in both the gas- and particle-phase. In this case a layer of PDMS with 1 mm thickness was prepared using the following recipe.

A mould was fabricated from 1.6 thickness copper-clad board using LPKF 2.5D milling technic (Figure 3.4). The mould was fabricated from 14×14 mm copper clade and the active area was milled from it with actual equal to 12×12×1 mm. 1 mm depth will be the PDMS thickness and it can vary based on application requirements.

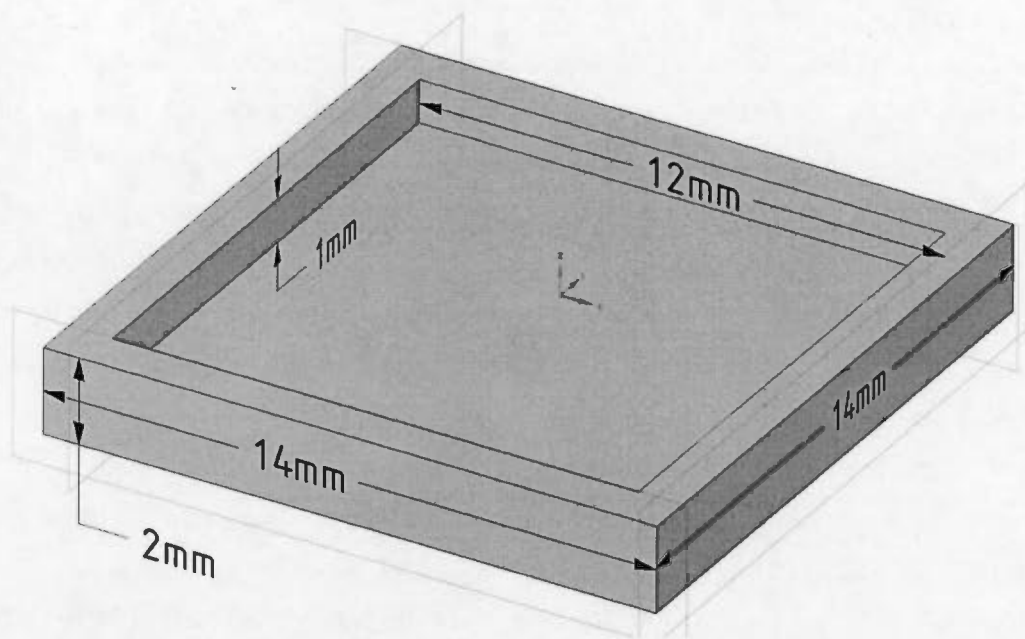


**Figure 3.4 : PDMS mould for forming the uncured PDMS to the 1 mm layer thickness**

PDMS (1.12-1.16 g.cm<sup>-3</sup> density; Specialty Silicone Products, Ballton Spa, NY, USA) was prepared by mixing Sylgard 184 and Sylgard 184 curing agent with 10:1 m/m ratio. The mixed materials were vacuumed for 10 minutes in order to eliminate all the bubble air. The mould was put into the flat plastic container and the PDMS were cast on it slowly until the PDMS fill the mould 1 mm depth. The container was kept in the oven for 10 minutes with a temperature of 80 °C. After curing, PDMS was peeled off from mould manually and cut into elliptic-shaped piece for usage.

### 3.2.4 Graphene oxide

Graphene oxide is a compound of three elements are carbon, oxygen and hydrogen. It obtains by treating graphite with oxidizers (Hummers Jr et Offeman, 1958). It is as a kind of mono molecular sheet which uses to prepare strong paper-link material (Dreyer *et al.*, 2010). The form and its body structure depends on the treating solution. As an adsorbents, the following treatment was used by Doctor Sujitra Poorahong to form it as a foam. To address this, a thick layer of PDMS was used as a mould with the same size as the PAS adsorbent place. Since the PDMS is flexible it would be easier to bring out the graphene oxide foam after drying. For graphene oxide treatment, aqueous GO dispersion was prepared by a modified Hummers' method (Marcano *et al.*, 2010) using the natural flake graphite. Then it was sonicated for 60 min before use. To prepare GO foam, 5 mL of GO dispersion (1.76 mg mL<sup>-1</sup>) was mixed with 200 mg of polyethyleneimine (PEI). Then, the mixture was sonicated for about 1 min. The gel precursor was stored in the oil bath at 60 °C for 24 h to obtain GO-PEI hydrogel. Then the hydrogel was transferred to the mould and froze at -80 °C for 4 hours. Finally, the material in the mould was placed in a freeze-drying instrument to eliminate the water and obtain the GO foam.

### 3.3 PAS onsite testing

In this section, PAS onsite tests and results are presented which was done in collaboration with the biology department. A part of the tests process and results are provided by Manon Sorais (The PhD candidate in biology who will work on more ecotoxicological aspect of global work).

The study was continued by mounting the 3D printed PAS on the restricted mounting surface area in the middle back of the ring-billed gulls (*Larus delawarensis*) (the surface

mounting area is extended along the birds body and not along the wings) (Figure 3.5) to minimize the effect of mounted PAS on the bird's body aerodynamic. In order to avoid compromising the bird's flying (Vandenabeele *et al.*, 2014), a customized harness that was made from a protective neoprene patch and Teflon® ribbon (Bally Ribbon Mills, Bally, PA, USA), while the Bird-born air sampling method is described elsewhere (Sorais *et al.*, in prep).

6-120 nests were selected when presenting 2 eggs laid, in order to be able to estimate the induction of the incubation. The selected nests were evenly distributed on the 3 sections of the island. 28 birds on 28 preselected nests were captured when they presented 3 eggs, in order to assure the bond between the bird and its nest (just to be sure the birds will be back).

The birds were trapped with a dip net or a trap triggered by a remote control. The feathers were coloured at the back of the head in blue to be able to recognize them at distance. 28 PAS were deployed on the birds for one, two and three weeks and at the end only 24 PAS were bought back. Two types of adsorbents were tested in this study: a PUF disk coupled to a GFF and . Among those 24, 12 carried a PAS with PUF coupled to GFF and 12 carried a PAS with PDMS. Among birds carrying the PUF-GFF PAS, 3 were deployed for one week, 5 for two weeks, and 4 for three weeks. For PDMS PAS, 3 birds were deployed for one week, 6 for two weeks, and 3 for three weeks. Also other types of the adsorbent was tested which was prepared from graphene oxide in order to test the PAS versatility (the numerical results are not presented in this work). The PAS housing and adsorbents (PDMS, GFF, and PUF) were cleaned before operations using methanol and chloroform solution with the volume ratio equal to 50:50. Then they were evaporated and dried under a fume hood for two hours. After equipping the PAS with absorbers, the top and bottom parts were glued together using a HFR-free glue (RapidFix, Norton Shores, Michigan, USA), then they were kept in the dark place at -20°C until deployment.

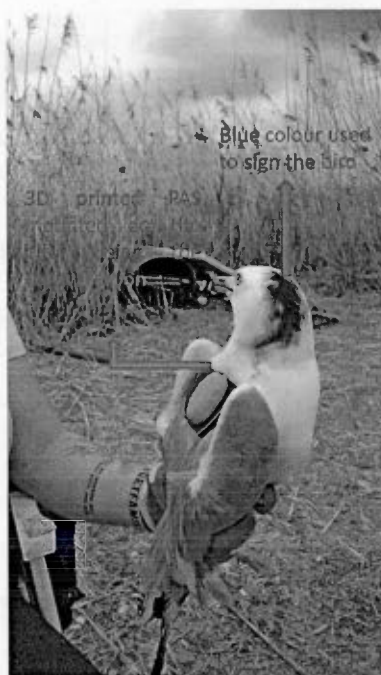


Figure 3.5 : Mounted PAS on a bird, using the Teflon ribbon in bird's colony

24 sampling mediums that were brought back, analyzed by biology department and the following results (Figure 3.6) were achieved.

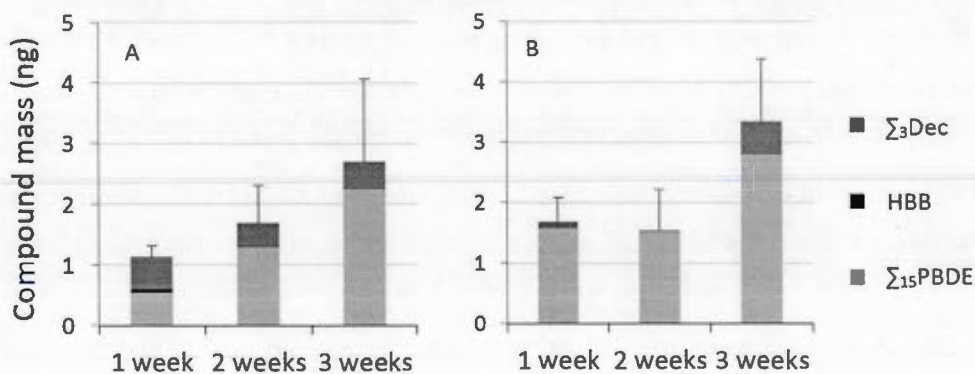


Figure 3.6 : Mean total mass (ng) of  $\Sigma_{15}\text{PBDE}$ , HBB, and  $\Sigma_{3}\text{Dec}$  (sum of syn- and anti-DP, and Dec-604 CB) determined in A) PUF-GFF PAS and B) PDMS PAS carried by ring-billed gulls in Montreal (QC, Canada) area during one, two and three weeks. The error bar represents the SEM of  $\Sigma_{19}\text{HFR}$

These results show the PAS functionality. It indicates that during certain period of time, three different kinds of flame retardants was detected. The detected compounds are three kinds of Dechlorane ( $\Sigma$ 3DEC), Hexabromodenzene (HBB) and fifteen kinds of PBDE ( $\Sigma$ 15PBDE). These indicate that our miniaturized passive air sampler is capable of carrying different types of adsorbents which brings the advantage of sampling all types of compounds. This was achieved by using the PUF and GFF to collect the gas and particulate phase of compounds and PDMS for more volatile compounds. As the first miniaturized PAS which can be carried by birds in order to collect HFF (halogenated flame retardants), the results are so satisfactory while some improvements can be made in future such as precision modification, which will be discussed in future work section. More detailed results are available in the paper with the title of “A Miniature Bird-Borne Passive Air Sampler for Monitoring Halogenated Flame Retardants” from Manon Sorais et al., (in prep).

### 3.4 Resume

Nowadays, fabricating the rapid prototypes and even mass productions are getting faster and easier due to the 3D printing technology since it provides a variety of printing methods and materials with high printing accuracy. Based on PAS fabrication limitations such as resolution, weight and cleaning process standard, many PAS were fabricated using 3D printing technology. Different kinds of absorbents were used to test the PAS by mounting them on signed birds. Based on project study plan, they were deployed on birds for certain times and then they were sent to analyze. Fortunately, the target compounds were captured and recorded to be compared with results that will be obtained in future.



## CHAPTER IV

### EMBEDDED ELECTRONIC CIRCUIT

This chapter is divided in five sections which present the procedure of equipping the miniaturized passive air sampler with some electronic sensors. These sensors do not change the role of the passive air sampler to active air sampler. They will just provide some complementary data in order to help biologist for better evaluation on results of the adsorbents analysis. It begins with sensors description and more details of using the pressure sensor for airspeed calculation. Then the electronic circuit (schematics and PCB) which is responsible to control the sensors will be presented. In the third section, all the modification that was done on approved PAS, in order to equip it with electronic parts will be presented. Following that the CFD simulation results for modified PAS will be presented for better comparison with previous designs. In the last section the results of active sensors that was embedded into the PAS will be shown and compared with an anemometer results to show its reliability.

#### 4.1 Sensors and their utilization

As it was explained in chapter 1, the sampling air velocity around and inside the PAS can affects the sampling rate results (May *et al.*, 2011; Thomas *et al.*, 2006; Tuduri *et al.*, 2006) where the PAS is installed in free space environment containing variable wind speed. This would be more significant when the PAS is mounted on a mobile object such as a bird or a vehicle since both PAS and sampling air can have their own velocity and depending on wind and bird's flying direction and also bird's flying speed,



the sampling air velocity would have variety values. In this case, in order to have a better analyze on absorbers' sampling rate and also better comparison with other studies, the PAS was equipped with a tiny digital electronic circuit in order to measure the velocity of the sampling air around the PAS by measuring the principle values which are necessary for airspeed calculation.

In order to equip the designed PAS with active airspeed sensors, it was necessary to consider several conditions. First, the combination of all electronic components, including active sensors, processor and PCB board, must be small enough to be mounted inside the miniaturized PAS, without needing for large modifications in PAS dimensions. Second, the maximum power supply should be 3.3 volt as generated by a small battery and the complete board must have minimum power consumption for long-term measurement. Finally, the total weight of all devices that will be mounted on the birds should not exceed the 3% of the bird's total weight. Then, the selected electronic components, processors and sensors must be as light as possible while having enough accuracy for the required measurements.

The typical anemometers use a simple structure to measure the airspeed. They use small propellers or a fan to power their generators. As the wind blows, it spins the fan blades and a tiny generator to which they're attached. The generator is connected to an electronic circuit that gives an instant readout of the wind speed on a digital display based on generated voltage but, this is not an appropriate solution for miniaturized PAS since it needs more space.

The other solution to measure the airspeed is the one that uses in aviation which calls Pitot-static system (Figure 4.1) (Elmajdub et Bharadwaj). In this system, the fluid velocity can be determined by measuring the related pressure (Pitot, 1732). It consists of a Pitot tube generates the Pitot pressure and static tube which generates static pressure. The Pitot pressure also called total pressure is a measure of ram air pressure (the air pressure which creates due to the moving objects) and can be measured by

placing the Pitot tube directly into the fluid flow. Usually the Pitot tubes installed on-under wings or in the front side of the aircraft's fuselage, facing forward while its pressure channels is exposed to the front wind (Elmajdub et Bharadwaj). Positioning the Pitot tubes on mentioned locations will lead us to accurate measurement since less vortex and deflected air will be generated due to the aircraft fuselage shape or engines power.

The static pressure can be measured through the static tube channel.usually it is installed in the same location as total pressure tube where there is less distributed flow and this will result in accurate measurement (Elmajdub et Bharadwaj). A Pitot-static tube is a mixed tube which the total pressure tube is located in the middle (facing to the fluid flow) and the static pressure is located around it but in such a way that the direct airflow cannot pass through it. In this case the higher altitude with decrease the static pressure.

The dynamic pressure is the difference between the total pressure and the static pressure. The dynamic pressure is then determined to use a diaphragm located inside the pressure sensors. The differential pressure sensor has to internal part. The static side and the total side. In this case the variation of the diaphragm will give us the dynamic pressure (Nelson, 1998).

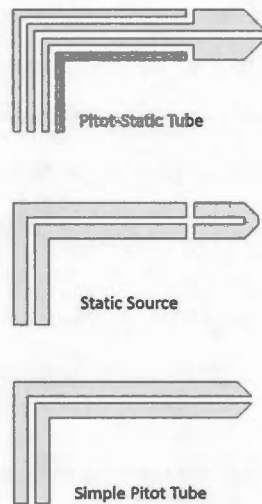


**Figure 4.1 : Pitot, Static and Pitot-Static tube diagram**

By having the dynamic pressure, airspeed can be calculated using Bernoulli's equation (Klopfenstein Jr, 1998):

$$V = \sqrt{(2 \times \Delta P) / \rho}$$

Where:

- $V$  is flow velocity in m/s;
- $\Delta P$  is differential pressure;
- $\rho$  is fluid density in  $kg / m^3$ ;

$\Delta P$  is differential pressure which is equal to the difference between total and static pressure.

$$\Delta P = P_t - P_s$$

The  $\rho$  value which is fluid density in  $kg/m^3$  can be calculated from following equation:

$$\rho = \frac{P \times M}{R \times T}$$

Where:

- $P$  is fluid pressure in Pascal;
- $M$  is the fluid molar mass;
- $R$  is the universal gas constant;
- $T$  is the absolute temperature in Kelvin;

As the miniaturized PAS will be mounted on a bird and these birds can fly in different altitudes with different air temperatures. As they mostly fly close to the sea level (not in very high altitudes), the first three variables can be fixed to the sea-level condition. In this case the air pressure at sea level can be fixed to 101.325 kilopascals. In presented equation the air molar mass is equal to  $28.9645 \text{ g.mol}^{-1}$  and air universal constant is  $8.3144 \text{ j.mol}^{-1}\text{k}^{-1}$ . However, the last variable which is absolute temperature should accurately measure in order to have the exact air density and then better airspeed calculation since there are a lot ambient temperature variation in Montreal area.

Based on PAS limitations (weight, size and power consumption), a differential pressure sensor was found from ALL Sensors company. It has some advantages which fit to project requirements. It has a small dimension as  $15.75 \times 12.70 \times 7.17 \text{ mm}$  which is small enough to put inside the PAS. The most important thing is its digital output data. Due to its inside digital circuit it is possible to communicate with sensor trough I2C or SPI interfaces. In this case no extra electronic components will be required to convert analogue output to digital value like what the most pressure sensors do. It works with

3.3 V power supply voltage and consume maximum 0.9 mA on low power mode and 5.0  $\mu$ A on sleep mode so, the total power consumption can be managed using its different operational mode (Figure 4.2). The output value is differential (dynamic) pressure and it can directly use with airspeed equation without needing the extra calculation and it can measure from 0 to 60 inH<sub>2</sub>O depends on selected models.

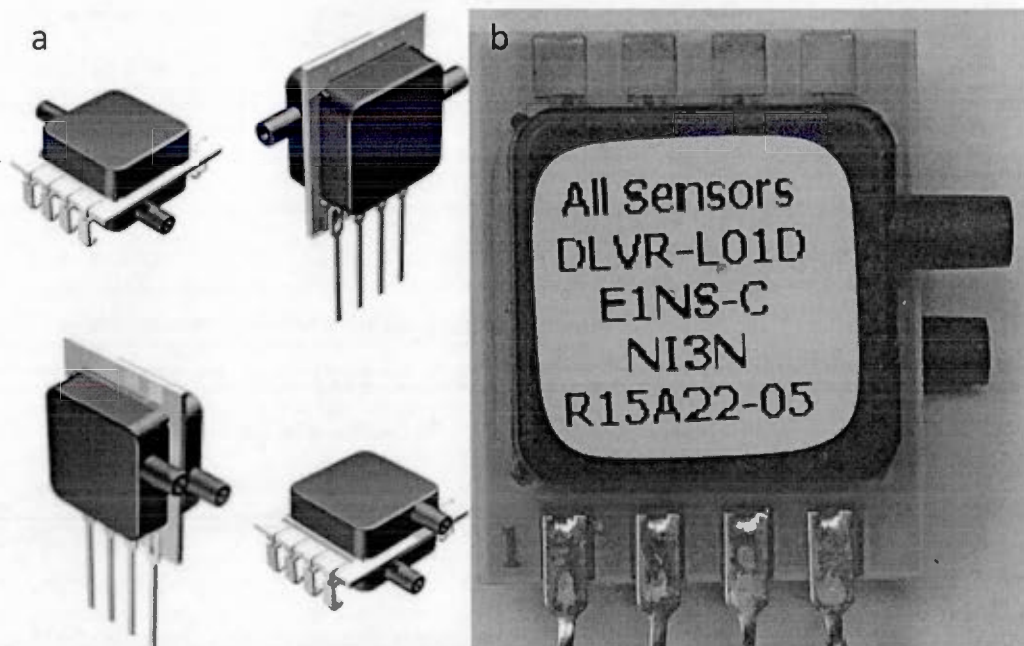


**Figure 4.2 : Differential pressure sensor. (a) Different packages and tube direction (Retrieved from <http://www.allsensors.com>), (b) pressure sensor model number used to implement in PAS**

Moreover, an accurate tiny temperature-humidity sensor was bought from SENSIRION Company with  $3 \times 3 \times 1.1$  mm dimension in order to measure the absolute temperature for air density calculation. As the humidity sensor was already included in this sensor, it was also tried to provide the related humidity results for biologists as

complementary data while this is not absolutely necessary for this project. It works with supply voltage between 2.1 to 3.6 V and the maximum current would be 330  $\mu\text{A}$  on measuring mode and 0.4  $\mu\text{A}$  in sleep mode. In the same way I2C protocol can be used to communicate with sensor for reading its digital output data (figure 4.3).

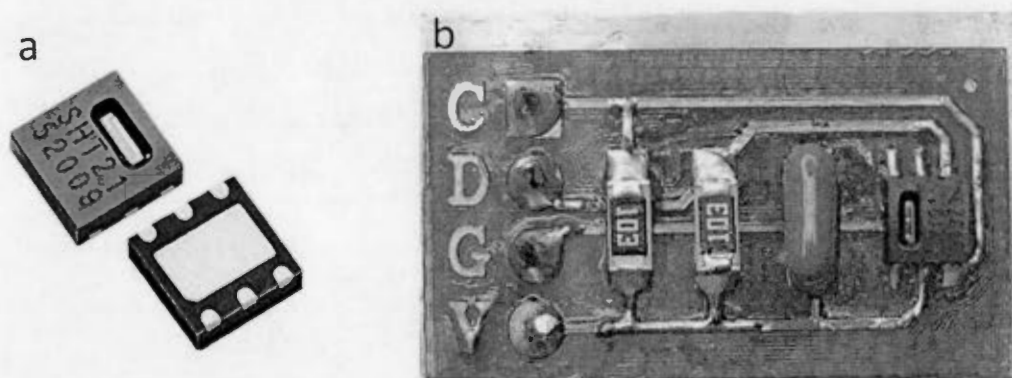


**Figure 4.3 : Temperature-humid sensor. (a) Top and bottom view of sensor package (Retrieved from <http://www.chipdip.ru/product/sht21/>) (b) soldered sensor behind the 10k pullup resistor with 1206 package**

#### 4.2 Airspeed measurement electronic circuit

In order to measure the airspeed based on presented sensors, a processor is needed to get all data from sensors and calculates the airspeed based on presented equation. In this case the Atmega81 microcontroller from Atmel Company was used based on figure 4.4 schematic diagram to address this.

Both differential pressure sensor and temperature-humid sensors were connected to the microcontroller I2C communication port. Two 4.7  $\text{k}\Omega$  resistors were considered as I2C

bus pullup. Memory chip, At45DB161, was used for data recording based on SPI communication protocol. The microcontroller read the temperature and humid value from related sensor, then it read the pressure value from differential sensor and after some calculation it records the airspeed, temperature and humidity value on memory. After each measurement, the microcontroller changes sensors active mode to sleep mode to reduce the power consumption and waits until the next measurement time-point. The measurement time-point could be determined by project requirements and is based on project sampling rate (the number of times that airspeed should be measured in hours). The airspeed can be measured on each millisecond utile hours and finally, when the measurements done and PAS will be brought back to the lab then, recorded data can be transferred to a computer using the USART communication port.

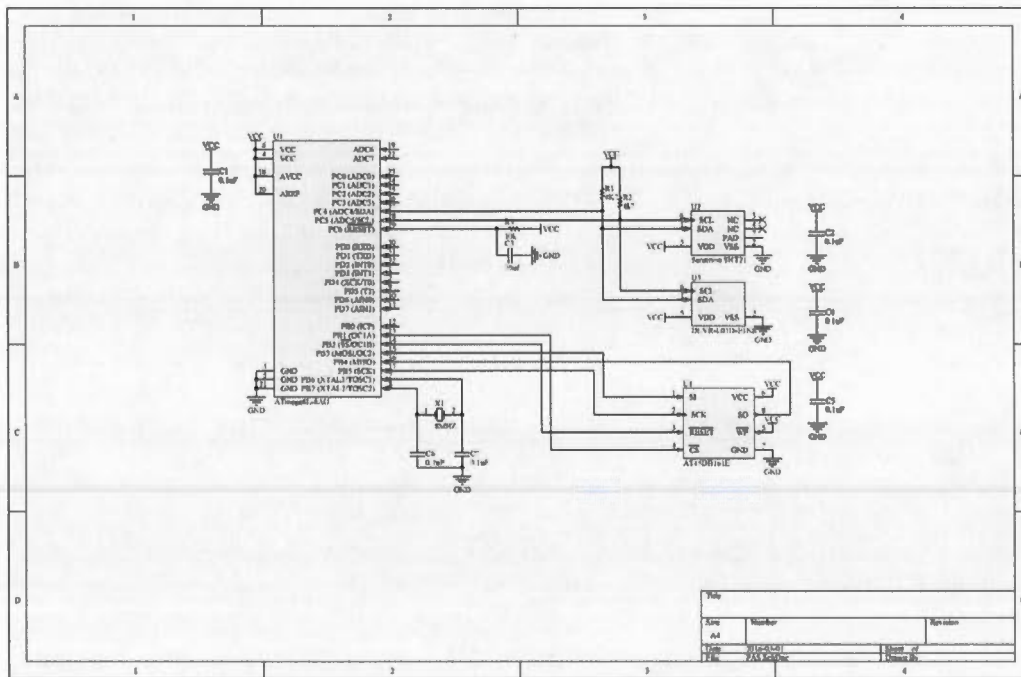


Figure 4.4 : Schematic diagram of sensors and controllers

In order to equip the miniaturized PAS with electronic circuits, the printed circuit board (PCB) keep-out layer should have the same shape as PAS (where the PCB should be installed). To address this, the inside diagram of PAS was exported from 3D design software and then imported as keep-out layer in PCB design circuit (circuit maker from Altium design). The rest of the electronic circuit should be designed inside this area. Figure 73 shows the designed and fabricated PCB including the sensors diagram for better imagination of their positioning. To minimize the weight and size of the complete board (Figure 4.6), copper clad with  $1/64$ ' (0.4 mm) thickness was used for PCB fabrication. After fabrication, the electronic components (Table 4.1) were soldered on the fabricated PCB to be ready for test.

As it was explained, one of the main objectives of the global project was tracking the source of the flame retardants. The miniaturized PAS is responsible to capture compounds in gas-particle phases. In order to track the bird's flying path, a small GPS including a small battery was used (the GPS and battery were bought, tested and mounted of birds by our colleagues in biology department). This battery (3.2V–250 mA) was used as a source of power for the presented electronic circuit. Since The GPS was programed to record the coordinates each 10 minutes, the presented electronic circuit was programed to do all its tasks at the same time as GPS. In order to save more energy, all the components were programed to be in sleep mode. Each 10 minutes, only for duration of 10 millisecond, the microcontroller changes the components statues to active mode, starts all measurements, records the data and changes the components statues to sleep mode again. The total power consumption of proposed circuit is 0.00008 Wh. By using the mentioned battery as a power source, without connecting any other circuits (GPS, accelerometer, etc.) to the battery, the proposed circuit can be used for duration of approximately 400 days.



Table 4.1: List of main electronic components

Part number	Manufacturer	Description	QTY	Package
DLVR-L01D-E1NS	All Sensors	Differential pressure sensor Dimension: 15.75 × 12.70 × 7.17 mm Communication protocol: I2C or SPI Supply voltage: 3.3V current consumption: 0.9mA low power, 5.0 μA sleep Range: 0 – 60 inH2O Accuracy: 1%	1	Dip
SHT21	SENSIRION	Temperature and humidity sensor Dimension: 3 × 3 × 1.1 mm Communication protocol: I2C Supply voltage: 2.1 - 3.3V current consumption: 330 μA low power, 0.4 μA sleep Range: 0 – 100 % RH, -40 – 125 °C Accuracy: ± 2 % humidity (20% - 80%) Accuracy: ± 0.3 % Temp (0 – 60 °C)	1	DFN
AT45DB161D	Atmel	Flash memory Dimension: 6 × 5 × 0.55 mm Communication protocol: SPI - 66MHZ Supply voltage: 2.5 - 3.6V current consumption: 11mA on active, 3 μA low power Memory size: 16 Megabit	1	MLF
Atmega328	Atmel	Microcontroller Dimension: 5 × 5 × 0.9 mm Communication protocol: I2C, SPI, Serial, Parallel protocol Supply voltage: 1.8 - 5.5 V Clock frequency: 0 - 20 MHz (Depends on supply voltage) current consumption: 3,6mA on active, 0.5 μA low power	1	VFQFN

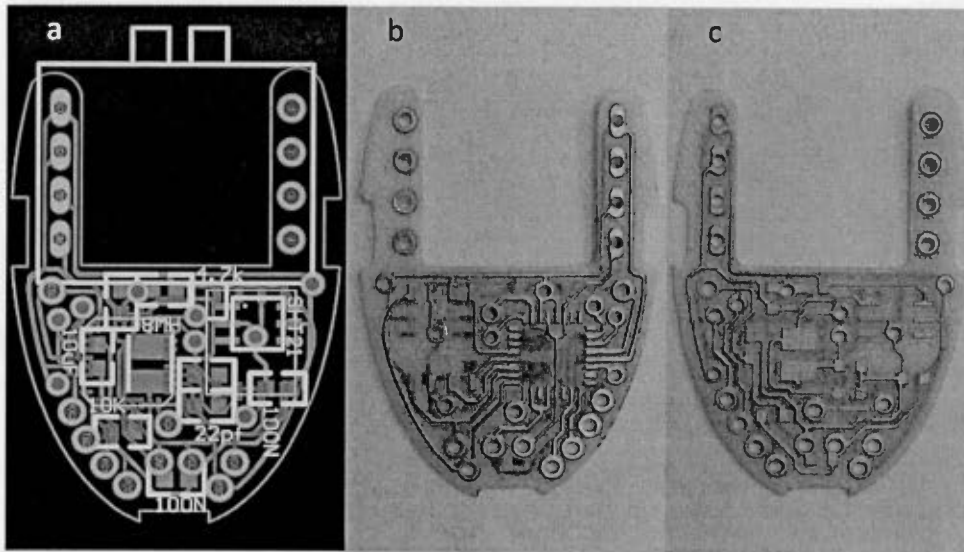


Figure 4.5 : Designed and adapted PCB to be installed inside the PAS. (a) PCB diagram. (b) Fabricated PCB – bottom layer. (c) Fabricated PCB – top layer

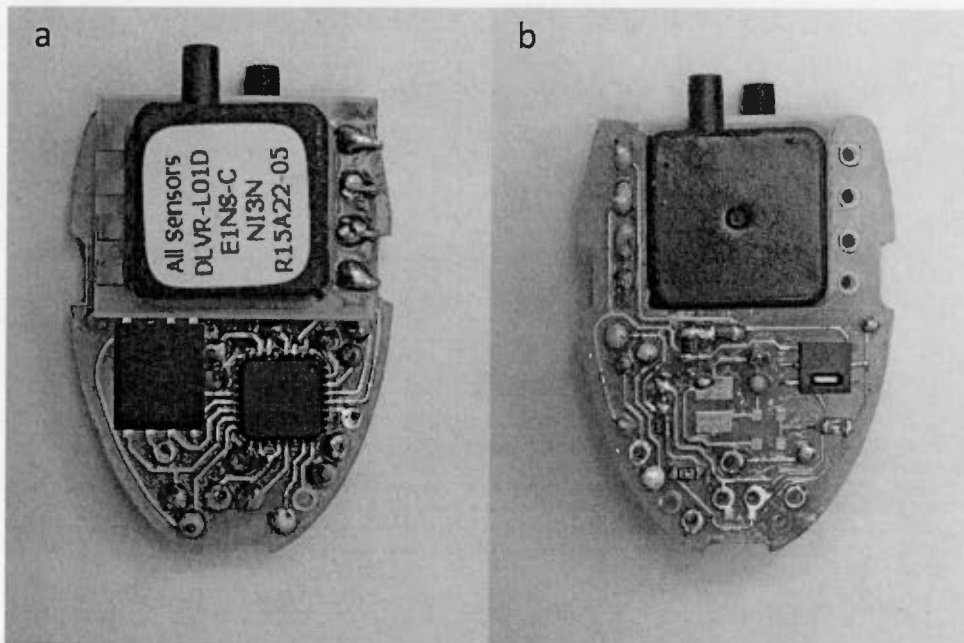


Figure 4.6 : A complete electronic board including all components. (a) Top view. (b) Bottom view

### 4.3 PAS concept design (modified to embed the sensors)

In order to equip the last miniaturized PAS with a new active electronic circuit, several modifications should be done. The height of the bottom part should increase to make enough space for electronic components and sensors especially for a pressure sensor which is the thickest components among all. The bottom part should be divided in two parts to insert the electronic components into the PAS while the top part keeps its first design (Figure 4.7). After components installation the third part (Figure 4.8) will cover the electronic board and can be glued to middle part. In order to have the optimized changes in bottom part dimensions, pressure sensor and electronic board including all components with their exact size was designed as a 3D module (Figure 4.9). Using these 3D modules could help for better imagination during PAS bottom part modifications.

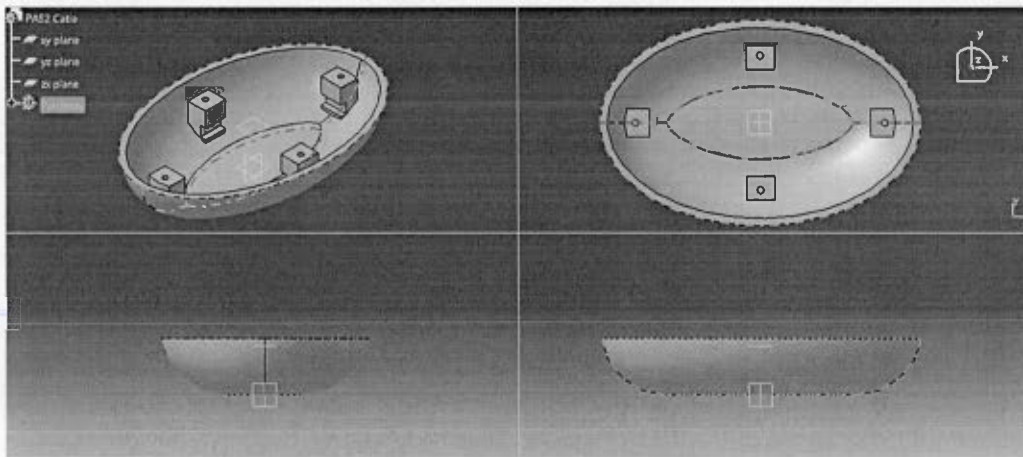
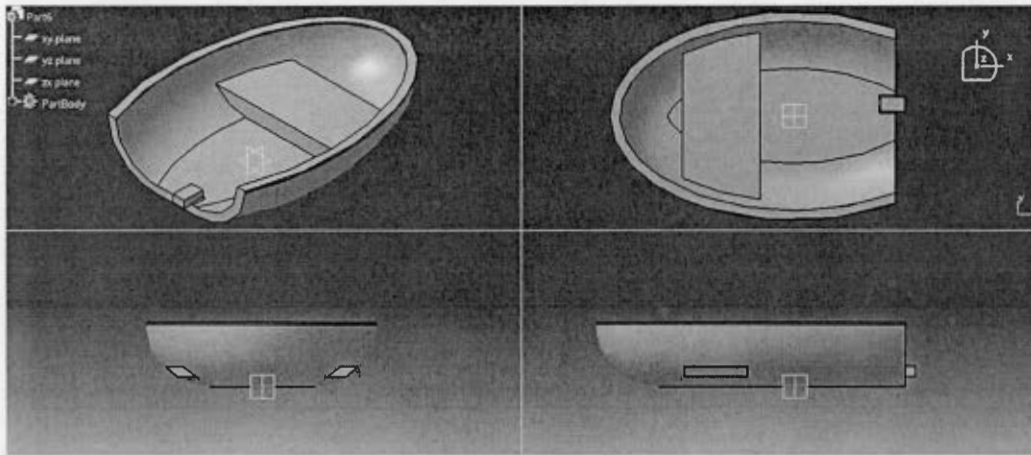
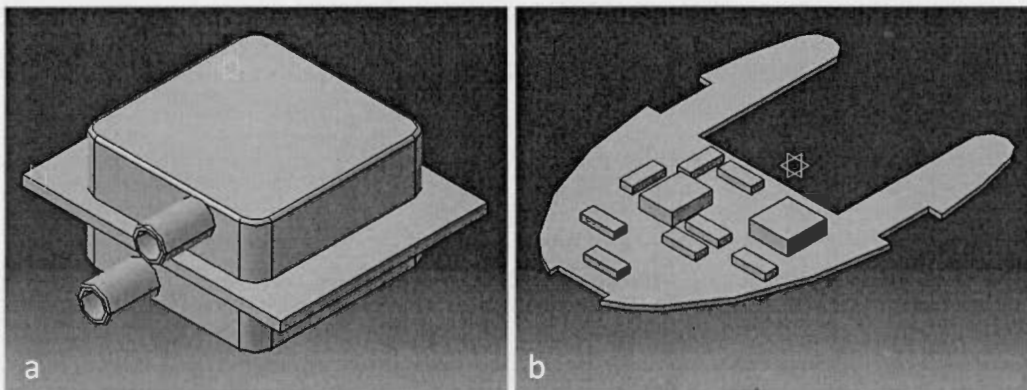


Figure 4.7 : Modified PAS concept design top part 4 side view



**Figure 4.8 : Modified PAS concept design third part 4 side view**



**Figure 4.9 : Electronic components 3D diagram. (a) Differential pressure sensor. (b) PCB board with all required components**

Two separated pressure tubes (Pitot and static) were considered in the front side of PAS middle part (Figure 4.10) where directly points to the fluid flow. For better temperature and humid measurement a square shape hole was added to the PAS middle part, close to the absorber's pin holders while a small piece of a water filter will cover the hole to prevent water penetration into the sensor and the rest of the electronic components.

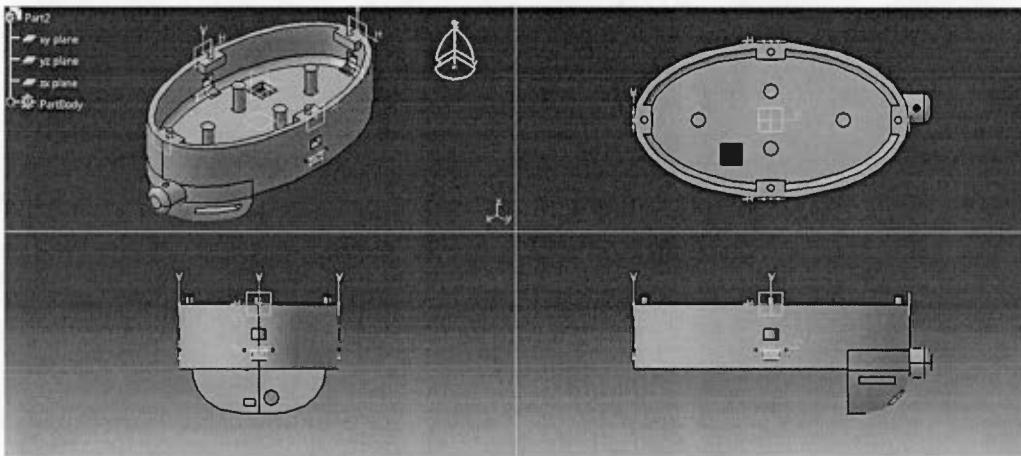


**Figure 4.10 : Modified PAS concept design middle part 4 side view**

Figure 4.11 shows the installation sequences of all part of the PAS including the electronic boards and Figure 80 shows the final PAS after installation and packing.

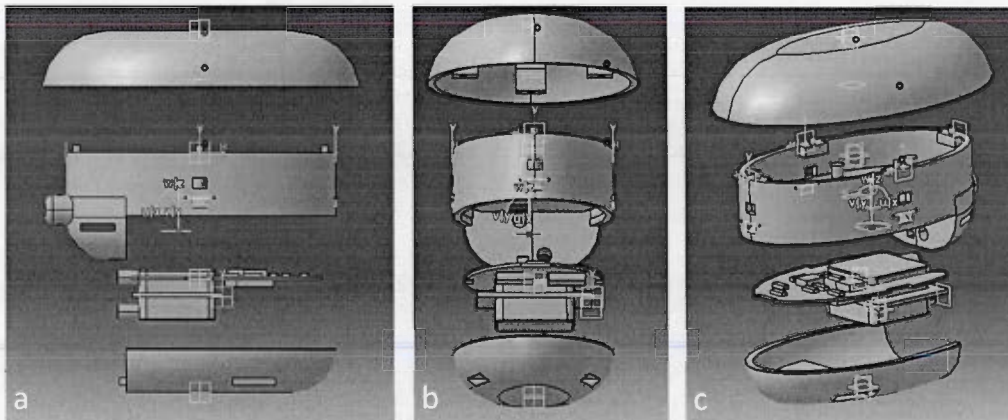


**Figure 4.11 : Modified PAS parts installation sequence. (a) Side view. (b) Back view including pressure holes. (c) 3D view**

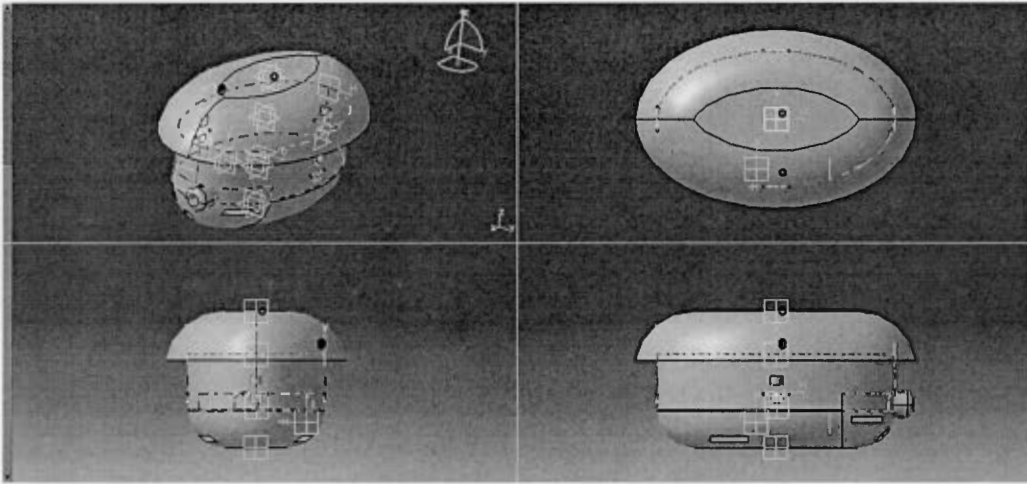


**Figure 4.12 : Modified PAS complete pack 4 side view, electronic parts included**

Figure 4.13 shows a cross-sectional cut of complete PAS including all electronic components. As it shows pressure tube were correctly fit to their tubes and the temperature-humid sensor is positioned exactly under its sampling hole. The inside space is well optimized to reduce the weight of the device.

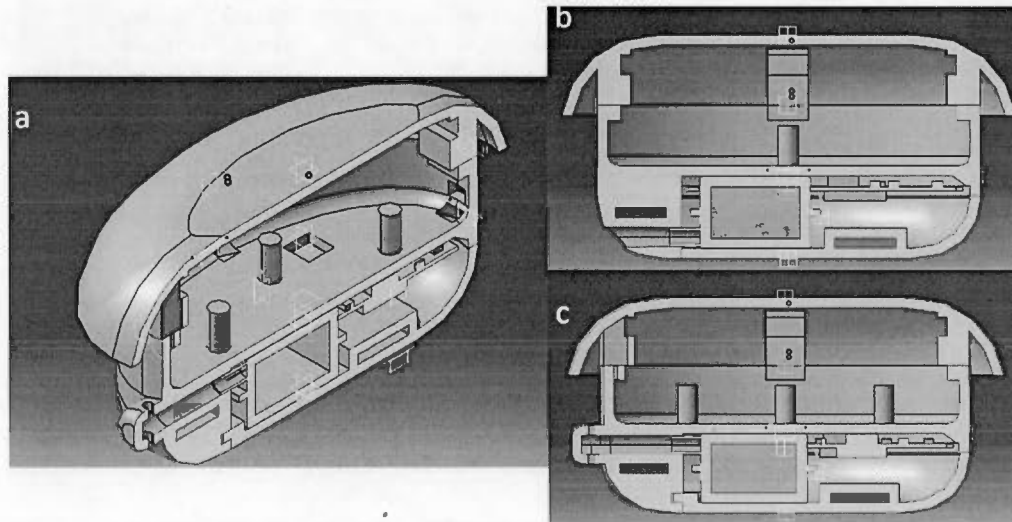


**Figure 4.13 : Complete and final modified PAS cross sectional cut including all electronic components. (a) 3D view. (b) Side view – Pitot tube view. (c) Side view – Static tube view**

#### 4.4 Simulation

CFD simulation was done on modified PAS in order to study the air circulation inside and outside the PAS, especially inside the static pressure tube and electronic component chamber.

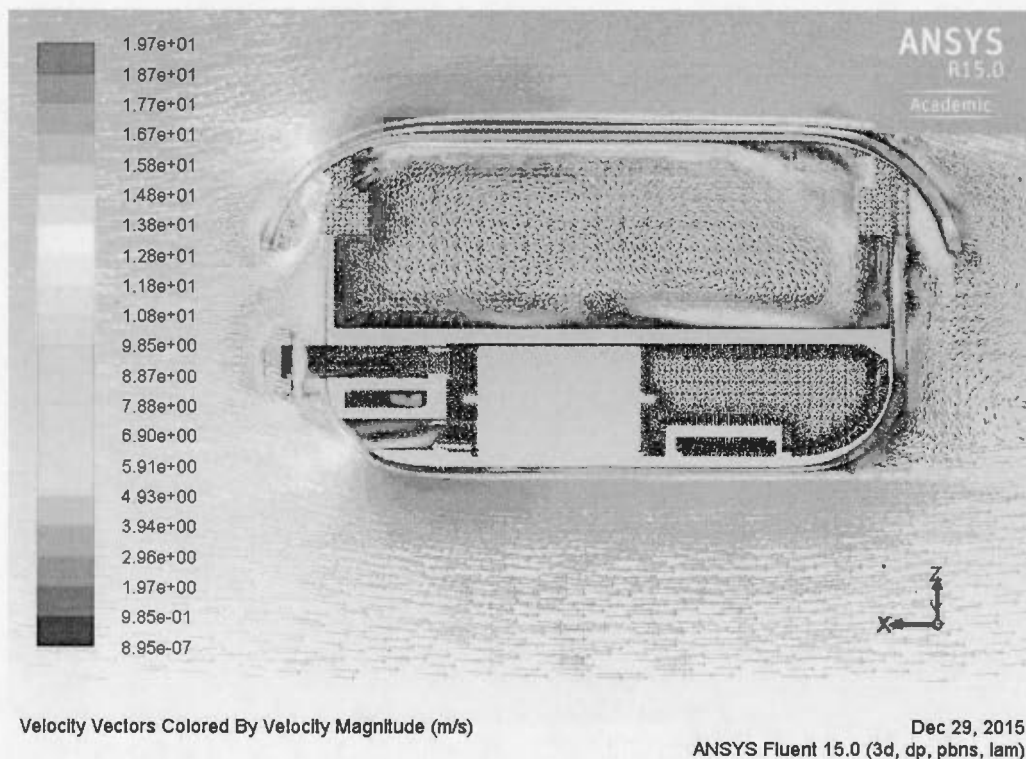


**Figure 4.14 : CFD simulation on complete PAS, results on Y plan, both static and Pitot tube included**

As figure 4.14 presents, sampling air circulation around (above and under) the PAS has approximately the same effects as the PAS without sensors. The fluid velocity inside the top part where the fluid first entered the PAS has the value around 10 m/s. Compared with the PAS without sensors the fluid velocity in this area has 4m/s increase but, it affects only a very thin layer of fluid which is close to the top part and after deflection with inside curve, located in the top part, it decreases to around 4-6 m/s which is equal to the last PAS. After distraction, the sampling air makes a good circulation inside the bottom part under and above the sampling media position. Also the CFD simulation shows that the sampling air penetrates into the static tube holes without strong circulation inside the tube. This means that it is perfectly closed the static holes and keeps the pressure inside the tube as same pressure as environment



while the fluid completely rams to the Pitot tube (Figure 4.14, 4.17) and due to the good alignment for third part (the one that covers that electronic chamber) there is no fluid circulation inside it and the velocity vector value is around 1 m/s.

Moreover, Figure 4.15 and Figure 4.16 show that the two parts have a good overlap and even by 4 mm height increases on the bottom part, the sampling air with velocity equal to 15 m/s could not enter to the PAS and after impacting to top and bottom part, it deflects around the PAS without highly increment in its velocity.

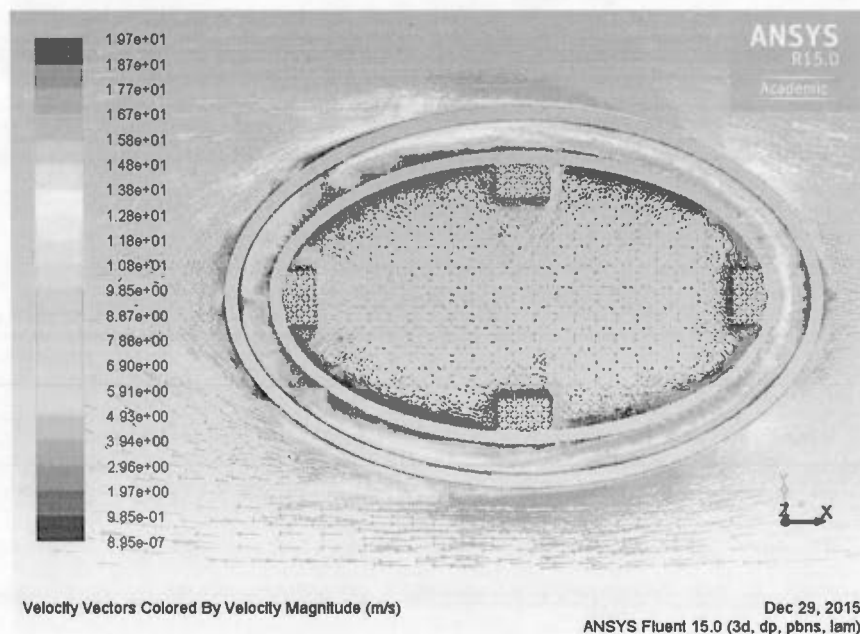


**Figure 4.15 : CFD simulation on modified PAS, results on Z plan and close to the top and bottom parts overlap area**

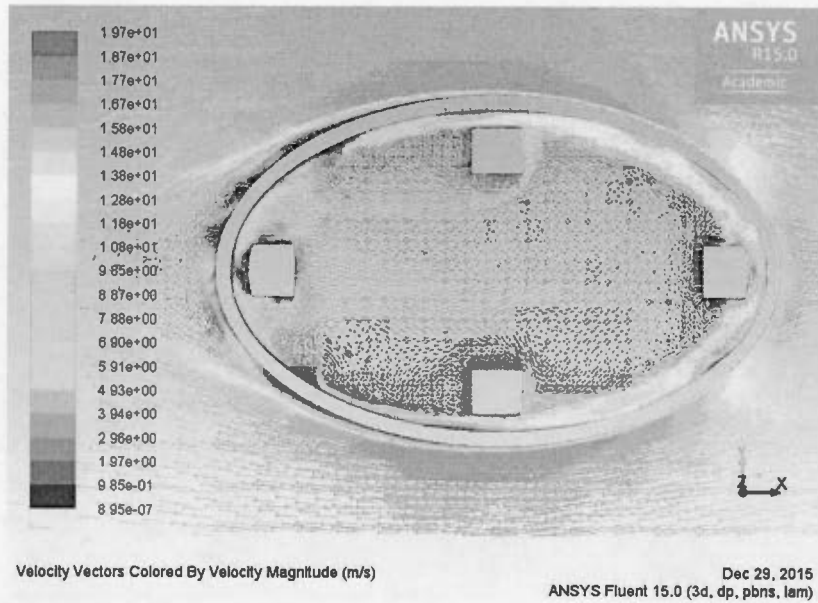


**Figure 4.16 : CFD simulation on modified PAS, results on Z plan and close to the top part close to the sampling media place**

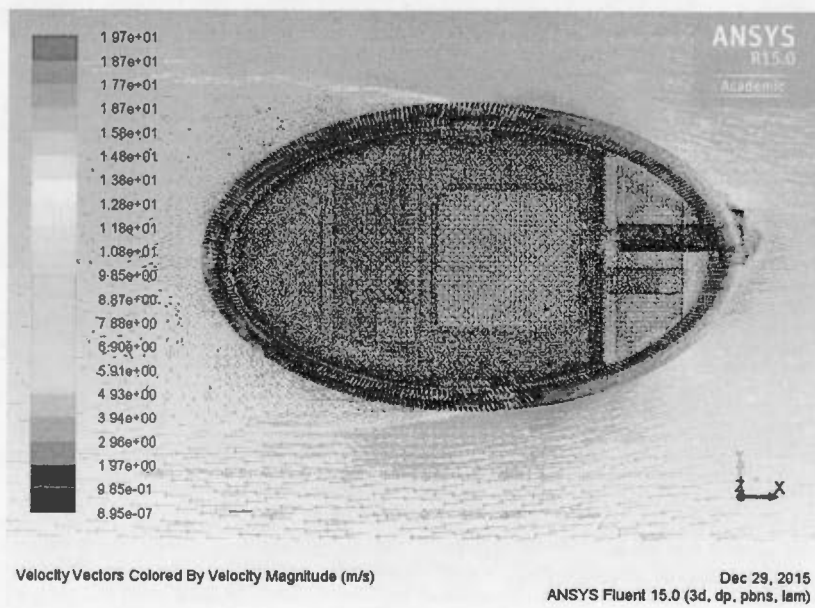


**Figure 4.17 : CFD simulation on modified PAS, results on Z plan top view, all parts, pressure tubes and electronic parts included**

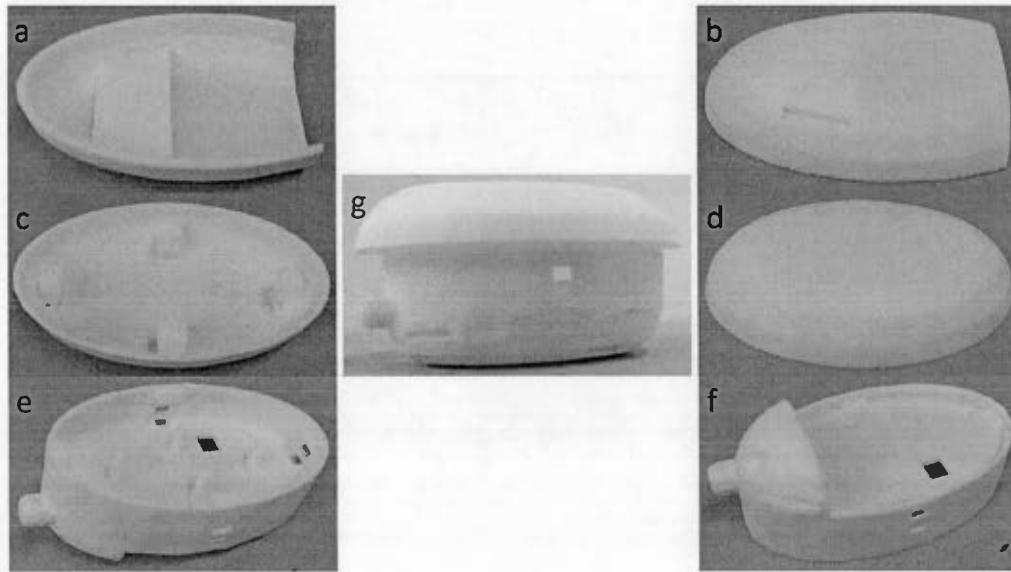


**Figure 4.20 : Modified accepted PAS for embedding the active sensors, fabricated with 3D printing technology. (a) Third part inside. (b) Third part outside. (c) Top part inside. (d) Top part outside. (e) Middle part top view. (f) Middle part bottom view. (g) Complete assembled PAS**

**Table 4.2 : Design 7 drag force calculation**

Design Number	Frontal surface area (mm <sup>2</sup> )	Drag coefficient	Drag force value (Newton)
Design7 (Sensor embedded)	755.5	0.040412487	0.00406647

#### 4.5 Sensor validation and calibration

In order to use sensor's data, they should be compared and validated with an anemometer which usually used as a measurement tool in the environment and biology department. PASCO 850 universal anemometer (Figure 4.21) was used for sensors

validation and calibration. It contains a software which might be installed on a PC, an interface which will be connected to all measurement tools and computer and the measurement tools. The measurement tool consists of, a temperature, a humid sensor and a fan. When the measurement tool is against the fluid flow, fluid passes through the sensors chamber and voltage generator fan. The fan will turn with a specific speed which depends on fluid velocity. Then it will generate a voltage which will be measured and converted to the fluid velocity.

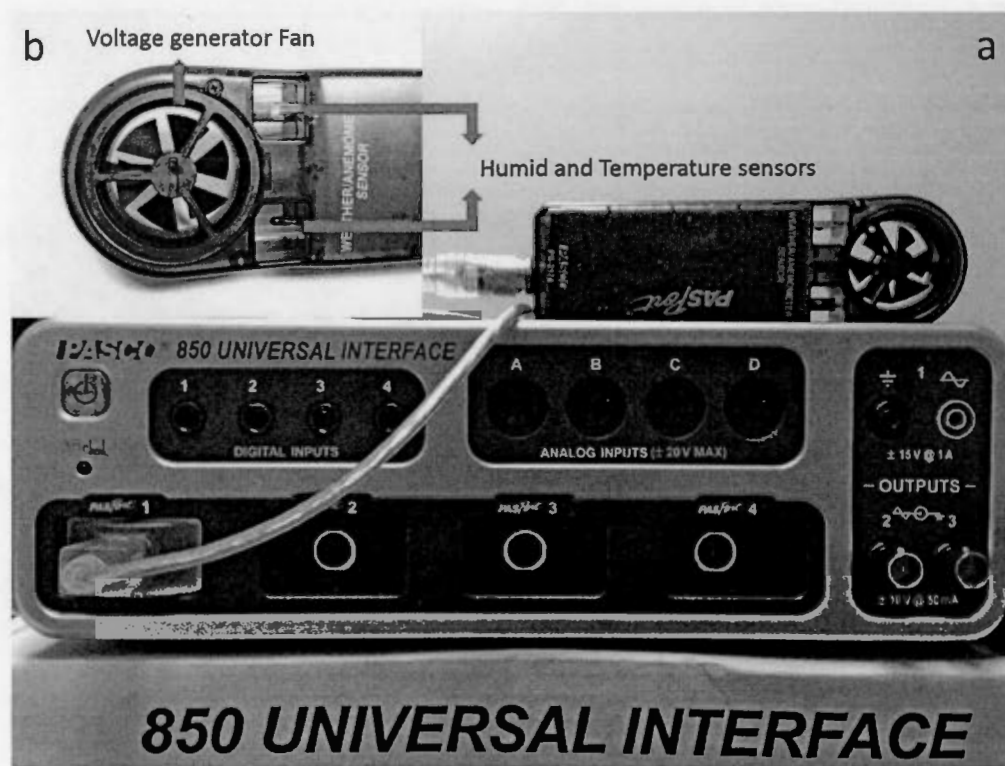
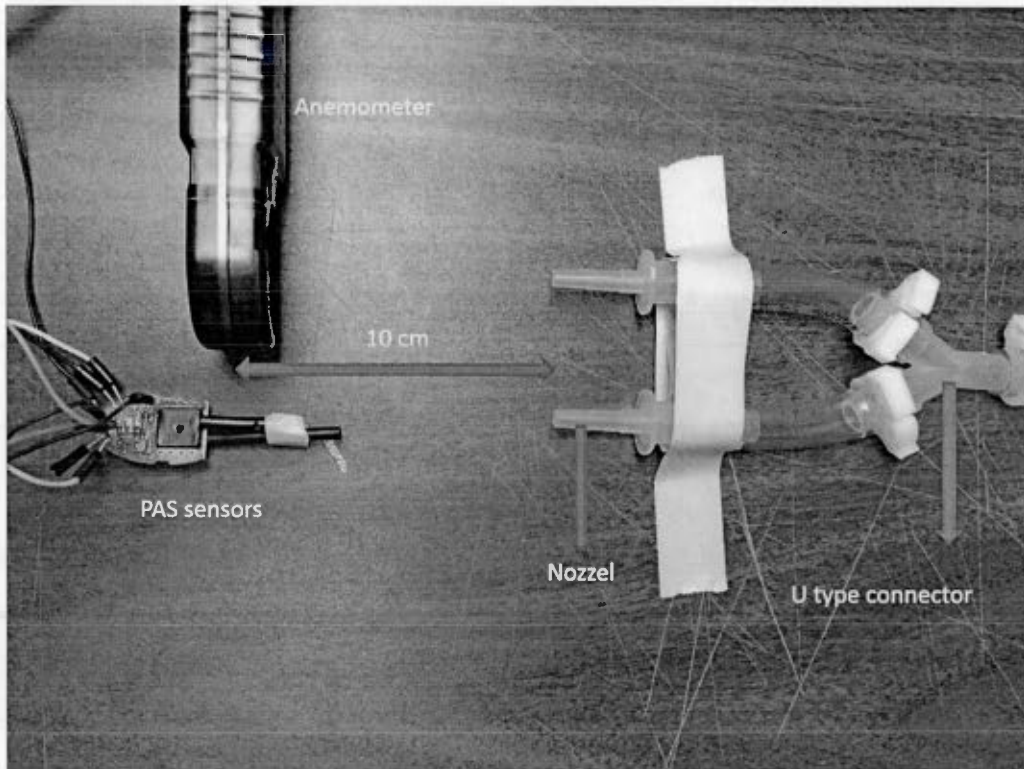


Figure 4.21 : PASCO 850 Universal anemometer. (a) Peripheral interface and measurement tools. (b) Measurement tool that uses separated humid and temperature sensors and a fan as a voltage generator

In order to validate the sensors output and compare them with anemometer outputs value, the following setup was used (Figure 4.22). A pump was used to flow the air into the anemometer and sensors. The airflow velocity was controlled with a manual valve in order to make several tests with different fluid velocities. The air was pumped into a tube which was connected to a U-type connector in order to divide the flowed air in two independent tubes. Each tube was connected to a nozzle to accelerate the air velocity. Anemometer measurement tool and PAS sensors were fixed in front of each nozzle with 10 cm distance and this setup was used for all tests.



**Figure 4.22 : Considered setup for validation and calibration the PAS sensors with an anemometer**

It was tried to have the same sampling frequency as anemometer which was 1 sample per 0.2 second. Each test was done for two minutes and it was repeated six times with six different airspeed (2, 4, 8, 10, 15, 20 m/s). As it is obvious in figures 4.23 and 4.24, the preliminary tests showed that the airspeed sensors outputs have more variation compared with the anemometer outputs. In order to solve the variation problem, the sampling frequency was increased to twenty times during each 0.2 second and the average of all these twenty samples was considered as output value for PAS airspeed sensor.

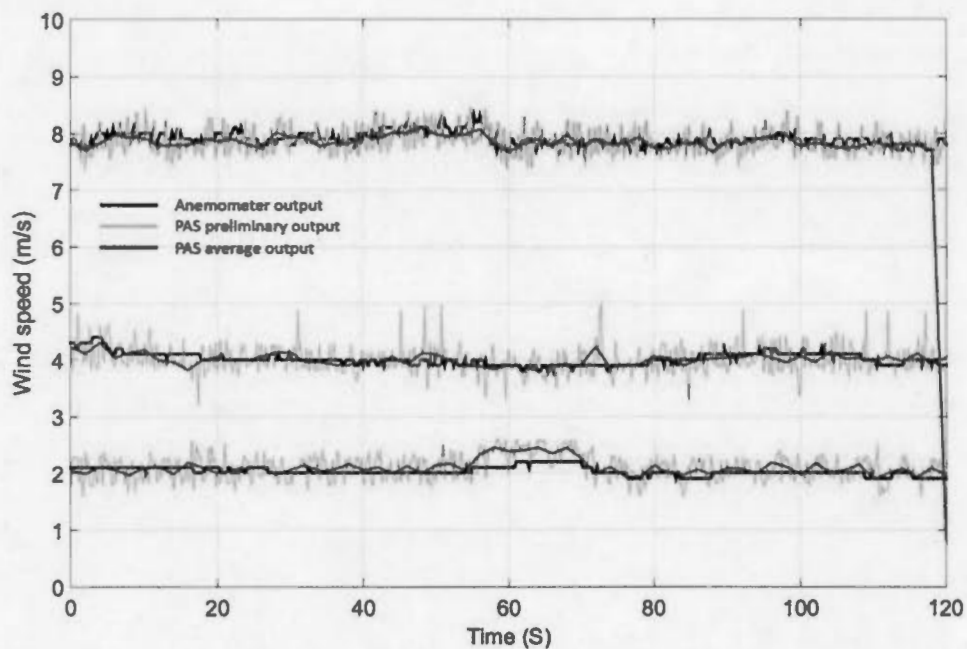


**Figure 4.23 : PAS preliminary and calibrated output results compared with anemometer output results (measured for 2, 4 and 8 m/s airspeed)**

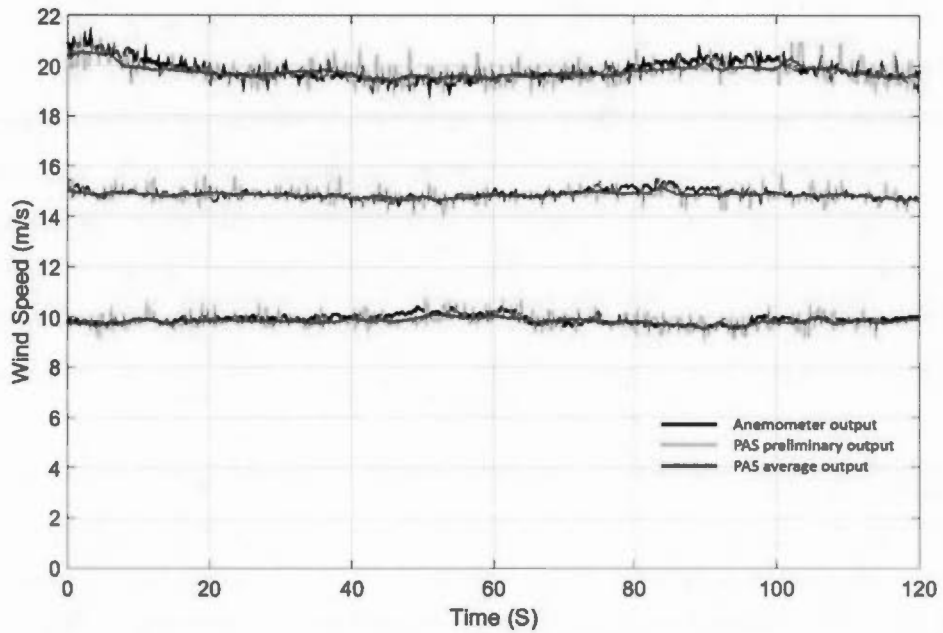


**Figure 4.24 : PAS preliminary and calibrated output results compared with anemometer output results (measured for 10, 15 and 20 m/s airspeed)**

For temperature and humidity sensors the PAS outputs was approximately as same as the anemometer outputs and there were no need for further calibration for these two type of the measurement (Figure 4.25, 4.26).

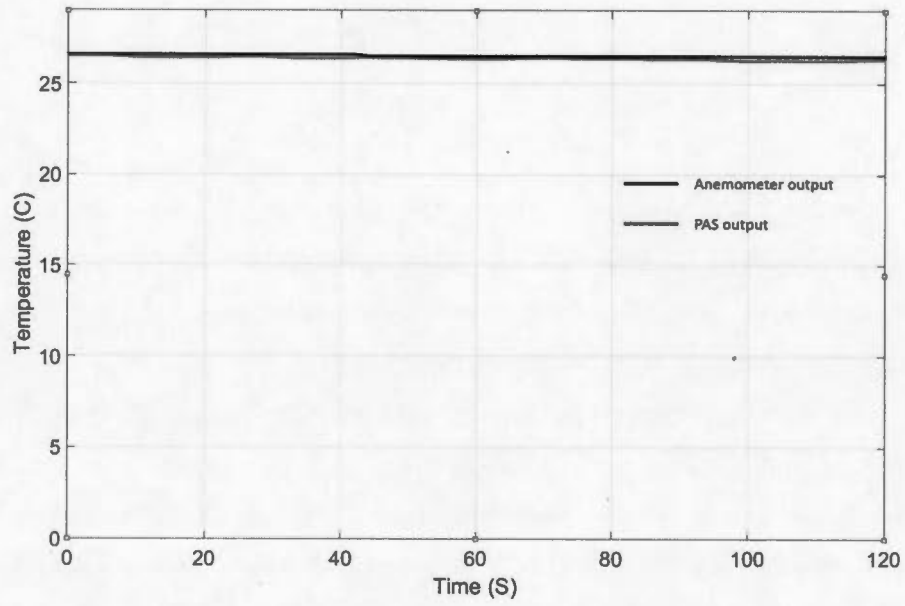


Figure 4.25 : Temperature comparison graph

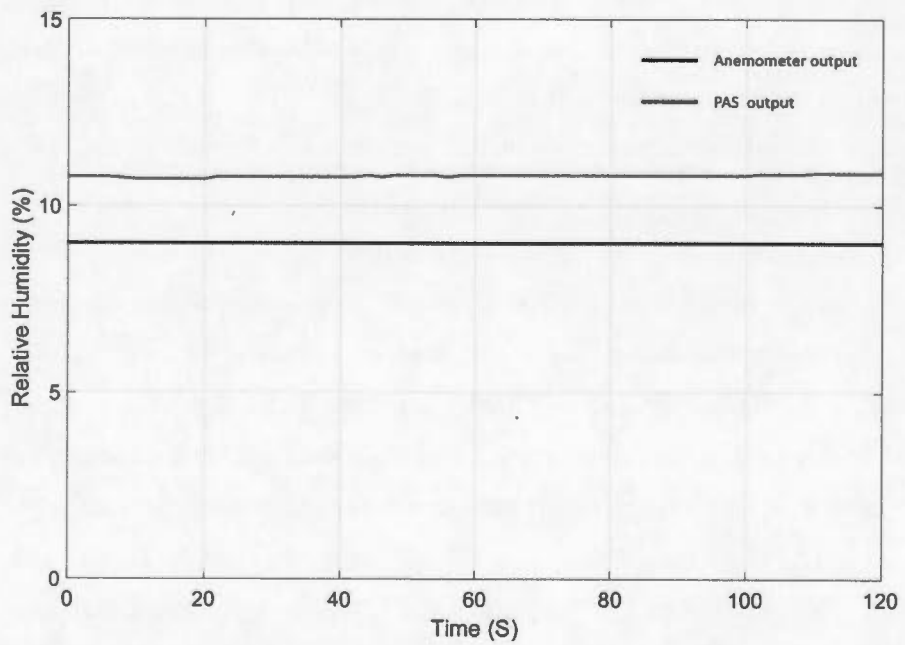


Figure 4.26 : Relative humidity comparison graph



## SUMMARY AND DISCUSSION

In recent years, the dramatic increase in the number of harmful chemicals discharging to the ecosystem causes an important challenges. These chemicals are constantly discharged into the ecosystems and can bioaccumulate in variety of species. In this work, as a part of a project in collaboration with biology department who study on bird's contamination, a traditional passive air sampler was miniaturized. In order to capture desired compounds, a usual passive air sampler designed and miniaturized under certain condition. These conditions depend on bird's physiology and environment, since these PASs should be mounted on the birds to carry to where ever they flight in order to find the source of these contamination.

To address this, several concept designs with different characteristics were presented and simulated with ANSYS-Fluent simulation software as miniaturized passive air sampler. The CFD (computational fluid dynamics) simulation was done on all concept designs in order to find: 1- air flow inside and outside of the PAS, 2- The way that air will expose to the surface of the absorbers 3- calculating the drag coefficient (CD) value to quantify the Drag or resistance of the designs in fluid (air) environment. Based on continuously design-modified process, the design 6 was approved by biology department since it covers project's limitations. It can inhale sampling air from all direction while it decrease the velocity of the sampling air by overlapping the top and bottom part. It is printed from non-transparent plastic material (Polyamide model PA2200) to protect the inside sampling mediums from sun light. This material is also persistent against organic solvent which used for cleaning the PAS before using and it is light enough to bring the advantage of 2.875gr weight per complete PAS (Top and bottom part). The miniaturized PAS can be equipped by multi-layer sampling mediums in three different layer which increases the sampling medium active surface area.

In continue the approved PAS is modified in the way that it can be equipped with some active electronic sensors while it respect all previous conditions. A precise humidity – Temperature and a differential pressure sensors were added to the PAS in order to record the air speed and its related humidity and temperature value. The sensors were calibrated with an anemometer with different air speed. All the electronic components was chose from ultra-low power components (total power consumption of all components = 0.00008 Wh) in order to reduce the power consumption of the device which will extend the sampling period time.

The approved miniaturized PAS was printed and mounted on the back of the birds, equipped with different type of absorbers. The polyurethane foam was used as a well-known absorbers accompanied by a glass fiber filter while, polydimethylsiloxane and graphene oxide was also used to study their functionality. The PASs were deployed on back of the birds for 1, 2 and three weeks and then brought back to the Lab for analysing. The analysis on adsorbents shows that different type of flame retardants including three type of Dechlorane, 15 type of the PBDEs and also Hexabromodenzene were captured. The results from the PASs which were equipped with PUF-GFF sampling media show that the total mass of mentioned compounds was equal to 1 ng for the ones which were studied for duration of 1 week, less than 2 ng for duration of 2 weeks and less than 3 ng for duration of 3 weeks. Also the same analysis on PASs which were equipped with PDMS shows the total mass of mentioned compounds around less than 2 ng for both duration of 1-2 weeks and less than 4 ng for duration of 3 weeks. The results indicate that Montreal clearly is a hotspot for different type of halogenated flame retardant both in gas and particulate phase.

This project consisted of several limitations which must considered due to the ethical regulation. The first and most important one was about the equipment's weight. The total weight of the PAS including adsorbents and custom harness should not exceed 3% of bird weight. The PAS should stand for duration of study in harsh weather. The colour of the PAS should be somehow as same as bird's feather in order to be

camouflaged from other birds. It should also stand during cleaning procedure with organic solvents. The aerodynamic shape of the design was another important thing which was considered in this work. PAS should be designed in such a way that it avoids compromising bird's flying. Moreover it should be considered that all of the materials including PAS, adsorbents, harness or glues must be HFR free in order to have a better evaluation on analysis.

## CONCLUSION

In this work, a miniaturized passive air sampler that can be mounted and carried by a medium size bird, is presented. CFD simulation was done on design in order to study the airflow inside and outside the design and also around the adsorbents position.

3D printing technology was used to fabricate the final device. Variety type of materials with different weights, colours and physical strength can be used by this technology. The fabricated device was equipped with different kinds of adsorbents and mounted on birds for study. Thereafter, the PAS was modified in such a way that it could be equipped with some sensors in order to measure the velocity, temperature and humidity of the sampling air as complementary data for better adsorbents analysis. Based on our knowledge, this is the first miniaturized passive air sampler that can be transported by a bird. Moreover, the adsorbents analysis show that by equipping this device with different type of adsorbents, both gas and particulate phase of flame retardant compounds can be captured which is a great advantage for tracking the source of the pollutions.

There are some points in this thesis that could be developed and there are several lines of research arising from this work which should be pursued. First, it would be interesting to test the PAS with other types of adsorbents specially Graphene oxide in order to know about its functionality and efficiency. It is recommended adding some other type of sensors which could help biologist for better evaluation on their results. In the next step the PAS can be equipped with an active sensor which specially designed for this type of gas or compounds. It can then be embedded inside the microfluidic device in such a way that it respect all PAS's characteristic. The PAS shape as points of precision and aerodynamic can be improved in order to be adapted

for high speed flying birds. Also it is recommended testing the modified PAS, equipped with presented electronic sensors on field, since due to the limited period of the project, there was no chance to test them on the field.

## References

- Abdallah, M.A.-E. et Harrad, S. (2010). Modification and calibration of a passive air sampler for monitoring vapor and particulate phase brominated flame retardants in indoor air: application to car interiors. *Environmental science & technology*, 44(8), 3059-3065.
- Barclift, M.W., Williams, C.B.. (2012). *Examining variability in the mechanical properties of parts manufactured via polyjet direct 3d printing*. International Solid Freeform Fabrication Symposium, August.
- Bayer, O. (1947). Das Di-Isocyanat-Polyadditionsverfahren (Polyurethane). *Angewandte Chemie*, 59(9), 257-272.
- Bohlin, P., Jones, K.C., Levin, J.-O., Lindahl, R. et Strandberg, B. (2010). Field evaluation of a passive personal air sampler for screening of PAH exposure in workplaces. [10.1039/C0EM00018C]. *Journal of Environmental Monitoring*, 12(7), 1437-1444.
- Bulbul, A., Hao-Chieh, H., Hanseup, K.. (2014, 26-30 Jan. 2014). *Microfluidic bubble-based gas sensor*. Micro Electro Mechanical Systems (MEMS), 2014 IEEE 27th International Conference on.
- Chua, C.K. et Leong, K.F. (2003). *Rapid prototyping: principles and applications*. (Vol. 1) : World Scientific.
- Dreyer, D.R., Park, S., Bielawski, C.W. et Ruoff, R.S. (2010). The chemistry of graphene oxide. *Chemical Society Reviews*, 39(1), 228-240.
- Elmajdub, E.N.F.A. et Bharadwaj, A. Important Pitot Static System in Aircraft Control System.

- European Centre for, E. et Toxicology of, C. (1983). Joint assessment of commodity chemicals. *Joint assessment of commodity chemicals*. /z-wcorg/.
- Hazrati, S. et Harrad, S. (2007). Calibration of polyurethane foam (PUF) disk passive air samplers for quantitative measurement of polychlorinated biphenyls (PCBs) and polybrominated diphenyl ethers (PBDEs): Factors influencing sampling rates. *Chemosphere*, 67(3), 448-455.
- Hoerner, S.F. (1965). *Fluid-dynamic drag: practical information on aerodynamic drag and hydrodynamic resistance*. : Hoerner Fluid Dynamics.
- Hull, C.W. (1986). *Apparatus for production of three-dimensional objects by stereolithography* : Google Patents.
- Hummers Jr, W.S. et Offeman, R.E. (1958). Preparation of graphitic oxide. *Journal of the American Chemical Society*, 80(6), 1339-1339.
- Khaing, M., Fuh, J. et Lu, L. (2001). Direct metal laser sintering for rapid tooling: processing and characterisation of EOS parts. *Journal of Materials Processing Technology*, 113(1), 269-272.
- Klopfenstein Jr, R. (1998). Air velocity and flow measurement using a Pitot tube. *ISA transactions*, 37(4), 257-263.
- Kumar, S. (2003). Selective laser sintering: a qualitative and objective approach. *Jom*, 55(10), 43-47.
- Li, S., Day, J.C., Park, J.J., Cadou, C.P. et Ghodssi, R. (2007). A fast-response microfluidic gas concentrating device for environmental sensing. *Sensors and Actuators A: Physical*, 136(1), 69-79.
- Marcano, D.C., Kosynkin, D.V., Berlin, J.M., Sinitskii, A., Sun, Z., Slesarev, A., Alemany, L.B., Lu, W. et Tour, J.M. (2010). Improved Synthesis of Graphene Oxide. *ACS Nano*, 4(8), 4806-4814.

- Martini, V., Bernardini, S., Bendahan, M., Aguir, K., Perrier, P. et Graur, I. (2012). Microfluidic gas sensor with integrated pumping system. *Sensors and Actuators B: Chemical*, 170(0), 45-50.
- May, A.A., Ashman, P., Huang, J., Dhaniyala, S. et Holsen, T.M. (2011). Evaluation of the polyurethane foam (PUF) disk passive air sampler: Computational modeling and experimental measurements. *Atmospheric Environment*, 45(26), 4354-4359.
- Mu, X., Ward, N., Li, L., Li, W., Mason, A.J., Covington, E., Serrano, G., Kurdak, C., Zellers, E. (2012, 20-23 May 2012). *CMOS monolithic chemiresistor array with microfluidic channel for micro gas chromatograph*. Circuits and Systems (ISCAS), 2012 IEEE International Symposium on.
- Nelson, R.C. (1998). *Flight stability and automatic control*. (Vol. 2) : WCB/McGraw Hill.
- Park, E.J., Cho, Y.K., Kim, D.H., Jeong, M.-G., Kim, Y.H. et Kim, Y.D. (2014). Hydrophobic Polydimethylsiloxane (PDMS) Coating of Mesoporous Silica and Its Use as a Preconcentrating Agent of Gas Analytes. *Langmuir*, 30(34), 10256-10262.
- Pitot, H. (1732). Description d'une machine pour mesurer la vitesse des eaux courantes et le sillage des vaisseaux. *Mémoires de L'Académie*.
- Prisacariu, C. (2011). Chemistry of polyurethane elastomers. Dans *Polyurethane Elastomers* (p. 1-22) : Springer.
- Qin, D., Xia, Y. et Whitesides, G.M. (2010). Soft lithography for micro- and nanoscale patterning. [10.1038/nprot.2009.234]. *Nat. Protocols*, 5(3), 491-502.
- Seymour, R.B. et Kauffman, G.B. (1992). Polyurethanes: A class of modern versatile materials. *J. Chem. Educ*, 69(11), 909.
- Thomas, J., Holsen, T.M. et Dhaniyala, S. (2006). Computational fluid dynamic modeling of two passive samplers. *Environmental Pollution*, 144(2), 384-392.



- Tuduri, L., Harner, T. et Hung, H. (2006). Polyurethane foam (PUF) disks passive air samplers: Wind effect on sampling rates. *Environmental Pollution*, 144(2), 377-383.
- Vandenabeele, S.P., Grundy, E., Friswell, M.I., Grogan, A., Votier, S.C. et Wilson, R.P. (2014). Excess baggage for birds: inappropriate placement of tags on gannets changes flight patterns. *PloS one*, 9(3), e92657.
- Ward, N., Mu, X., Serrano, G., Covington, E., Kurdak, C., Zellers, E.T., Mason, A.J. et Li, W. (2012). Microfluidic-packaged CMOS chemiresistor detector for micro-scale gas chromatograph. *Micro & Nano Letters, IET*, 7(8), 721-724.
- Xiao, H., Hung, H., Harner, T., Lei, Y.D., Johnston, G.W. et Wania, F. (2007). A flow-through sampler for semivolatile organic compounds in air. *Environmental science & technology*, 41(1), 250-256.